STUDYING PLATELET AND MONOCYTE FUNCTION IN ATHEROSCLEROSIS BY EMPLOYING QUANTITATIVE PROTEOMICS

by

Honghui Jiang

B.Sc., University of Windsor, 2011

A THESIS SUBMITTED IN PARTIAL FULFILLMENT OF

THE REQUIREMENTS FOR THE DEGREE OF

MASTER OF SCIENCE

in

THE FACULTY OF GRADUATE AND POSTDOCTORAL STUDIES

(Chemistry)

THE UNIVERSITY OF BRITISH COLUMBIA

(Vancouver)

August 2017

© Honghui Jiang, 2017

Abstract

Atherosclerosis is the major cause of cardiovascular diseases. Both monocytes and platelets are key players in the development and progression of atherosclerosis. Monocyte adhesion, transmigration, and differentiation contribute to atherosclerotic plaque formation. Activated platelets release their granule contents, platelet releasate, to activate and modulate monocytes. The platelet releasate consists of a large number of bioactive proteins, including multiple cytokines and chemokines. The binding of chemokines to specific G protein-coupled receptors in the plasma membrane of monocytes can initiate the intracellular signaling cascade that results in monocyte migration. Multiple small GTPases are critical elements in such intracellular signaling pathways. To determine the effect of platelet releasate on small GTPases in monocytes, the activity level changes of small GTPases were quantified by the quantitative multiplexed small GTPase activity assay. Upon lysophosphatidic acid (LPA)-induced platelet releasate treatment, the activation of both Rap1 and Rap2 GTPases in monocytes was found to be increased through chemokine CXCL12 binding. Like LPA, oxidized phosphatidylcholines (oxPCs) are also oxLDL derivatives. They can be released from plaques upon rupture. The effect of oxPCs on platelets is controversial, but involves the cAMP/cGMP signaling pathway. To define the response of the cAMP/cGMP interactome in platelets upon oxPC treatment, a targeted quantitative chemical proteomics approach was developed and applied to purify cAMP/cGMP binding proteins and quantify their amount change in platelets upon KDdiA-PC and POV-PC stimulation. The amount of PKA-RIα and -RIIα was decreased in POV-PC-stimulated platelets, which coincides with an increase in the intracellular cAMP level. However, sGC inhibitor treatment further decreased the amount of PKA-RIβ and -RIIβ, and PKG1 in POV-PC stimulated platelets, which implies the

reduction of intracellular cGMP upon POV-PC stimulation and the cross-talk between cAMP and cGMP signaling. The interaction between phosphodiesterases and cAMP/cGMP demonstrates the compartmentalization of cyclic nucleotide signaling. These findings may help recognize therapeutic targets for prevention of inappropriate monocyte activation and contribute to the application of platelet drugs in combination to avoid undesirable side effects like bleeding.

Lay Summary

Atherosclerosis is the prime cause of cardiovascular diseases, which account for about 30 percent of all global deaths. Platelets and monocytes (a type of white blood cell) play key roles in the development and progression of atherosclerosis. Activated platelets release signaling proteins (platelet releasate) which interact with monocytes, causing the monocytes to burrow into the inner-most layer of blood vessels (transmigration) and form atherosclerotic plaques. My study found that platelet releasate treatment increased the activity level of Rap GTPase proteins in the monocytes. Rap GTPases are essential to monocyte transmigration. Therefore, they can be targeted when treating inappropriate monocyte activation. I also analyzed the effect of oxidized phosphatidylcholines (oxidized lipid) on the components of platelet inhibition signaling pathway. The understanding of the interaction between oxidized phosphatidylcholines and these components may contribute to the application of platelet drugs in combination to avoid undesirable side effects like bleeding.

Preface

Ethical approval for platelet and monocyte isolation from whole blood from healthy blood donors was obtained from the Clinical Research Ethics Board at University of British Columbia (H12-00757) and written consent was granted by the blood donors.

Table of Contents

List of Tables

List of Figures

List of Abbreviations

AC	Adenylate cyclase
ACD	Acid citrate dextrose
ADP	Adenosine diphosphate
ATP	Adenosine triphosphate
BCA	Bicinchoninic acid
BD	Binding domain
cAMP	Cyclic adenosine monophosphate
CCL3	Macrophage inflammatory protein-1α
CCL5	RANTES
cGMP	Cyclic guanosine monophosphate
COX	Cyclooxygenase
CXCL4	Platelet factor 4
CXCL8	Interleukin-8
DAG	Diacyl glycerol
EDG	Endothelial differentiation gene
ESI	Electrospray ionization
GAP	GTPase-activating protein
GDI	Guanine nucleotide dissociation inhibitor
GDP	Guanosine diphosphate
GEF	Guanine nucleotide exchange factor
GPCR	G-protein-coupled receptor
GPIbα	Glycoprotein Ibα
GST	Glutathione S-transferase
GTP	Guanosine triphosphate
GTPase	Guanosine triphosphatase
HSP27	Heat shock protein 27
IP_3-R	Inositol 1,4,5-trisphosphate receptor
IRAG	IP_3-R-associated cGMP kinase substrate
LASP	Lim and SH3 domain protein
LB	Lysogeny broth
LC-MS/MS	Liquid chromatography-tandem mass spectrometry
LDL	Low density lipoprotein
LPA	Lysophosphatidic acid
m/z	Mass-to-charge
Mac-1	$\alpha_M\beta_2$ integrin
MALDI	Matrix-assisted laser desorption/ionization
MCP-1	Monocyte chemoattractant protein-1
MM-LDL	Minimally modified low density lipoprotein
MPA	Monocyte-platelet aggregate
MRM	Multiple reaction monitoring
MS	Mass spectrometry
MW	Molecular weight

NO	Nitric oxide
ODQ	1H-[1,2,4]oxadiazolo-[4,3-a]quinoxalin-1-one
oxLDL	Oxidized low density lipoprotein
oxPC	Oxidized phosphatidylcholine
PAPC	1-palmitoyl-2- arachidonyl-PC
PBD	Protein-binding domain
PBMC	Peripheral blood mononuclear cell
PBS	Phosphate-buffered saline
PDE	Phosphodiesterase
pGC	Particulate guanylate cyclase
PGI_2	Endothelial prostacyclin
PKA	Protein kinase A
PKC	Protein kinase C
PKG	Protein kinase G
PLCγ2	Phospholipase Cγ2
PLPC	1-palmitoyl-2-linoleoyl-PC
PR	Platelet releasate
PRP	Platelet-rich plasma
PSG-1	P-selectin glycoprotein ligand-1
PTM	Post-translational modification
PVDF	Polyvinylidene difluoride
QQQ	Triple quadrupole
Q-TOF	Quadrupole-time of flight mass spectrometer
rcf	Relative centrifugal force
ROS	Reactive oxygen species
RPMI	Roswell Park Memorial Institute medium
SDS-PAGE	Sodium dodecyl sulfate-polyacrylamide gel electrophoresis
SFK	Src-family kinase
sGC	Soluble guanylate cyclase
SILAC	Stable isotope labelling by amino acids in cell culture
SMC	Smooth muscle cell
SRM	Selected reaction monitoring
SYK	Spleen tyrosine kinase
THP-1	The human acute monocytic leukemia cell line
TXA2	Thromboxane A2
VASP	Vasodilator-stimulated phosphoprotein
VCAM-1	Vascular cell adhesion molecule-1
VWF	Von Willebrand factor

Acknowledgements

I would like to thank all the people who contributed in some way to the work described in this thesis. First and foremost, I thank my academic advisor, Professor Jürgen Kast, for accepting me into his group and guiding me all the time through this study.

I owe particular thanks to all the blood donors for contributing their time and blood to support my research. NSERC and CIHR are also acknowledged for providing financial support to my study.

Next, I would like to thank our lab technician Shujun Lin for training me to use the MS instruments and helping me when I encounter problems. Many thanks are given to fellow PhD students Jiqing Huang and Ru Li for their help with my project. I also would like to thank Dr. Nikolay Stoynov and Jason Rogalski for helping me run samples on mass spectrometers.

A special thank-you goes out to Dr. Yanni Wang, Dr. Hermann Ziltener, and Dr. Doug Carlow for giving me input on my research.

Finally, the continual encouragement and support of my family has been a source of strength, which is sincerely appreciated.

Chapter 1: Introduction

1.1 Atherosclerosis

Atherosclerosis, the main cause of heart attack, stroke, and peripheral vascular disease, accounted for 31 percent of all global deaths in 2013. The American Heart Association estimates that cardiovascular diseases caused more than 17.3 million deaths per year and cost 863 billion dollars in 2010.

Atherosclerosis is the narrowing of the arteries due to the build-up of cholesterol-rich plaques inside the artery wall. Arteries, with the exception of the pulmonary artery, carry oxygenated blood to all parts of the body. Plaque build-up narrows the lumen of arteries and slows down the flow of blood. Eventually, the surface of a plaque can rupture. After a plaque breaks open, blood clots form on the surface of the arteries. A large blood clot can mostly or completely block blood flow resulting in tissue death. Occlusion of brain arteries causes stroke. Blockage of coronary arteries leads to myocardial infarction.

Usually the clinical manifestations of atherosclerosis do not appear until people reach middle age. However, the process of atherosclerosis can begin during childhood (Young, M. H., 2010). Most scientists believe that atherosclerosis starts with vessel endothelium damage. Hyperlipidemia, hypertension, and smoking are possible factors that contribute to the damage of the arterial wall (Munro, et al., 1988). Endothelial dysfunction increases the permeability to lipids and leukocytes. Low density lipoprotein (LDL) enters the arterial wall and undergoes oxidation. Endothelial damage also stimulates an inflammatory response, in which monocytes

and T-lymphocytes migrate from the blood into the intima and monocytes differentiate into macrophages. After taking up oxidized LDL, macrophages form the lipid core of the atherosclerotic plaque (foam cells). T-lymphocytes and foam cells release cytokines and growth factors that induce the migration and proliferation of smooth muscle cells (SMCs) to form a distinct fibrous capsule (Figure 1-1). Plaques with thicker fibrous caps tend to be stable and are not prone to rupture. Conversely, plaques with thin fibrous caps tend to be more fragile and rupture.

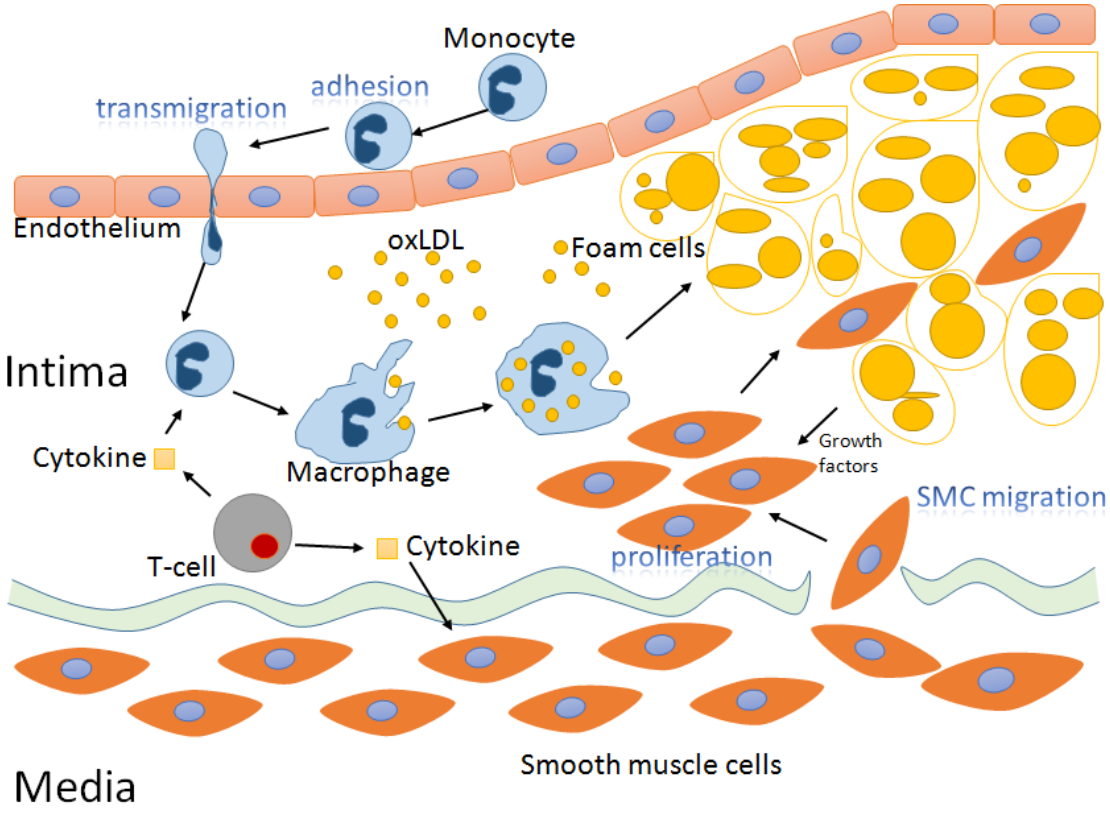

Figure 1-1. The mechanism of atherosclerotic plaque formation.

Endothelial dysfunction triggers monocyte adhesion and transmigration. Monocytes migrate beneath the endothelium and differentiate into macrophages. LDL also passes through the more permeable endothelium to enter the intima and is oxidized to be oxLDL. Macrophages engulf the oxLDL and become foam cells. T-cells in the intima secrete cytokins that induce smooth muscle cells to migrate from the media to the intima. Under the influence of growth factors, these smooth muscle cells begin to proliferate and join foam cells to form plaques.

Recent research has recognized that activated platelets contribute to the inflammatory processes underlying atherosclerosis by enhancing leukocyte recruitment, activation, and transmigration (Rainger, et al., 2015). The number of activated platelets can be elevated by the risk factors of atherosclerosis such as hypercholesterolemia (Broijersen et al., 1998), hypertension (Nityanand et al., 1993), and smoking (Nowak et al., 1987).

Lifestyle changes may slow down the progression of atherosclerosis but are not enough to reduce the risk of atherosclerosis complications. Cholesterol medications such as statins and anti-platelet medications such as aspirin are normally used for protection from atherosclerosis. Statins are cholesterol-lowering drugs and work through reducing the production of cholesterol by the liver. Statins can reduce the plaque volume, but do not induce a significant change for fibrotic and fibro-fatty compositions (Tian et al., 2012). Therefore, they do not reduce the risk of plaque rupture. Moreover, most statin drug trials demonstrate that they do not induce regression of atherosclerosis (Crouse et al., 2007). Aspirin reduces the ability of platelets in the blood to form clots through inhibiting the cyclooxygenase (COX) enzyme. Aspirin given can decrease the risk of heart attacks and strokes. However, it suppresses the normal function of platelets causing bleeding.

In order to improve the therapeutic treatment of atherosclerotic disease, it is necessary to understand the mechanisms of platelet activation, monocyte function, and platelet-monocyte interaction in atherosclerosis.

1.1.1 Platelets in atherosclerosis

Platelets are small disk-shaped anucleate cell fragments. They are derived from the cytoplasm of megakaryocytes in the bone marrow and circulate in the blood with physiological concentration of 200×10^9/L to 400×10^9/L. Platelets lack DNA but they contain messenger RNA (mRNA) therefore can synthesize a limited number of proteins. α granules, dense granules, and lysosomes are three major types of platelet granules. The most abundant granules are α granules which contain proteins for supporting platelet adhesion, aggregation, and coagulation such as fibrinogen, von Willebrand factor (vWF), vitronectin, and integrin $\alpha_{IIb}\beta_3$ (GPIIb/IIIa). The contents of α granules also include membrane-bound proteins such as P-selectin, which is only expressed on the platelet surface after platelet activation, and a diverse range of chemokines such as CXCL1, platelet factor 4 (PF4 or CXCL4), CXCL5, CXCL7, interleukin-8 (IL8 or CXCL8), CXCL12, macrophage inflammatory protein-1α (MIP-1α or CCL3), and RANTES (CCL5) (Blair et al., 2009). Dense granules store nucleotides (ADP and ATP), serotonin, and cations (Rendu, et al. 2001). Lysosomes contain the lysosomal-associated membrane proteins, LAMP1, LAMP2, and LAMP3 (CD63) (Silverstein, et al., 1992).

The main physiological function of platelets is initiating blood clotting to stop bleeding at the sites of damaged vessel endothelium. Under physiological conditions, endothelial prostacyclin and nitric oxide inhibit platelet functions. After vascular injury or atherosclerotic plaque rupture, platelets immediately adhere to exposed subendothelial matrix proteins, collagen and von Willebrand factor (vWF). The platelet glycoprotein (GP) Ib/V/IX complex first interacts with vWF (Kroll et al., 1996), and then collagen binds to platelet GPVI receptors (Furie et al., 2005). The binding of collagen to GPVI induces platelet activation (Varga-Szabo et al., 2008).

Thrombin, the most potent platelet stimulator, is generated at the site of vascular injury and causes platelet shape change, integrin activation, and granule secretion. Upon firm adhesion, platelets release the contents of their granules such as Adenosine diphosphate (ADP) and thromboxane A_2 (TXA_2) to further promote platelet activation leading to platelet aggregation. Platelet aggregation is triggered by the activation of the GPIIb/IIIa receptor which binds to fibrinogen. The receptor-bound fibrinogen acts as a bridge to connect two GPIIb/IIIa on adjacent platelets, which results in the formation of blood clots (Varga-Szabo et al., 2008).

Besides their function in the hemostatic process, platelets also play a major role in inflammation and atherosclerosis. The interaction of platelets and inflamed endothelium results in the activation of platelets. Activated platelets release an enormous number of inflammatory mediators which promote monocytes and other leukocytes to adhere and transmigrate through endothelium. Activated platelets also modulate inflammation through directly interacting with monocytes to form platelet-monocyte aggregates. The binding of platelets to monocytes is initiated by the interaction between P-selectin on platelets and P-selectin glycoprotein ligand-1 (PSGL-1) on monocytes (Yokoyama et al., 2005). Crosslinking of P-selectin and PSGL-1 activates the β2 integrin (Mac-1) and congregates Mac-1 on the monocyte surface, resulting in the further binding interaction between platelet glycoprotein Ibα (GPIbα) and Mac-1 ($\alpha_M\beta_2$ integrin). The platelet-monocyte interactions may also be mediated by platelet CD40L-monocyte CD40 and platelet TREM-1 ligand- monocyte TREM-1 (Thomas et al., 2015).

Platelets can be activated not only by physiological stimuli such as thrombin, ADP, epinephrine, and thromboxane A_2 (TXA_2) but also by pathological stimuli such as lysophosphatidic acid

(LPA). Normally, agonist-induced platelet activation is achieved through binding to membrane G-protein-coupled receptors (Offermanns, S., 2006). These receptors are coupled to G proteins in platelets and in turn activate their downstream intracellular signaling pathways. There are four groups of G proteins, G_q, $G_{12/13}$, G_i, and G_s, expressed in platelets. G_q, $G_{12/13}$, and G_i are involved in activation pathways, whereas G_s is responsible for inhibition signaling.

1.1.1.1 Lysophosphatidic acid (LPA) and platelets

LPA, a bioactive phospholipid, is a component of oxidized LDL and the lipid core of atherosclerotic plaques (Siess et al., 2004). Two LPA molecular species, acyl-LPA (80%) and alkyl-LPA (20%), are found in atherosclerotic lesions and alkyl-LPA (16:0) has higher platelet-activating potency than acyl-LPA (16:0) (Rother et al., 2003). Chemical structures of acyl-LPA and alkyl-LPA are shown in Figure 1-2.

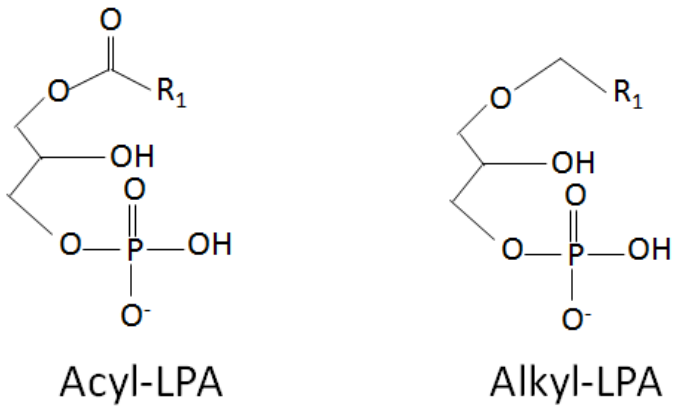

Figure 1-2. The chemical structures of acyl-LPA and alkyl-LPA.
$R_1 = (CH_2)_{14}CH_3$

LPA induces platelet shape change and aggregation through G-protein-coupled receptors (GPCRs) in an autocrine fashion. The seven identified LPA receptors can be divided into two subfamilies according to their structure. The Endothelial Differentiation Gene (EDG-) subfamily of GPCRs consists of LPA_1, LPA_2, and LPA_3 (Chun et al., 2002), and the purinoreceptor (P2Y) cluster of GPCRs consists of LPA_4, LPA_5, LPA_6, and LPA_7 (Noguchi et al., 2003). Human platelets express mRNA for LPA_1 to LPA_6; LPA_4 and LPA_5 are the most abundant transcripts (Amisten et al., 2008). However, the LPA receptors mediating LPA responses in platelets are not pinpointed. LPA-induced platelet shape change is inhibited by antagonists of LPA_1 and LPA_3 receptors (Rother et al., 2003), but the LPA_1 and LPA_3 receptors do not show any ligand specificities (Bandoh et al., 2000). Although different LPA molecular species have dissimilar platelet-activating potency, the response of LPA_{1-4} receptors to LPA molecules with different structure is the same (Smyth et al., 2008). This suggests that these receptors are not the only major mediators of LPA-induced platelet activation.

The downstream signaling pathways of LPA-stimulated platelet activation are also not very clear. LPA activates Rho GTPase and its target Rho kinase resulting in myosin light chain kinase and moesin phosphorylation to control actin organization and shape change (Retzer et al., 2000). LPA works through receptors coupled to $G_{12/13}$ to activate Rho/Rho kinase and provoke shape change (Klages et al., 1999). Furthermore, LPA-induced platelet aggregation may be achieved by activating ADP receptors (Haserück et al., 2004).

LPA stimulates platelet shape change (Retzer et al., 2000) and platelet-monocyte aggregate formation (Haserück et al., 2004). However, platelet aggregation induced by LPA is donor

dependent and platelets from 20% of healthy donors do not aggregate with LPA stimulation (Pamuklar et al., 2008). The elevation of expression of LPA_4 mRNA in non-responders suggests that LPA_4 mediates inhibitor signaling by LPA (Pamuklar et al., 2008). However, LPA stimulation does not affect platelet cAMP levels (Khandoga et al., 2008). Therefore, further study is needed to reveal the receptors mediating LPA-induced platelet activation and signaling mechanisms.

1.1.1.2 Oxidized low-density lipoprotein (oxLDL), oxidized phosphatidylcholines (oxPC) and platelets

Low-density lipoproteins (LDLs) are cholesterol carriers to transport cholesterol from blood to cells. When cholesterol uptake is blocked, excess LDL cholesterol accumulates in the blood resulting in high risk of developing atherosclerosis.

Oxidative modification of LDL increases its proinflammatory and proatherogenic properties. The oxidized LDL can be classified into two main groups, minimally modified LDL (MM-LDL) and (extensively) oxidized LDL (oxLDL). MM-LDL is chemically different from unmodified LDL and still recognized by the LDL receptor, but not by scavenger receptors. OxLDL are recognized by scavenger receptors but not by the LDL receptor. Class B scavenger receptor, CD36, is identified as a receptor for oxLDL. Both extensively oxidized LDL and mildly-oxidized LDL can be recognized by CD36 (Kunjathoor et al., 2002). Most oxidation of LDL takes place in the tunica intima of the arteries. However, small amounts of oxidized LDL (mainly the MM-LDL) are found in normal plasma and increased significantly in coronary heart disease (Tsimikas, S., 2006). Many new compounds in oxLDL are generated during LDL oxidation and contribute to

some biological effects of oxLDL. These compounds include phospholipid products such as LPA and sn-2 short chain PCs (oxPC), sphingolipid products, and free fatty acid products.

Most previous studies have demonstrated that oxidized LDL can increase platelet activation. OxLDL-stimulated platelet activation induces vascular inflammation and atherosclerosis (Daub et al., 2010). OxLDL-induced platelet activation and shape change require CD36 and work through tyrosine kinase and Rho kinase-signaling pathways (Wraith et al., 2013). The LPA-independent platelet activation by oxLDL is mediated through CD36 and scavenger receptor-A (Korporaal et al., 2007). The mechanism by which oxLDL promotes platelet activation is through inhibition of the cGMP/PKG signaling pathway (Magwenzi et al., 2015). However, some reports also have shown that oxLDL preparation affects their platelet-activating properties. Between 0% and 15% oxidation, LDL sensitizes the thrombin receptor-activating peptide (TRAP)-induced platelet aggregation. When oxidation is greater than 15%, oxLDL inhibits TRAP-induced platelet aggregation and secretion (Korporaal et al., 2005). Native LDL and fully oxidized LDL inhibit ADP-induced platelet aggregation, but minimally modified LDL induces primary platelet aggregation and elevates ADP-induced platelet aggregation (Naseem et al., 1997).

Oxidized phosphatidylcholines (oxPCs) are generated in the oxidation of LDL by multiple distinct pathways (Podrez et al., 2002a) and in atherosclerotic lesions (Podrez et al., 2002b). Four oxPC species derived from oxidized 1-palmitoyl-2- arachidonyl-PC (PAPC) and four species derived from oxidized 1-palmitoyl-2-linoleoyl-PC (PLPC) were identified and their structures were confirmed by multinuclear NMR and high resolution mass spectrometry (Podrez et al.,

2002a) (Figure 1-3). All of these oxPCs serve as high affinity ligands for CD36 receptor (Podrez et al., 2002a; Podrez et al., 2002b) and the ligand-binding properties of oxLDL for CD36 can be attributed significantly to the oxPC (Hazen, S. L., 2008).

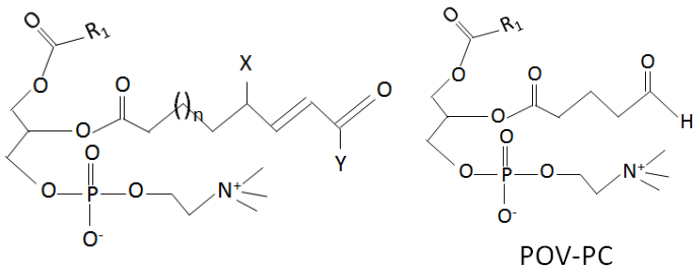

PAPC, n=1		PLPC, n=5	
HOdiA-PC	X=OH, Y=OH	HDdiA-PC	X=OH, Y=OH
KOdiA-PC	X=O, Y=OH	KDdiA-PC	X=O, Y=OH
HOOA-PC	X=OH, Y=H	HODA-PC	X=OH, Y=H
KOOA-PC	X=O, Y=H	KODA-PC	X=O, Y=H

Figure 1-3. The core structural motif of oxdized phospholipids and chemical structure of POV-PC.
$R_1 = (CH_2)_{14}CH_3$

OxPCs can activate platelets and induce monocyte differentiation. Therefore, they can be used as biomarker for atherosclerosis (Ashraf et al., 2008). The Src-family kinase (SFK)-spleen tyrosine kinase (SYK)-phospholipase Cγ2 (PLCγ2) pathway is downstream of CD36 receptor and important for oxPC-induced platelet activation (Zimman et al., 2014). OxPCs activate platelets through inhibition of the cGMP/PKG signaling pathway (Magwenzi et al., 2015). Some of the oxPCs also display anti-inflammatory activities. KOdiA-PC and POV-PC can inhibit TLR-2 and TLR-4 binding of LPS (Walton et al., 2003). Previous researches have demonstrated that oxPCs affect platelet function through binding to the CD36 receptor. However, the mechanism of how oxPCs act on platelets is not characterized.

1.1.2 Monocytes in atherosclerosis

Monocytes are large mononuclear white blood cells with bean-shaped or kidney-shaped nuclei. They are derived from monoblasts in the bone marrow and account for 3% to 8% of peripheral blood leukocytes (Ghattas et al., 2013). Normally, monocytes circulate in the bloodstream for a few days and then migrate to tissues where they differentiate into macrophages and dendritic cells.

The main function of monocytes in the immune system is counteracting exogenous bacterial and viral infections by phagocytosis and antibody-dependent cell-mediated cytotoxicity. However, monocytes are also involved in inflammation and contribute to atherosclerotic plaque formation (Yang et al., 2014). As pro-inflammatory cells, monocytes produce a broad panel of cytokines, chemokines, and reactive oxidative species that promote LDL oxidation and endothelial cell activation. Activated endothelial cells interact with monocytes by releasing monocyte chemoattractant protein-1 (MCP-1). Moreover, MCP-1 also induces diapedesis of monocytes from the blood to the subendothelial tissue, where they differentiate into macrophages, engulf the oxLDL, and become foam cells. Various chemokines such as CXCL1, CCL5, CXCL4, CXCL12 and their monocyte receptors CXCR2, CCR5, CXCR4 are also involved in monocyte-endothelium interactions (Pamukcu et al., 2010).

To remove activated platelets from circulation, circulating monocytes can interact with platelets to form monocyte-platelet aggregates (MPAs) (Shantsila et al., 2009). However, MPAs activate expression of receptors on monocytes to adhesion molecules (Simon et al., 1993). The upregulation of monocyte receptors to adhesive molecules is closely associated with monocyte

transmigration and atherosclerotic plaque formation. Therefore, MPAs play an important role in atherosclerosis development.

1.1.2.1 Lysophosphatidic acid (LPA) and monocytes

Lysophosphatidic acid is produced by a variety of activated cells, especially platelets (Aoki et al., 2002), and acts as a mediator associated with multiple cellular effects such as platelet aggregation and smooth muscle cell proliferation. Moreover, LPA increases endothelium-monocyte interaction by elevating E-selectin and vascular cell adhesion molecule-1 (VCAM-1) cell surface expression (Rizza et al., 1999). LPA treated endothelial cells enhance monocyte recruitment and migration through upregulating Interleukin-8 (IL-8) and monocyte chemoattractant protein-1 (MCP-1) expression (Lin et al., 2006; Gustin et al., 2008). LPA not only promotes monocyte adhesion and migration but also affects monocyte differentiation (Lee et al., 2002). LPA activates human monocyte-derived dendritic cells (Chen et al., 2006; Martino et al., 2006) and induces macrophage formation through the AKT/mTOR pathway (Ray et al., 2017).

LPA-induced platelet-monocyte aggregate formation is P-selectin-mediated and insensitive to aspirin inhibition. Unlike LPA-induced platelet aggregation, MPA formation stimulated by LPA is blood donor independent (Haserück et al., 2004).

1.1.2.2 LPA platelet releasate and monocytes

Upon stimulation, activated platelets release the soluble content of granules and microparticles, which is known as the releasate. The platelet releasate consists of a large number of bioactive

proteins, multiple cytokines and chemokines, which induce monocyte migration (McClelland et al., 2010) and differentiation (Gleissner et al., 2010). Platelet releasate also can increase reactive oxygen species (ROS) production in both human monocytic cell line (THP-1 cells) and primary monocytes (Li et al., 2016). Releasate from thrombin-activated platelets enhances the expression of CXCR5 (Halvorsen et al., 2014) and CXCL13 (Smedbakken et al., 2012) in monocytes and CXCL-13-CXCR5 interaction modulates atherogenesis and plaque destabilization.

1.2 Signal transduction and protein-protein interaction

Signal transduction (cell signaling) is the process by which molecular signals are transmitted from the outside of a cell to its inside resulting in the cell's function change (Cary et al., 2000). Most of the cell signals are chemical molecules including growth factors, hormones, neurotransmitters, and extracellular matrix components (Jose et al., 1990). Once the cell-surface receptors receive a signal, the receptors undergo a shape change and initiate a series of biochemical changes within the cell, which is called intracellular signal transduction cascades. Most components of signal transduction are proteins and protein phosphorylation is the most common biochemical change in cell signaling (Roach et al., 1991). Protein kinase A (PKA) and Protein kinase C (PKC) (Nishizuka, Y., 1984; Takasago et al., 1991), two enzymes, phosphorylate protein substrates by adding phosphate groups to protein molecules. Phosphate groups are typically attached to the amino acids serine, threonine, and tyrosine in proteins for phosphorylation (Ben-David et al., 1991). Phosphorylation works as a switch to control the activity of many enzymes in signal transduction. Although proteins are critical in cell signaling, several small molecules also participate as second messengers. Such second messengers include

Ca^{2+} ions, cyclic AMP (cAMP), cyclic GMP (cGMP), nitric oxide, diacylglycerol (DAG), and lipids (Mahajan et al., 2005).

Proteins are involved in all cell functions and most of them interact with others to facilitate their biological activity. Various protein-protein interactions play fundamental roles in the process of signal transduction (Simons et al., 2000). The interactions between binding domains and their recognition motifs control the routes for signal transduction pathways. The signaling cascades that are mediated by heterotrimeric G-proteins reveal the importance of protein-protein interactions (Neer, E. J., 1995). After specific ligands bind to a membrane G-protein-coupled receptor (GPCR), the GPCR activates and then transmits the signal into the cell through activation of the bound G proteins. G proteins have three subunits (α, β, γ). The activated receptors promote the exchange of bound GDP for GTP on the α subunit of G proteins, resulting in the dissociation of the α subunit (G_α) from the β and γ subunits ($G_{\beta\gamma}$). The G_α continually activates different downstream effectors such as calcium ions, adenylyl cyclase, Phospholipase C (PLC), and protein kinases. The $G_{\beta\gamma}$ dimer activates the muscarinic K^+ channel, PLC-β, and beta-adrenergic receptor kinase. Then, these effectors initiate distinct intracellular signaling responses. The signal can be terminated by the hydrolysis of α subunit-bound GTP to GDP, which causes the re-association of the α and βγ subunits (Tuteja, N., 2009).

1.2.1 Small GTPase-effector binding protein interaction leads to signal cascades

Small guanosine triphosphatases (GTPases), having molecular weights of 21 to 30 kDa, are a family of monomeric guanine nucleotide binding proteins and homologous to the alpha subunit of heterotrimeric G-proteins (Yang, Z., 2002). They are encoded by human *ras* genes thereby

sometimes called Ras superfamily GTPases. Small GTP binding proteins of the Ras superfamily regulate major cellular processes such as signal transduction, cell adhesion, migration, differentiation, proliferation, vesicle transport and cytoskeleton reorganization (Delprato, A., 2012). This superfamily consists the Ras/Ral/Rap, Rho, Rab, Ran, and Arf/Sar subfamilies. All small GTPases have four guanine nucleotide binding domains and an effector binding domain (Takai et al., 2001).

Upstream factors regulate small GTPases, which in turn activate downstream targets. Once stimulated by upstream signals, guanine nucleotide exchange factors (GEFs) alternate small GTPases from the GDP-bound inactive form to the GTP-bound active form by dissociating the tightly bound GDP and binding GTP. Then, the GTP-bound active form switches on downstream pathways by binding to effector proteins. Each small GTPase affects numerous downstream effector proteins to engage specific signaling cascades, all of which carry out critical cellular functions. GTP hydrolysis is very slow. Therefore, GTPase-activating proteins (GAPs) are needed for efficient deactivation (Figure 1-4). Small GTPases that have a farnesyl or geranylgeranyl group in their C-terminus, cycle between membrane-bound and cytosolic forms thereby requiring the regulation of guanine nucleotide dissociation inhibitors (GDIs) (Cherfils et al., 2013).

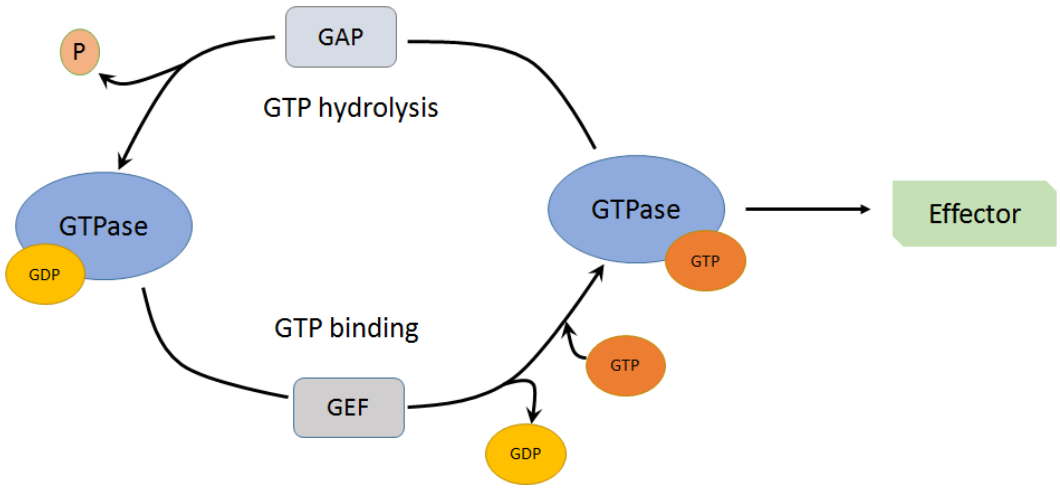

Figure 1-4. **The mechanism of the small GTPase switch.**
GDP-bound small GTPase is activated by GEF through catalyzing the exchange of GDP for GTP. GAP inactivates small GTPase by GTP hydrolysis.

1.2.2 Signal amplification by binding of cAMP/cGMP to PKA/PKG

Many life processes are achieved via signaling through a cAMP/cGMP-dependent pathway, and many cell responses are mediated by cAMP/cGMP, such as the regulation of glycogen metabolism and the inhibition of platelet functions. Epinephrine signals the breakdown of glycogen by increasing the intracellular concentration of cAMP (Rall et al., 1958). Endothelial prostacyclin (PGI_2) and nitric oxide (NO) inhibit platelet activation by elevating the cAMP and cGMP, respectively (Moncada et al., 1976; Mellion et al., 1981).

Levels of cytosolic cAMP are controlled by adenylyl cyclase (AC) and phosphodiesterase (PDE). AC is activated by G-protein-coupled receptor signaling. Binding of epinephrine (or PGI_2) to its membrane receptor triggers the activation of the G_s alpha subunit. Activated G_s binds to AC, which in turn stimulates the synthesis of cAMP from ATP. The effect of cAMP is mediated by PKA. The inactive form of PKA is a tetramer composed of two catalytic and two regulatory subunits. Binding of cAMP to the regulatory subunits results in their dissociation from

the catalytic subunits. The free catalytic subunits activate and phosphorylate their downstream proteins (Figure 1-5).

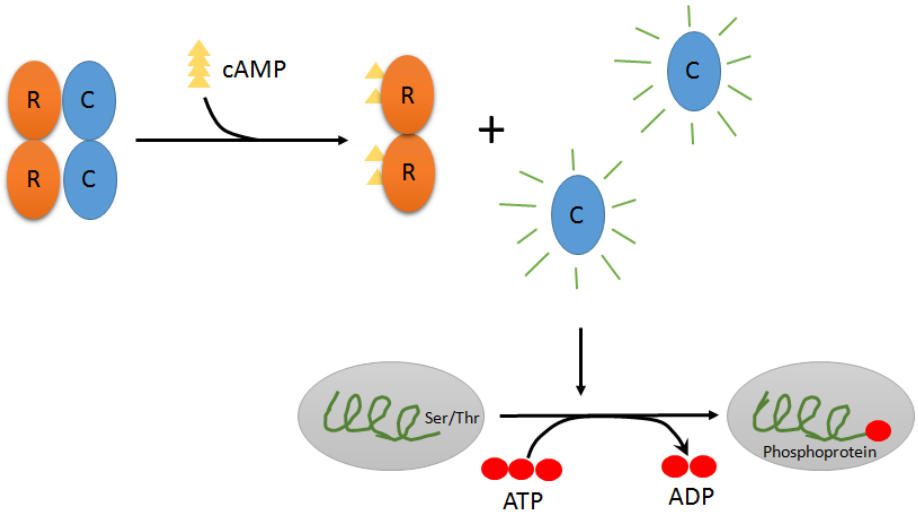

Figure 1-5. **The mechanism of the PKA activation.**
Binding of cAMP to the regulatory subunits dissociates and activates the catalytic subunits, which phosphorylate their target proteins.

In the regulation of glycogen metabolism, PKA phosphorylates phosphorylase kinase, which in turn phosphorylates and activates glycogen phosphorylase. The enzyme glycogen phosphorylase catalyzes the breakdown of glycogen. In parallel, PKA phosphorylates and inactivates glycogen synthase, which catalyzes glycogen synthesis (Roach, P. J., 2002). The signaling pathway of glycogen metabolism demonstrates the signal amplification during intracellular signal transduction. Each epinephrine receptor can activate many G_s molecules. Each G_s molecule activates AC, which can catalyze the synthesis of many cAMP molecules. Once activated by cAMP, each PKA molecule can phosphorylate a large number of phosphorylase kinase molecules, which successively phosphorylate numerous glycogen phosphorylase molecules.

In the inhibition of platelet activation, NO permeates the plasma membrane of platelets and activates cytosolic soluble guanylyl cyclase (sGC) to produce cGMP (Rukoyatkina et al., 2011; Dangel et al., 2010; Zhang et al., 2011). Cyclic GMP stimulates cGMP-dependent protein kinase (PKG) to phosphorylate target proteins. PKA and PKG substrate proteins can be catalogued to two groups, signaling regulators and actin-binding proteins. Signaling regulators include Rap1B, Rap1GAP2, inositol 1,4,5-trisphosphate receptor (IP_3-R), IP_3-R-associated cGMP kinase substrate (IRAG), PDE5A, PDE3A, and Glycoprotein Ibβ (GPIbβ). Actin-binding proteins include vasodilator-stimulated phosphoprotein (VASP), Lim and SH3 domain protein (LASP), and Heat shock protein 27 (HSP27) (Smolenski, A., 2012). Phosphorylation of PKA and PKG substrates results in the inhibition of platelet activation, adhesion, granule release, and aggregation.

1.3 Proteomics

Proteomics is the large-scale study of all proteins in cells or tissues to illustrate protein expression and changes under the influence of biological perturbations such as disease or drug treatment (Anderson et al., 1998). Proteomics generally refers to mass spectrometry (MS)-based proteomics because proteome analysis heavily relies on mass spectrometry (Altelaar et al., 2013). Powerful mass-spectrometry-based technologies make the identification and quantification of nearly all expressed proteins practicable in a single experiment (Altelaar et al., 2013). Furthermore, multiple protein properties, including protein-protein interactions, post-translational modifications (PTMs), and protein turnover rates, can be measured by mass spectrometry-based proteomic approaches (Larance et al., 2015; Boisvert et al., 2012).

Typically, MS-based proteomics experiments include three steps: sample preparation, sample ionization, and mass analysis. In the first step, proteins are isolated from lysed cells or tissues, separated on one-dimensional/two-dimensional polyacrylamide gel electrophoresis (1-D/2-D-PAGE), and then digested into peptides by proteases. Subsequently, the extracted peptides are introduced to an ion source for ionization. Two common methods for this are electrospray ionization (ESI) (Fenn et al., 1989) and matrix-assisted laser desorption/ionization (MALDI) (Karas et al., 1988). In ESI, a liquid sample is converted to a fine mist of charged droplets by the potential difference between the capillary and the inlet of the mass spectrometer. The development of nanospray improved ESI by reducing the amount of sample consumed and increasing the time available for analysis (Shevchenko et al., 1996; Shevchenko et al., 1997). In MALDI, the sample is mixed with matrix molecules and irradiated by a pulsed laser, which promotes the ionization. MALDI outcompetes ESI by directly using samples without purification after protease digestion (Qin et al., 1997). After ionization, masses are separated by mass analyzers based on their mass-to-charge ratios. Four types of mass analyzers that are normally used in a mass spectrometry are quadrupole, time of flight, ion trap, and ion cyclotron resonance. Finally, the relative abundance of each ion type is recorded by a detector.

Top-down proteomics, focusing on study of intact proteins, has the advantage of measuring diverse modifications and identifying proteoforms (Tran et al., 2011; Smith et al., 2013). However, bottom-up proteomics, focusing on the study of peptides derived from enzymatic digestion of intact proteins, is more manageable experimentally and computationally and has been widely used (Aebersold et al., 2016). In a bottom-up proteomics experiment, peptides are fractionated and analyzed by liquid chromatography tandem-mass spectrometry (LC-MS-MS). A

tandem mass spectrometer has two stages of mass spectrometry, MS1 and MS2. After ionized molecules are separated in MS1, precursor ions are selected and fragmented by collision-induced dissociation (CID), electron capture dissociation (ECD), or electron transfer dissociation (ETD). The resulting product ions are then separated in MS2 for detection (Figure 1-6).

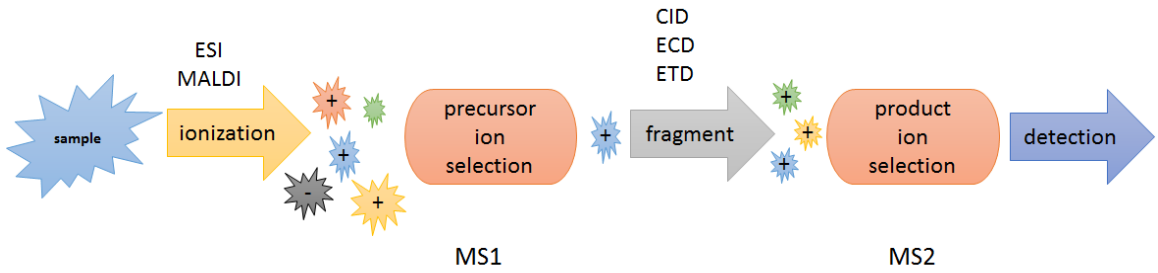

Figure 1-6. **Principle of tandem mass spectrometry (MS/MS).**

There are several types of tandem mass spectrometers, including triple quadrupole (QqQ), quadrupole time-of-flight (QqTOF), quadrupole-linear ion trap (QLIT), and time-of-flight-time-of-flight (TOF/TOF) instruments. Triple quadrupole and Quadrupole time-of-flight are popular techniques. A triple quadrupole instrument consists of two quadrupole mass analyzers (Q1 and Q3) and a radio frequency collision quadrupole (q). Both mass analyzers are controlled by direct current and radiofrequency potentials, and can either be set to a fixed or to scan a range of m/z values, while the collision cell is only controlled by radio-frequency potential which allows all selected ions to pass through the collision quadrupole. A triple quadrupole instrument can perform qualitative and quantitative analyses, and allows for increased sensitivity and specificity yielding a lower resolution. It is particularly suitable for targeted compound analysis, when both mass analyzers are set to fixed m/z values. In quadrupole time-of-flight instruments, the third quadrupole of a triple quadrupole is replaced by a TOF mass spectrometer. As this overcomes

the inherent sensitivity of a scanning quadrupole due to the higher duty cycle of a TOF analyzer, the advantages of quadrupole time-of-flight are high sensitivity, mass resolution and mass accuracy. QqTOF are particularly useful for the analysis of unknown compounds such as protein-derived peptide mixtures, and are used for e.g. proteomic discovery.

1.3.1 Functional proteomics

Proteins are involved in all cellular processes and regulatory mechanisms. Most of them work together like molecular machines to carry out cellular functions (Alberts, B., 1998). Functional proteomics is the study of protein-protein interactions to identify unknown proteins and clarify their functions in cellular mechanisms (Monti et al., 2007). There are some functional proteomic techniques for detection of protein-protein interactions, such as tandem affinity purification, yeast two hybrid, and domain-pairs-based sequence approach (Rao et al., 2014). Tandem affinity purification is based on affinity purification procedures (Puig et al., 2001). Yeast two hybrid is based on genetic readout systems (Chien et al., 1991). Domain-pairs-based sequence approach is based on computational prediction methods (Singhal et al., 2007).

The process of signal transduction relies on various protein-protein interactions. Therefore, functional proteomics is widely used to analyze the global changes of signaling pathways and identify the signaling components (Graves et al., 2003; Yan, et al., 2008; Lewis et al., 2000). Purification of protein complexes followed by mass spectrometry-analysis can fulfill the goal of functional proteomics, which is to identify all molecular machines and to characterize their function, their response to external stimuli and their interconnectivities (Kocher et al., 2007).

1.3.2 Purification and identification of interacting proteins by mass spectrometry-based functional proteomics

To identify interacting proteins, endogenous protein complexes need to be isolated from cell lysate by using affinity purification-based techniques. In the affinity-based procedure, the bait protein with a suitable tag is utilized to fish protein of interest, which is the other proteins in the same protein complexes. Multiple protein complexes can be isolated by several anti-tag systems, which include His tags, glutathione S-transferase (GST) tags, Flag tags, biotin, and calmodulin-binding peptide (Monti et al., 2005). Methods for purifying endogenous protein complexes also include immunochemical (antibody/antigen) approach, biochemical purification (enzyme/substrate) approach, and other affinity chromatography (receptor/ligand).

After purification, protein mixtures are separated by one-dimensional sodium dodecyl sulfate-polyacrylamide gel electrophoresis (SDS-PAGE) to remove unwanted contaminants such as bait proteins and detergents. Protein bands of interest are excised and in-gel digested by proteases such as trypsin to produce peptides for mass spectrometry analysis (Shevchenko et al., 2006). Another protein digestion method is in-solution digestion. If the bait proteins are not eluted with protein of interest, purified proteins can be directly digested in solution and analyzed by LC-MS-MS (Link et al., 1999).

1.3.2.1 Effector binding proteins as bait to isolate active small GTPases

Small GTPases act as molecular switches to control diverse cellular processes and the GTP-bound active form switches on downstream pathways by binding to effector proteins. Therefore, the active small GTPase purification method is based on the affinity of downstream effector

proteins for the active form of GTPases. The specific protein-binding domain (PBD) of downstream effectors is expressed as a GST-fusion protein, which can be immobilized onto agarose beads. The PBD-bound agarose beads are incubated with cell lysate to pull down corresponding active small GTPases. Active small GTPases form non-covalent interactions with the immobilized PBD, whereas the unbound proteins will be washed away. Then, active small GTPases retained on the agarose beads are eluted with protein-binding domain and subjected to SDS-PAGE. After in-gel trypsin digestion, resulting peptides are analyzed by LC-MS/MS for protein identification (Figure 1-7).

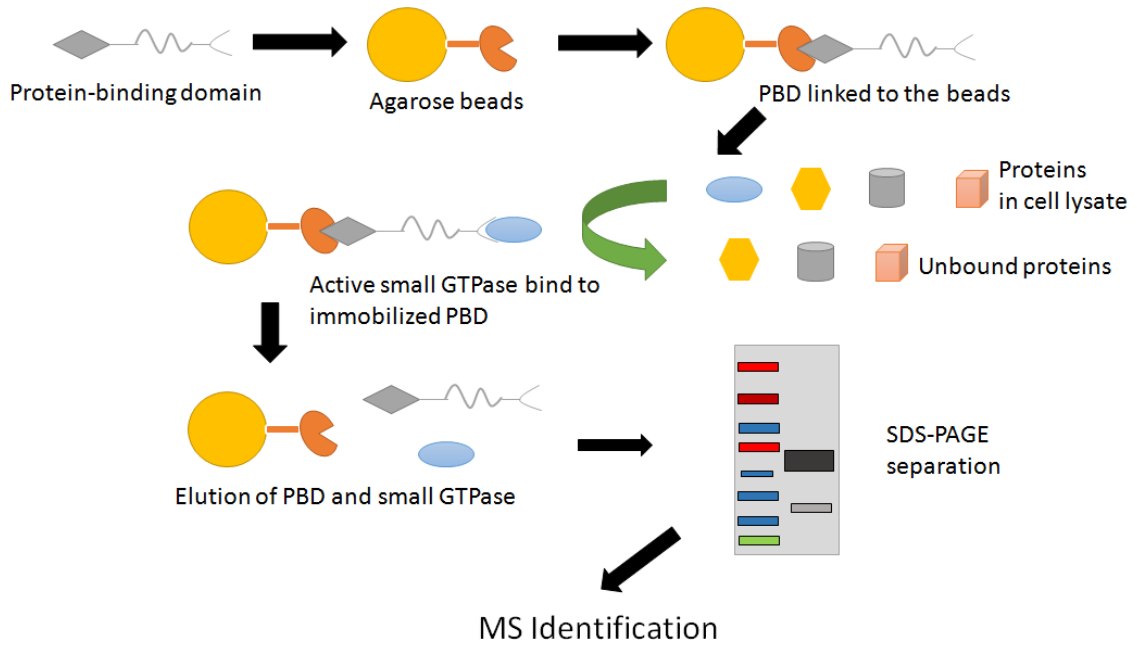

Figure 1-7 The precipitation of active small GTPases by protein-binding domian of downstream effectors.

1.3.2.2 Cyclic AMP and cyclic GMP to precipitate protein partners

Both cAMP-dependent protein kinase (PKA) and cGMP-dependent protein kinase (PKG) play key roles in cellular processes by phosphorylating a number of biologically important proteins.

The activation of PKA and PKG depends on their binding of cAMP and cGMP, respectively. Therefore, the cAMP/cGMP interactome purification method is based on the affinity of cyclic nucleotides for PKA and PKG. Cyclic AMP and cyclic GMP can be immobilized on agarose beads to pull down PKA, PKG, and their binding proteins in cell lysate. After washing away nonspecific binding proteins, proteins retained on the cAMP/cGMP beads are eluted and in-solution digested. The digested peptides are analyzed by LC-MS/MS for protein identification. For quantification, they are often also stable isotope labeled prior to LC-MS/MS analysis.

1.3.3 Quantitative proteomics

Quantification of protein changes in response to different environments is the most important part of proteomics. The ability of quantifying thousands of peptides in a single experiment has made mass spectrometry-based quantitative proteomics increasingly popular in the last decade. The main three quantitative methods include label-free quantification such as label-free selected reaction monitoring (SRM) (Wong et al., 2010; Martínez-Aguilar et al., 2013), *in vivo* metabolic stable-isotope labelling such as stable isotope labelling by amino acids in cell culture (SILAC) (Ong et al., 2002), and *in vitro* stable-isotope labelling using chemical tags such as dimethyl-labelling (Boersema et al., 2009). In label-free quantitative proteomics, protein quantification is based on the measurements of ion intensity changes and the spectral counting of identified proteins. In stable-isotope labelling method, the protein abundance in differentially labeled samples is reflected by the peak intensities of the corresponding isotope-labeled peptides.

1.3.3.1 Stable isotope dimethyl labeling

Stable isotope dimethyl labeling as a quantitative strategy was reported by Hsu et al in 2003 (Hsu et al., 2003). This method is very straightforward. After protein samples are digested, the resulting peptides of the different samples are labeled with isotopomeric dimethyl labels. Then, the labeled samples are mixed and analyzed by LC-MS/MS.

In the dimethyl labeling, formaldehyde reacts with the N-terminus or lysine residue side chain of a peptide to form a Schiff base, which is then reduced by cyanoborohydride to form a secondary amine. Subsequently, the secondary amine immediately reacts with another formaldehyde molecule to form a dimethylamino group (Figure 1-8A). All primary amines in the sample can be dimethylated except for N-terminal prolines, which are monomethylated by the reaction. Three differential stable isotopes can be used for labelling and the differentially labeled peptide triplets have mass differences of 4 Da from each other (Figure 1-8B). Dimethyl labelling is an efficient and inexpensive approach for relative quantification and can precisely quantify all sample types including cell line, primary cells and tissues (Boersema et al., 2008; Margarucci et al., 2011).

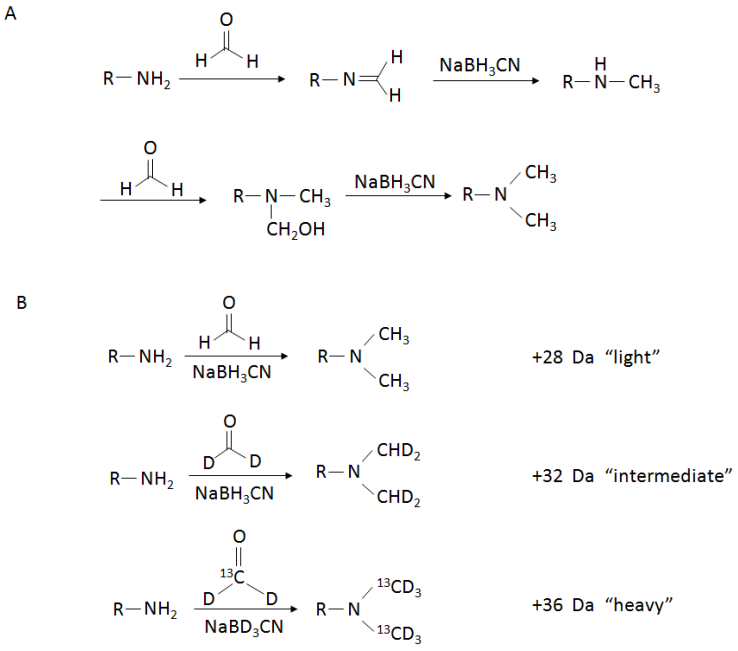

Figure 1-8 The mechanism of stable isotope dimethyl labeling.

(A) Dimethylation of primary amines by using formaldehyde and cyanoborohydride. (B) Labeling schemes for differential isotope dimethyl labeling.

As an illustration of the result, Boersema et al. have relied on the exemplary mass spectrum of the dimethyl-labeled BSA peptide YICDNQDTISSK to demonstrate the LC-MS outcome of triplex stable isotope dimethyl labeling at equal ratios (Figure 1-9) (Boersema et al., 2009).

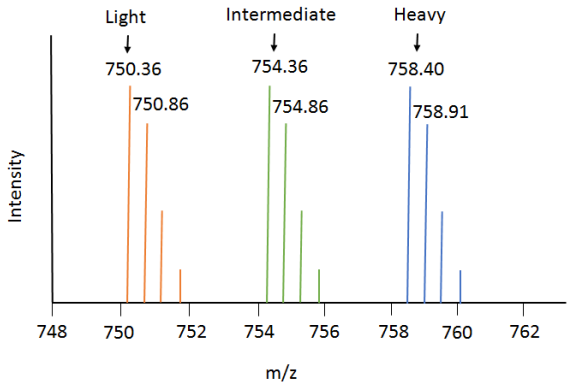

Figure 1-9 Mass spectra of the BSA peptide YICDNQDTISSK.

Digested peptides are dimethyl labeled in 1:1:1 light/intermediate/heavy ratio.

1.3.3.2 Multiple reaction monitoring

Selected/multiple reaction monitoring (SRM/MRM) is an emerging method for targeted quantitative proteomics. It is capable of sensitive detection and quantification of predetermined proteins/peptides by utilizing triple quadrupole (QQQ) mass spectrometers. In an MRM experiment, the first and third quadrupoles work as mass filters to selectively monitor a predefined peptide ion (precursor ion) and several fragment ions (product ions), which are generated from the precursor ion in the second quadrupole by collisional dissociation (Yost et al., 1978; Kondrat et al., 1978). A precursor/product ion pair is called a transition. Several transitions are detected over time resulting in a set of chromatographic traces with retention time and signal intensity as coordinates. The label-free relative quantification of MRM is based on the signal intensities of specific transitions. The peak areas for MRM transitions accurately reflect peptide abundance and can be used as the measurement for quantitative comparisons.

Comparing to normal label-free quantification, an MRM assay is more complex because of the selection of unique proteotypic peptides. However, MRM can specifically, sensitively, and speedily quantify targeted proteins. Furthermore, an MRM assay can be employed for absolute quantification by spiking isotopically labelled proteotypic peptides (Gerber et al., 2003).

1.4 Aims

Both platelets and monocytes play crucial roles in atherosclerosis. Monocytes directly participate in the formation of atherosclerotic lesion and activated platelets promote monocyte adhesion, transmigration and differentiation, which facilitate the development of the atherosclerotic plaque.

Activated platelets affect monocytes by forming platelet-monocyte aggregates or by releasing soluble factors, which is called platelet releasate. Some chemokines in platelet releasate contribute to monocyte activation. Multiple small GTPases are also associated with the migration and differentiation of monocytes. Therefore, the first aim of this study was to test the hypothesis that platelet releasate can stimulate monocyte migration through small GTPase signaling pathway. Here, a previously developed MRM-based quantitative assay was optimized and used to monitor the activity changes of multiple small GTPases in monocytes with platelet releasate stimulation.

Upon plaque rupture, some oxLDL derivatives such as LPA and oxPC are released to the blood and affect platelet activity. Numerous reports have proved that LPA is platelet agonist. However, the effect of oxPC on platelets is still arguable. A recent report exhibits that oxLDL/oxPC activates platelets by inhibition of cGMP pathway. Hence, my second aim was to study the response of the cAMP/cGMP binding proteins in platelets with oxPC stimulation. To fulfill this goal, a targeted quantitative chemical proteomics approach was developed and applied to quantify the cAMP/cGMP interactome in resting and oxPC treated platelets.

Chapter 2: Methods

2.1 THP-1 cell culture and LPA stimulation

Human monocytic cell line THP-1 cells (American Type Culture Collection, MD, USA) were cultured in RPMI 1640 medium (Gibco, Life Technologies, Canada) supplemented with 10% FBS and 1% penicillin/streptomycin in 5% CO_2 at 37°C to give a final concentration of approximately 5×10^5 cells/ml.

THP-1 cells were cultured at 1×10^7/mL in phosphate-buffered saline (PBS) before lysophosphatidic acid (LPA) stimulation. To stimulate THP-1 cells, 25 μM LPA was added to 1mL of THP-1 cells at 1×10^7/mL and incubated for 2 or 10 minutes at 37°C. Stimulated THP-1 cells were immediately lysed by adding 2X lysis buffer (2% NP-40, 100 mM Tris·HCl, pH 7.4, 400mM NaCl, 5mM $MgCl_2$, 20% glycerol, with protease inhibitor cocktail (1 tablet / 50 mL, Roche, USA)). Lysate prepared from non-treated THP-1 cells served as negative control, corresponding to cells treated the same way but in the absence of LPA. As positive control, lysate prepared from non-treated THP-1 cells was incubated with 0.1 mM GTPγs for 15 minutes at 30°C and then used.

2.2 Platelet isolation and stimulation

Ethical approval for platelet and monocyte isolation was granted by the University of British Columbia Research Ethics Board (certificate number H12-00757), and a consent form was signed by each blood donor. 50 ml whole blood was drawn into vacutainer blood collection tubes containing ACD (Acid Citrate Dextrose). Platelet-rich plasma (PRP) was separated from red

blood cells by centrifugation at 150 x g (rcf) for 15 minutes at room temperature (all other isolation steps were also performed at room temperature). After adding a half volume of ACD, isolated PRP was centrifuged at 720 x g for 10 minutes. The platelet pellet was re-suspended by using 2ml of CGSA buffer (10 mM trisodium citrate, 30 mM dextrose and 1 unit/ml apyrase) and centrifuged at 720 x g for 10 minutes. The platelet wash step was repeated and platelets were re-suspended in 2 ml of HEPES buffer (10 mM HEPES, 137 mM NaCl, 2.9 mM KCl, 12 mM $NaHCO_3$, pH 7.4). Platelets were counted by employing a hemocytometer and diluted to physiological concentration (300×10^9/L) using HEPES buffer with 1.8mM $CaCl_2$. Platelets were rested at room temperature for 30 minutes before stimulation.

Washed platelets were divided into three equal portions. To induce the "stimulated" condition, platelets were incubated with 5 μM KDdiA-PC or POV-PC for 15 minutes at 37°C. For inhibitor studies, platelets were treated with 10 μM ODQ for 15 minutes, which was followed by 5 μM POV-PC incubation for 15 minutes at 37°C.

2.3 Platelet lysis

After stimulation, platelets were pelleted by centrifugation at 720 x g and lysed by 1.5 mL of lysis buffer (50 mM KH_2PO_4/K_2HPO_4 buffer, pH 7.0, 150 mM NaCl, and 0.1% Tween 20, with protease inhibitor cocktail (1 tablet / 50 mL, Roche, USA)). Dounce homogenization was used to completely lyse platelets. Lysate was centrifuged at 10000 rpm for 10 minutes at 4°C and supernatant was carefully collected. The pellet was re-suspended in 500 μL lysis buffer. By repeat centrifugation (10000 rpm, 10 minutes, 4°C), the second supernatant was collected and added to the previous one. The protein concentration of supernatant was determined using a

BCA (bicinchoninic acid) protein assay. The resting and stimulated platelet samples were treated identically and in parallel.

2.4 Platelet releasate preparation and inhibitor treatment

Washed platelets at a physiological concentration (300×10^9/L) in PBS with 1.8 mM $CaCl_2$ were stimulated with 50 μM LPA (alkyl-LPA 16:0, Avanti Polar Lipids, AL, USA) for 10 minutes at 37°C. Platelet releasate (supernatant) was separated from platelets by centrifuging twice at 750 x g for 10 minutes at 4°C, and then collected in a fresh tube.

For inhibitor treatment, platelet releasate was incubated with 10 μg/mL anti-human CXCL12/SDF-1 antibody (R&D systems, MN, USA) for 30 minutes at room temperature.

2.5 Monocyte isolation and stimulation

Peripheral blood mononuclear cells (PBMC) were isolated through differential gradient centrifugation (2000 rpm, 20 minutes) in Ficoll gradient (GE Healthcare, BC, Canada). After three HBSS (GIBCO® Hank's Balanced Salt Solution, Life Technologies, Canada) washes (one time 1500 rpm for 10 mins, twice 800 rpm for 10 mins), PBMCs were re-suspended in RoboSep® buffer (StemCell Technologies, BC, Canada) at a concentration of 50×10^6/mL. Peripheral Blood monocytes were separated from PBMCs by negative selection using the EasySep™ Human Monocyte Enrichment Kit without CD16 depletion (StemCell Technologies, BC, Canada). Isolated monocytes were re-suspended at a concentration of 1×10^7/mL and separated into four fractions before LPA or platelet releasate stimulation.

To stimulate monocytes, 25 μM LPA or equal volume of platelet releasate was added and monocytes were incubated for 2 or 10 minutes at 37°C. Stimulated monocytes were immediately lysed by adding 2X lysis buffer (2% NP-40, 100 mM Tris·HCl, pH 7.4, 400mM NaCl, 5mM $MgCl_2$, 20% glycerol, with protease inhibitor cocktail (1 tablet / 50 mL, Roche, USA)). For the positive control preparation, lysate from resting monocytes was incubated with 0.1 mM GTPγs for 15 minutes at 30°C.

2.6 Effector binding domain expression

Four binding domain plasmids, Addgene plasmid 13338, Addgene plasmid 15247, Addgene plasmid 12217, and a special plasmid obtained from Dr. Michael Gold's lab, were transformed into *Escherichia coli* to express effector binding domains, GST-Raf1-RBD, GST-Rhotekin-RBD, GST-PAK1-PBD, and GST-RalGDS-RBD, respectively.

To express the effector binding domains, bacteria containing binding domain plasmids were inoculated in 100 mL Lysogeny broth (LB) with 100 μg/mL ampicillin (Sigma, USA) and incubated overnight at 37°C with shaking. The 100 mL bacteria culture was transferred into 1L LB with 100 μg/mL ampicillin for further incubation at 37°C with shaking until the bacteria concentration reached 0.8 OD600. For GST-RalGDS-RBD and GST-PAK1-PBD expression, 0.1 mM IPTG (Invitrogen life technologies, USA) was added and incubated overnight at 26°C with shaking. For GST-Raf1-RBD expression, 0.1 mM IPTG was added and incubated for 4 hours at 26°C with shaking. For GST-Rhotekin-RBD expression, 0.5 mM IPTG was added and incubated for 2 hours at 37°C with shaking. After IPTG-induced binding domain expression, bacteria were collected by centrifugation at 5000 rpm for 10 minutes at 4°C and lysed by using 10 mL lysis

buffer (1% NP-40, 50 mM Tris·HCl, pH 7.4, 150 mM NaCl, 1 mg/mL lysozyme, 1:10000 Benzonase, and protease inhibitor cocktail). Bacteria lysate was sonicated 6 times (15 seconds each) at 14 W on ice. Bacteria debris was removed by ultracentrifugation at 30000 rpm for 45 minutes at 4°C. Supernatant was collected, aliquoted, and stored at -80°C for late use. A purification step was required to retain GST-Rhotekin-RBD activity before storage. The supernatant obtained from GST-Rhotekin-RBD expression was incubated with glutathione resin (Thermo Fisher Scientific, USA) for 45 minutes at 4°C. Then the resin was washed three times with 1X lysis buffer (1% NP-40, 50 mM Tris·HCl, pH 7.4, 200 mM NaCl, 2.5 mM $MgCl_2$, 10% glycerol, with protease inhibitor cocktail (1 tablet / 50 mL, Roche, USA)), re-suspended in the same lysis buffer, and stored at -80°C in aliquots.

2.7 Active small GTPase precipitation

Around 20 μg (50 μL) of each binding domain was incubated with glutathione resin for 45 minutes at 4°C. This step was performed for GST-Rhotekin-RBD binding domain before storage. For coupling, equal amounts of resin were mixed with the four different binding domains and washed six times with 1X lysis buffer (1% NP-40, 50 mM Tris·HCl, pH 7.4, 200 mM NaCl, 2.5 mM $MgCl_2$, 10% glycerol, with protease inhibitor cocktail). The resin mixture was incubated with monocyte lysate for 45 minutes at 4°C by rotary shaking. The unbound fraction was removed and the resin was washed 3 times with 1 mL of 1X lysis buffer. After washing, the bound small GTPases and binding domains were eluted with 50 μL of 2X SDS sample buffer (25 mM Tris·HCl, pH 6.8, 2% glycerol, 4% SDS, and 0.05% bromophenol blue) and heated at 99°C for 5 minutes.

2.8 Pulldown assay

2.8.1 Elution of different nucleotide binding fractions from THP-1 lysate

1×10^7 THP-1 cells were harvested by centrifugation at 1500 rpm for 5 minutes and washed once in ice-cold PBS. Cells were re-suspended in ice-cold lysis buffer (50 mM KH_2PO_4/K_2HPO_4 buffer, pH 7.0, 150 mM NaCl, and 0.1% Tween 20, with protease inhibitor cocktail). After Dounce homogenization on ice, lysate was centrifuged at 16000 x g for 15 minutes at 4°C and supernatant was carefully collected. The protein concentration of supernatant was determined using a BCA protein assay and diluted to 2 mg/mL with lysis buffer. Prior to pulldown, the agarose cyclic nucleotide affinity beads, 2-AH-cGMP-Agarose beads (Biolog life science institute, Germany), were washed with lysis buffer. The volume of beads used in each pulldown was 10 μL /mg of protein. Diluted THP-1 lysate was incubated with pre-washed 2-AH-cGMP-Agarose beads for 2 hours at 4°C by rotary shaking. Then the beads were washed 6 times in lysis buffer. The washed beads were subsequently subjected to 50 μL of 10 mM ADP, 10 mM GDP, 5 mM cGMP, and 200 mM cAMP in lysis buffer for 10 minutes on ice for stepwise elution. Beads were washed with 1 mL of lysis buffer in between the different elution steps. After the final elution step, proteins bound on the beads were eluted with 50 μL of 2X SDS sample buffer and heated at 99°C for 5 minutes. Previously eluted ADP, GDP, cGMP, and cAMP samples were treated with 1/5 volume of 6X SDS sample buffer and also boiled at 99°C for 5 minutes. All eluted samples were subjected to 12% SDS-PAGE electrophoresis.

2.8.2 Elution of cAMP/cGMP binding proteins from platelet lysate

A beads mixture composed of two immobilized cyclic nucleotides, 2-AHA-cAMP and 2-AH-cGMP (Biolog life science institute, Germany) (1:1), was used to carry out this pulldown

experiment. Prior to pulldown, beads were washed with lysis buffer. Platelet lysate was diluted to a final concentration of 2 mg/mL and incubated with 10 mM ADP/GDP for 30 minutes at 4°C. The volume of beads used in each pulldown was 10 μL /mg of protein. The lysate-bead suspension was incubated for 2 hours at 4°C by rotary shaking. The unbound fraction was removed and the beads were washed 6 times in lysis buffer. The washed beads were subjected to 50 μL of 10 mM ADP/GDP in lysis buffer for 10 minutes to reduce non-specific binding. After another 4 time washing, the bound proteins were eluted with 50 μL of 2X SDS sample buffer or 50 μL of 8 M urea in 50 mM of ammonium bicarbonate buffer. Eluted sample in SDS sample buffer was boiled at 99°C for 5 minutes and subjected to 12% SDS-PAGE electrophoresis. Eluted samples in urea were subjected to in solution digestion.

2.9 Protein concentration determination

Protein concentration was determined using a BCA (bicinchoninic acid) protein assay. A bovine serum albumin (BSA) standard curve was prepared by serial dilution. The stock solution was 2 mg/mL BSA in water and the serial dilution was made up of 1.5, 1.0, 0.75, 0.5, 0.25, 0.125, 0.025, and 0 mg/mL. The sample was 5X and 10X diluted. Working reagent was prepared by mixing 50 parts of reagent A with 1 part of reagent B. 30 μL of either sample or BSA standard were added to wells of a 96-well plate in triplicate. 200 μL of working reagent were added to each well. The plate was allowed to stand for 30 minutes at 37°C and then read on a SpectraMax Plus384 plate reader (Molecular Devices, Sunnyvale, CA, USA) at 562nm. The protein concentration of sample was extrapolated from the BSA standard curve.

2.10 Western blotting

Samples were loaded and run on a 12% SDS-PAGE gel. Then the proteins on the gel were transferred to a methanol activated PVDF (polyvinylidene difluoride) membrane. Blocking buffer (5% milk in PBST) was used to block the membrane for 1 hour at room temperature on a shaking platform. The membrane was rinsed five times with PBST and then incubated with a primary antibody overnight at 4°C. After five time washing with PBST, the membrane was incubated with a secondary antibody in the blocking buffer for 1 hour at room temperature in the dark. Finally, the protein level on the membrane was detected by using an Odyssey infrared imaging system (LI-COR Biosciences, Lincoln, NE, USA).

Rabbit polyclonal anti-Rap1 (Pierce, Rockford, IL, USA), rabbit polyclonal anti-Rho (Pierce, Rockford, IL, USA), mouse monoclonal anti-Cdc42 (Pierce, Rockford, IL, USA), and mouse monoclonal anti-Ras (Pierce, Rockford, IL, USA) were used as primary antibodies. Alexa Fluor 680 goat anti-rabbit or anti-mouse IgG (H+L) (MolecularProbes, Eugene, OR, USA) was used as secondary antibody.

2.11 In-gel trypsin digestion

Small GTPases (21-25 kDa) and effector binding domains (34-42 kDa) were separated by polyacrylamide gel electrophoresis. After Coomassie staining and destaining, the 15-25 kDa gel region was excised and chopped into cubes (~ 1×1 mm). The gel pieces were reduced in 10 mM dithiothreitol (Sigma, USA) for 30 minutes at 56°C and then alkylated in 55 mM iodoacetamide (Sigma, USA) for 45 minutes at room temperature in the dark. After thorough washing, the gel pieces were incubated with trypsin in 50 mM of ammonium bicarbonate buffer overnight at

37°C. Supernatant of the digest was collected and gel pieces were incubated with 5% formic acid and acetonitrile (1:2 (vol/vol)) for 15 minutes at 37°C. The second supernatant was collected and added to the previous one.

2.12 Heavy isotope-labeled proteotypic peptides for MRM quantitation

Heavy isotope-labeled proteotypic peptides with $^{13}C_6{}^{15}N_4$-arginine and $^{13}C_6{}^{15}N_2$-lysine incorporated were obtained as custom-synthesized PEPOtec SRM crude peptide from Thermo Pierce (Rockford, IL, USA). For MRM quantitation, heavy isotope-labeled peptides were added to the digested peptides. Samples were desalted by stage-tip and re-suspended with 0.5% acetic acid before LC-MRM-MS analysis.

2.13 In-solution trypsin digestion

Proteins eluted with 50 μL of 8 M urea in 50 mM of ammonium bicarbonate buffer were reduced in 10 mM dithiothreitol (Sigma, USA) for 1 hour at room temperature and then alkylated in 55 mM iodoacetamide (Sigma, USA) for 1 hour at room temperature in the dark. Solution was 4-fold diluted with 50 mM of ammonium bicarbonate buffer and then digested by trypsin overnight at 37°C.

2.14 Stable isotope dimethyl labeling

Digested peptides were passed through a C18 SepPak column (Waters, ON, Canada) and Dried by vacuum centrifugation. The digested samples were reconstituted in 100 μL of 100 mM Triethylammonium bicarbonate buffer (Sigma, USA). In-solution stable isotope dimethyl labeling was performed as described in the literature (Boersema et al., 2009). 4 μL of 4%

(vol/vol) different isotopomers of formaldehyde (light (CH_2O), intermediate (CD_2O), and heavy ($^{13}CD_2O$)) was added to the sample to be labeled with light, intermediate, and heavy dimethyl, respectively. Then 4 μL of 0.6M cyanoborohydride ($NaBH_3CN$) was added to the samples to be light and intermediate labeled and $NaBD_3CN$ was added to the sample to be heavy labeled. After incubation in a thermomixer for 1 hour at room temperature, the labeling reaction was quenched by adding 16 μL of 1% ammonia solution. Then, 8 μL of formic acid was added to further quench the reaction and to acidify the sample. The differentially labeled samples were mixed and purified by solid phase extraction on a C-18 stage-tip (Rappsilber et al., 2007).

2.15 LC-MS/MS analysis and quantification

Purified peptides were analyzed using an orthogonal quadrupole – time of flight mass spectrometer (Q-TOF, Impact II; Bruker Daltonics) on-line coupled to an Easy nano LC 1000 HPLC (ThermoFisher Scientific) using a Captive spray nanospray ionization source (Bruker Daltonics) including a 75-μm-inner diameter fused silica analytical column with an integrated spray tip (10 – 15 μm-diameter opening, pulled on a P-2000 laser puller from Sutter Instruments). The analytical column was packed with 1.9 μm-diameter Reprosil-Pur C-18-AQ beads (Dr. Maisch, www.Dr-Maisch.com). Buffer A consisted of 0.1% aqueous formic acid and 2% acetonitrile, and buffer B consisted of 0.1% formic acid and 80% acetonitrile in water. Samples were resuspended in buffer A and loaded with the same buffer. For 120 min runs, the gradient was from 10% B to 45% B over 90 min, then to 100% B over 5 min, held at 100% B for 15 min. Before each run the analytical column was conditioned with 4 μL of the same buffer and the sample loading was set at 8 μL + sample volume. The LC thermostat was set at 7°C. The sample was loaded on the trap column at 850 Bar and the analysis was performed at 0.25 μL/min

flow rate. The Captive spray tip holder was modified similarly to an already described procedure (Beck et al., 2015) – in order to reduce the dead volume, the fused silica capillary and the tubing that holds it were removed, and the analytical column tip was fitted in the Bruker spray tip holder using an 8 mm long piece of 1/16" x 0.015 PEEK tubing (IDEX), an 1/16" metal two-way connector, and a 16-004 Vespel ferrule. The Impact II mass spectrometer used OTOF Control 1.8 Ver. 4.0.17.1840, HyStar 3.2 and Compass 4.2 software. The Impact II was set to acquire in a data-dependent auto-MS/MS mode with inactive focus fragmenting the 20 most abundant ions (one at the time at 18 Hz rate) after each full-range scan from m/z 200 Th to m/z 2000 Th (at 5 Hz rate). The isolation window for MS/MS was 2 to 3 Th depending on precursor ion mass to charge ratio and the collision energy ranged from 23 to 65 eV depending on ion mass and charge. Precursor ions were then excluded from MS/MS for the next 0.4 min and reconsidered if their intensity increased more than 5 times. Singly charged ions were excluded since in ESI mode peptides usually carry multiple charges. Strict active exclusion was applied. Precursor ion threshold was 500 counts. Mass accuracy: error of mass measurement was typically within 5 ppm and was not allowed to exceed 10 ppm. The nano ESI source was operated at 1700 V capillary voltage, 0.20 Bar nano buster pressure, 3 L/min drying gas and 150°C drying temperature.

Analysis of Mass Spectrometry Data was performed using MaxQuant 1.5.2.8 (Cox et al., 2008). The search was performed against a database comprised of the protein sequences from the source organism plus common contaminants using the following parameters: peptide mass accuracy 10 parts per million; fragment mass accuracy 0.05 Da; trypsin enzyme specificity, fixed modifications - carbamidomethyl, variable modifications - methionine oxidation, deamidated N,

Q and N-acetyl peptides. Only those peptides exceeding the individually calculated 99% confidence limit (as opposed to the average limit for the whole experiment) were considered as accurately identified. For protein quantitation, a minimum of 1 unique peptide in addition to having two or more quantitated peptides were required. The reported protein ratios were the normalized ratios between two different label partners. The median of the total ratio population was shifted to 1. Paired *t*-tests were performed to determine whether differences between two sets of data were significant at a 95% confidence level.

2.16 LC-MRM-MS analysis

MRM analysis was performed using an Agilent triple quadruple 6460 (Agilent, Santa Clara, CA, USA) with the ChipCube nanospray ion source coupled with an Agilent 1200 nanoflow HPLC. 150 mm 75 μm ID C18 chip was used as the analytical column. Solvent A consisted of 0.1% formic acid and 3% acetonitrile, and solvent B consisted of 0.1% formic acid and 90% acetonitrile in water. For the 40 min run, the gradient was from 5% to 27% of solvent B over 29 min, then to 80% B over 1 min, held at 80% B for 10 min. The analysis was performed at 0.3 μL/min flow rate. Resolution of both MS1 and MS2 was set to 'unit'. The dwell time of each transition for 11 protein detection was set to 20 ms and for 6 protein detection was set to 50 ms. 11 proteotypic peptides with the highest signal intensity for each of the 11 small GTPase isoforms were showed in Table 2-1 (Zhang et al., 2015). Skyline (2.5.0.5675) (MacLean et al., 2010) was used for transition peak identification and quantification.

Table 2-1. MRM parameters used to detect proteotypic peptides of small GTPase isoforms.

C* is cysteine carbamidomethylation and M* is methionine oxidation.

Small GTPase	Proteotypic peptide sequence	Precursor charge state	Q1 m/z	Q3 m/z	Fragmentor voltage (V)	Collision energy (V)	Product ion type
NRas	SFADINLYR	+2	549.783	565.309	200	18	y4+
			549.783	793.420	200	15	y6+
			549.783	864.457	200	13	y7+
HRas	SYGIPYIETSAK	+2	664.840	454.740	220	18	y8++
			664.840	908.472	220	19	y8+
			664.840	1078.578	220	15	y10+
KRas	VKDSEDVPMVLVGNK	+3	543.955	417.246	120	12	y4+
			543.955	429.249	120	9	y8++
			543.955	857.491	120	12	y8+
KRas	VKDSEDVPM*VLVGNK	+3	549.287	417.246	120	14	y4+
			549.287	437.251	120	12	y8++
			549.287	873.496	120	15	y8+
RhoA	IGAFGYMEC*SAK	+2	667.299	725.296	200	18	y6+
			667.299	888.359	200	19	y7+
			667.299	945.380	200	18	y8+
RhoA	IGAFGYM*EC*SAK	+2	675.297	554.725	200	19	y9++
			675.297	741.291	200	23	y6+
			675.297	961.375	200	20	y8+
RhoC	ISAFGYLEC*SAK	+2	673.326	707.339	180	18	y6+
			673.326	927.424	180	18	y8+
			673.326	1074.492	180	18	y9+
Rap1A	VKDTEDVPMILVGNK	+3	553.299	417.246	165	10	y4+
			553.299	436.257	165	10	y8++
			553.299	871.507	165	11	y8+

Small GTPase	Proteotypic peptide sequence	Precursor charge state	Q1 m/z	Q3 m/z	Fragmentor voltage (V)	Collision energy (V)	Product ion type
Rap1A	VKDTEDVPM*ILVGNK	+3	558.631	417.246	165	14	y4+
			558.631	444.255	165	10	y8++
			558.631	887.502	165	14	y8+
Rap1B	VKDTDDVPMILVGNK	+3	548.627	417.246	140	11	y4+
			548.627	436.257	140	9	y8++
			548.627	530.330	140	10	y5+
Rap1B	VKDTDDVPM*ILVGNK	+3	553.959	417.246	140	11	y4+
			553.959	444.255	140	10	y8++
			553.959	887.502	140	10	y8+
Rap2B	ASVDELFAEIVR	+2	674.859	587.351	240	10	y5+
			674.859	734.420	240	19	y6+
			674.859	847.504	240	19	y7+
Rac1	LTPITYPQGLAMAK	+2	752.416	645.350	220	10	y12++
			752.416	815.444	220	26	y8+
			752.416	1079.555	220	23	y10+
Rac1	LTPITYPQGLAM*AK	+2	760.413	653.347	220	10	y12++
			760.413	831.439	220	23	y8+
			760.413	1095.550	220	24	y10+
Rac2	LAPITYPQGLALAK	+2	728.432	636.372	220	14	y12++
			728.432	797.488	220	23	y8+
			728.432	1061.599	220	23	y10+
Cdc42	TC*LLISYTTNK	+2	657.342	713.346	240	18	y6+
			657.342	826.431	240	21	y7+
			657.342	939.515	240	21	y8+

Chapter 3: Quantitative analysis of small GTPase activity in monocytes

3.1 Introduction

Monocytes/macrophages play an important role in the initiation and progression of atherosclerosis (Ghattas et al., 2013). Monocyte adhesion and transmigration are crucial events in the development of atherosclerotic lesions. Activated platelets can directly interact with monocytes or release soluble factors (platelet releasate) to activate and modulate monocytes. A variety of pro-inflammatory mediators including the chemokine CXCL12 (SDF-1) can be released from activated platelets. Platelets store an abundant amount of CXCL12 in their α-granules and release this chemokine after activation (Badimon et al., 2012; Chatterjee et al., 2013). CXCL12 binds to its receptors CXCR4 and CXCR7 on monocytes and regulates their functions (Chatterjee et al., 2015). CXCL12/CXCR4 mediates monocyte migration and CXCL12/CXCR7 mediates monocyte adhesion.

Small GTPases of the Ras superfamily are master regulators of diverse cellular behaviors, including cell adhesion, migration, differentiation, vesicle transport and cytoskeleton reorganization (Bos, J. L., 2005; Wennerberg, K., et al., 2005). This superfamily consists the Ras/Ral/Rap, Rho, Rab, Ran, and Arf/Sar subfamilies. The significance of Rap small GTPases in promoting cell adhesion and migration has been recognized. The Rap GTPases regulate the migration of B-cell lymphomas and Rap activation is important for CXCL12 induced B cell migration (Lin, et al., 2010a; McLeod, et al., 2002). Cellular motility through CXCL12/CXCR4 depends on the activation of the Rho small GTPases

including RhoA, Cdc42, and Rac1. Rac1 is specifically involved in controlling signaling efficiency of the CXCR4 (Zoughlami et al., 2012).

Since CXCL12 regulates the migration of monocytes, and small GTPases such as Rap and Rho play an essential role in cell migration, I hypothesized that CXCL12 rich platelet releasate might affect the activation of small GTPases in monocytes. A previous study in our lab demonstrated that LPA-induced platelet releasate contains more abundant proteins than thrombin- or collagen-induced platelet releasates, but all three types of platelet releasate cause the same number of THP-1 cells to migrate (Khosrovi-Eghbal, A., 2012). In this thesis, soluble factors released from LPA-stimulated platelets were employed to treat monocytes.

To monitor the change of small GTPase activity in monocytes with LPA stimulated-platelet releasate treatment, I decided to modify and apply a previously developed quantitative multiplexed small GTPase activity assay (Figure 3-1). Primary monocytes isolated from whole blood were separated into two fractions. One fraction was treated with platelet releasate. Both resting and platelet releasate-treated monocytes were lysed. Small GTPases in these two samples were purified by four different effector binding domains which were coupled with glutathione resin. Both small GTPases (20.8 - 22.1 kDa) and binding domains (34 - 42 kDa) were eluted out and separated through SDS-PAGE. Small GTPase bands were excised and in-gel digested. After adding heavy isotope-labeled synthetic peptides as standards, samples were analyzed by LC-MRM-MS (MRM assay) for protein quantification.

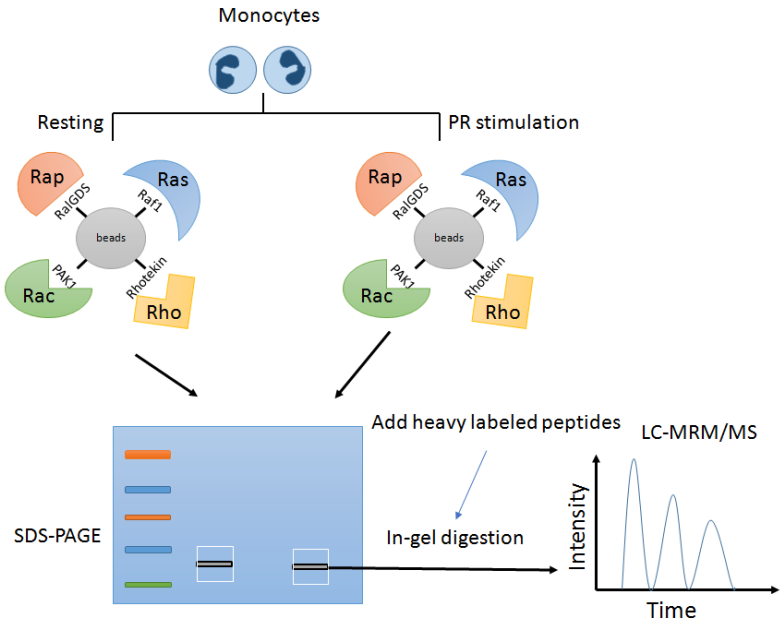

Figure 3-1. **Quantitative multiplexed small GTPase activity assay for enrichment and quantitation of active small GTPases in resting and platelet releasate stimulated monocytes.**

In this assay, four types of effector binding domains were used to precipitate multiple small GTPases. Therefore, the first objective of this chapter was to check the function of binding domains. However, this assay was previously employed to pull down small GTPases only in platelets but not in monocytes. Also, the amount of small GTPases in monocytes was not clear. Therefore, the second objective was to validate the MRM assay, determine the small GTPase expression levels in monocytes, and compare them to those in platelets. LPA can activate both platelets and monocytes. Therefore, the third objective was to examine the effect of LPA on small GTPases in monocytes which was used as a control, and evaluate the effect of LPA stimulated-platelet releasate on small GTPases in monocytes.

3.2 Results and discussion

3.2.1 Functionality check of effector binding domains

The protein purification part of the quantitative multiplexed small GTPase activity assay is a functional proteomics approach in which effector binding domains are used to pull down active small GTPases in monocytes. Our lab had showed that four groups of active small GTPases in platelets, Rap isoforms, Rho isoforms, Ras isoforms and Rac isoforms, could be precipitated by four binding domains, GST-RalGDS-RBD, GST-Rhotekin-RBD, GST-Raf1-RBD and GST-PAK1-PBD, respectively (Zhang et al., 2015). However, it was unknown whether or not these four binding domains could also pull down active small GTPases in monocytes. To check their pull-down function, the four binding domains expressed from bacteria were used to precipitate active small GTPases in a human monocytic cell line (THP-1 cells) and the eluted proteins were analyzed by Western blotting. Active Rap, Rho, Ras, and Cdc42 small GTPases were precipitated from GTPγs-treated THP-1 cell lysate by GST-RalGDS-RBD, GST-Rhotekin-RBD, GST-Raf1-RBD and GST-PAK1-PBD, respectively, as apparent by the bands in the Western blots (Figure 3-2). Small GTPases exist as GTP-bound active form and GDP-bound inactive form. GTPγs treatment locks small GTPases in their active form and therefore was used as a positive control. It produced strong bands at the same molecular weight as in the lysate pulldown, confirming that these bands corresponded to the individual small GTPases.

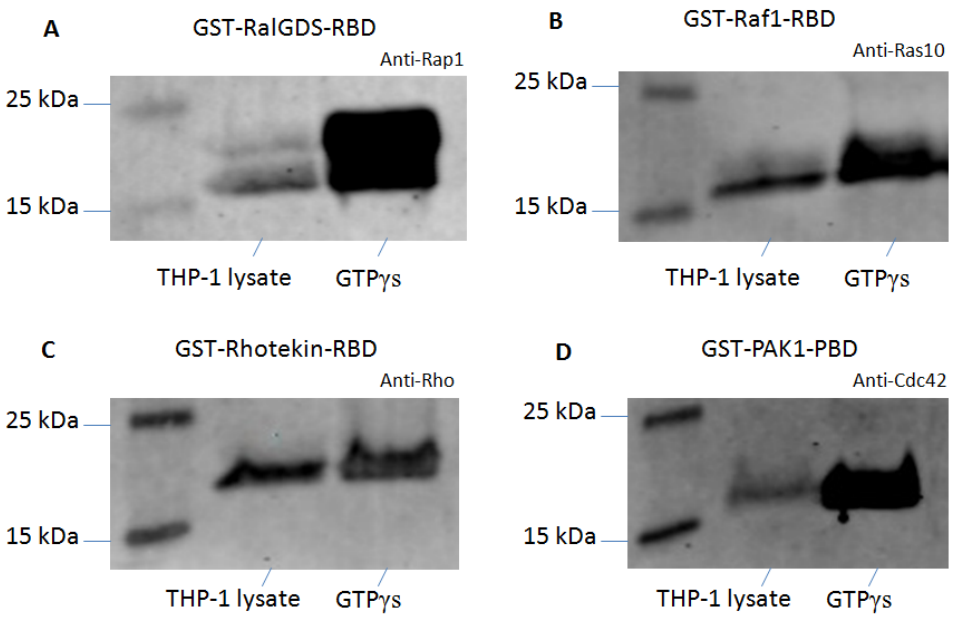

Figure 3-2. Functionality check of effector binding domains using western blotting.
(A) GST-RalGDS-RBD pull down active Rap1, (B) GST-Raf1-RBD pull down active Ras, (C) GST-Rhotekin-RBD pull down active Rho, and (D) GST-PAK1-PBD pull down active Cdc42.

This Western blot analysis demonstrated that newly prepared binding domains could efficiently pull down active small GTPases. However, the isoforms of each small GTPase group could not be identified by Western blotting. Therefore, non-targeted mass spectrometry was utilized to distinguish the precipitated small GTPase isoforms in each family. The active small GTPase isoforms for each group are shown in Table 3-1 together with the Mascot score. Rap1A, Rap1B, and Rap2B were precipitated by GST-RalGDS-RBD. Rac1, Rac2, and Cdc42 were precipitated by GST-PAK1-PBD. RhoA and RhoC were precipitated by GST-Rhotekin-RBD. NRas, HRas, and KRas were precipitated by GST-Raf1-RBD. Since the Mascot score represents how well the experimental data matches the database sequence and is a measure of abundance when proteins have similar molecular weights, Rap1A, Rap1B, Rac1, and Rac2 with higher Mascot score are the most abundant small GTPases in THP-1 cells. This result matches the small GTPase

isoforms precipitated in platelets (Zhang et al., 2015), demonstrating the general suitability of this approach also for monocytes.

Table 3-1. The small GTPase isoforms in THP-1 cells pulled down by effector binding domains.

Effector binding domain	Small GTPase	Mascot score
GST-RalGDS-RBD	Rap1A	2455.25
	Rap1B	2658.86
	Rap2B	267.83
GST-PAK1-PBD	Rac1	3542.58
	Rac2	3117.29
	Cdc42	82.27
GST-Rhotekin-RBD	RhoA	608.52
	RhoC	512.82
GST-Raf1-RBD	NRas	526.88
	HRas	94.59
	KRas	498.57

3.2.2 Relative expression level of small GTPases in platelets, THP-1 cells, and monocytes

To validate the MRM assay and confirm the ability to identify the 11 small GTPase isoforms in platelets, THP-1 cells, and monocytes, 100 μg of each lysate was subjected to a 12% SDS-PAGE gel and the 15 - 25 kDa regions were digested by trypsin. Finally, digested peptides were analyzed on a triple quadruple (QQQ) mass spectrometer using the MRM assay. Each light proteotypic peptide with all three transitions was used to identify the corresponding small GTPase (Table 3-2). Nine small GTPases (all except HRas and Cdc42) were identified for platelets and eight small GTPases (all except HRas, Rap2B, and Cdc42) were identified for THP-1 cells. Only five small GTPases (RhoA, RhoC, Rap1B, Rac1, and Rac2) were found in monocytes. This suggests that primary

monocytes may have lower small GTPase-expression or -basal activation levels than platelets and THP-1 cells.

Table 3-2. Identification of multiple small GTPase isoforms in platelet, THP-1, and monocyte lysate.

Small GTPase	Proteotypic peptide sequence	platelet	THP-1	Monocyte
NRas	SFADINLYR	X	X	
HRas	SYGIPYIETSAK			
KRas	VKDSEDVPMVLVGNK			
KRas	VKDSEDVPM*VLVGNK	X	X	
RhoA	IGAFGYMEC*SAK	X	X	
RhoA	IGAFGYM*EC*SAK	X	X	X
RhoC	ISAFGYLEC*SAK	X	X	X
Rap1A	VKDTEDVPMILVGNK	X	X	
Rap1A	VKDTEDVPM*ILVGNK	X		
Rap1B	VKDTDDVPMILVGNK	X	X	
Rap1B	VKDTDDVPM*ILVGNK	X	X	X
Rap2B	ASVDELFAEIVR	X		
Rac1	LTPITYPQGLAMAK	X	X	
Rac1	LTPITYPQGLAM*AK	X	X	X
Rac2	LAPITYPQGLALAK	X	X	X
Cdc42	TC*LLISYTTNK			

Notes: 100ug of each lysate was used to prepare samples. "x" indicates this peptide found. C*, cysteine carbamidomethylation; M*, methionine oxidation.

Table 3-2 shows that fewer small GTPase isoforms were identified in monocytes than in platelets. To quantitatively analyze the relative expression levels of the 11 small GTPase isoforms in monocytes and platelets, active small GTPases from the same total amount of GTPγs-treated monocyte and platelet lysate were precipitated, processed, and analyzed using the MRM assay. Peak area ratios of light/heavy proteotypic peptides were employed to calculate the relative activity level of each small GTPase and normalized to those observed in platelets (Table 3-3). Only the expression levels of Rap1B and Rac1 in monocytes were much lower than in platelets. In contrast, monocytes expressed more

Rap2B, Rac2, and Cdc42 than platelets, with all other small GTPases showing similar amounts on both types of blood cells. Therefore, the basal activation levels of most small GTPases in monocytes are much lower than those in platelets.

Table 3-3. Relative activity levels of multiple small GTPase isoforms in monocytes and platelets with GTPγs treatment.

Small GTPase	Proteotypic peptide sequence	Relative activity level	
		monocyte+GTPγs	Platelet+GTPγs
NRas	SFADINLYR	1	1
HRas	SYGIPYIETSAK	1	1
KRas	VKDSEDVPMVLVGNK	0.76	1
KRas	VKDSEDVPM*VLVGNK	0	1
RhoA	IGAFGYMEC*SAK	0.62	1
RhoA	IGAFGYM*EC*SAK	3.2	1
RhoC	ISAFGYLEC*SAK	0	1
Rap1A	VKDTEDVPMILVGNK	1	1
Rap1A	VKDTEDVPM*ILVGNK	0.38	1
Rap1B	VKDTDDVPMILVGNK	0.19	1
Rap1B	VKDTDDVPM*ILVGNK	0.45	1
Rap2B	ASVDELFAEIVR	2.36	1
Rac1	LTPITYPQGLAMAK	0.42	1
Rac1	LTPITYPQGLAM*AK	0.41	1
Rac2	LAPITYPQGLALAK	1.64	1
Cdc42	TC*LLISYTTNK	1.86	1

Notes: 0.6mg of platelet and monocyte lysates with GTPγs treatment was used to do pull down. 0.6 mg of platelet lysate was prepared from 0.44ml platelets at physiological concentration; 0.6 mg of monocyte lysate was prepared from 2.5 million monocytes.

3.2.3 Quantitative analysis of the small GTPase activity in THP-1 cells and monocytes

3.2.3.1 Activation profiles of multiple small GTPases in THP-1 cells stimulated by LPA

LPA can not only activate platelets but also promote monocyte adhesion and migration. In order to examine the effect of LPA stimulation on small GTPases in monocytic THP-1 cells, the activation profiles of the 11 small GTPases in LPA-treated THP-1 cells were studied. Small GTPases in platelets have the highest activation level within the first two minutes after LPA stimulation and then the activity gradually decreases after that (Zhang et al., 2015). In this study, I used the MRM assay to investigate the activation profiles of the 11 small GTPases in THP-1 cells stimulated with LPA for 2 or 10 minutes. The activity levels of small GTPases in GTPγs treated THP-1 lysate served as positive controls and were normalized to 100%. The data was obtained from eight independent biological replicates (Figure 3-3).

Compared to the activity levels of small GTPases in non-treated THP-1 cells, the amount of active NRas in THP-1 cells with two-minute LPA stimulation and the amount of active Rap2B in THP-1 cells with two-minute and ten-minute LPA stimulation was significantly increased. The activation pattern of Rap2B in THP-1 cells is similar to that previously reported for small GTPases in platelets. The activity level of Rap2B in non-treated THP-1 cells was 39%. After two-minute LPA stimulation, its activation increased to 77% and then decreased to 66% after another eight minutes. In contrast, the activity of Rap1A and Rap1B was not altered upon LPA stimulation. Rho and Rac GTPases were also not affected by LPA treatment. Interestingly, the activation level of NRas was very high in all experiments. This is explained by the known presence of a mutation in NRas in THP-1 cells that permanently locks it in its active conformation.

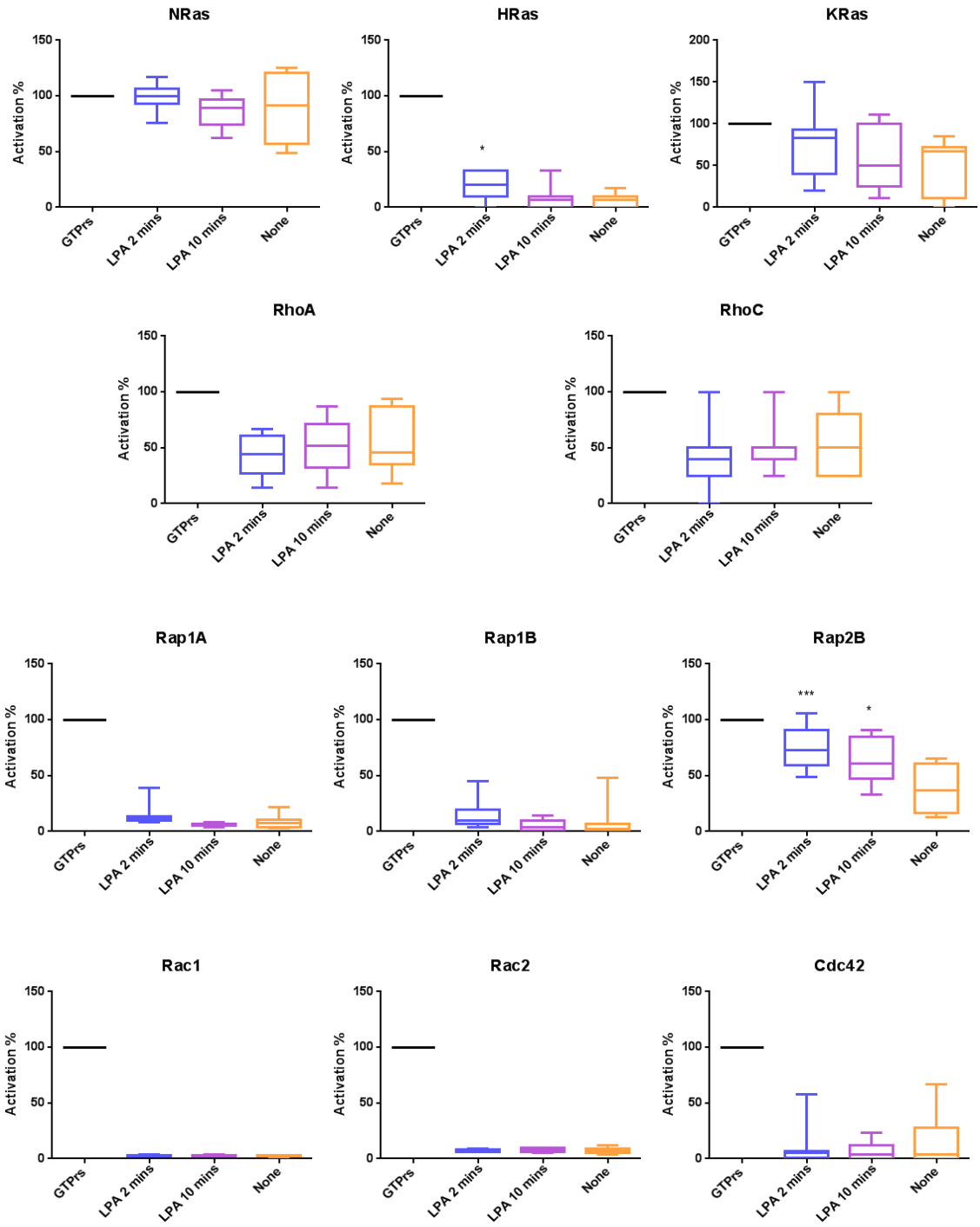

Figure 3-3. LPA stimulation increased the activity of HRas and Rap2B in THP-1 cells.

THP-1 cells were treated with LPA for 2 minutes or 10 minutes. The activity levels of small GTPases in GTPγs-treated THP-1 lysate were assigned a value of 100 to calculate the relative ratio of activation (one-way ANOVA with Dunnett's test, Significant changes are marked with a * $p < 0.05$, *** $p < 0.001$, n=8).

To check the effect of LPA-induced platelet releasate stimulation on small GTPases in primary monocytes, the activation profiles of the 11 small GTPases were studied in three independent experiments with monocytes from three donors. For each different donor, between 5 and 8 million total monocytes per 50 mL of whole blood were obtained. Samples (one for resting and the other for two-minute platelet releasate stimulation) in these three replicates were prepared from 2.5 million, 3.5 million, and 4 million monocytes. However, most of the peptides in the MRM assay could not be identified due to very low abundance of active small GTPases in resting and platelet releasate-stimulated monocytes. This result proves that most small GTPases in monocytes exist in their inactive form. Only Rac1 and Rac2 were identified and quantified, but their activity was not changed upon platelet releasate stimulation (data not shown).

3.2.3.2 Quantitative analysis of the Ras and Rap small GTPase activity in monocytes stimulated by LPA

The maximum number of monocytes that could be isolated from 50 mL of whole blood was 8 million, and the sensitivity of the MRM assay was not high enough to detect all 11 small GTPases prepared from 8 million monocytes in a single run. Therefore, I decided to increase the sensitivity of the MRM assay by reducing the number of small GTPases analyzed in each run. My previous data showed that LPA stimulation increased the activation of HRas and Rap2B in THP-1 cells. Therefore, Ras and Rap small GTPases were further explored. Before investigating the effect of LPA-induced platelet releasate on monocytes, the activation of Ras and Rap small GTPases in monocytes stimulated by LPA as a control was quantitatively analyzed (Figure 3-4). The activation of Rap1B in monocytes with two-minute LPA stimulation was significantly increased, but ten-minute LPA stimulation did not alter the extent of Rap1B activation

significantly. LPA stimulation also did not significantly affect the activation of Rap1A, Rap2B and Ras GTPases.

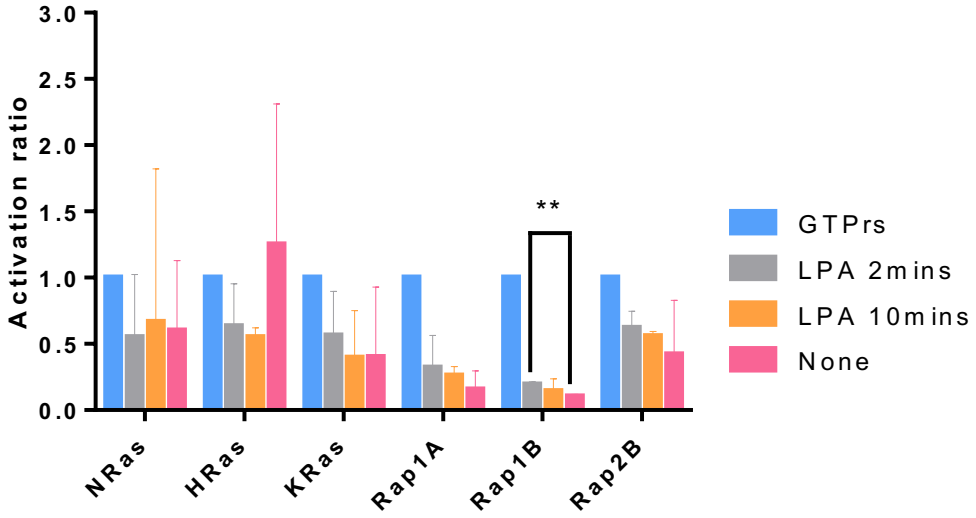

Figure 3-4. Two-minute LPA stimulation increased the activity of Rap1B in monocytes.
Monocytes were treated with LPA for 2 minutes or 10 minutes. The activity levels of small GTPases in GTPγs-treated monocyte lysate were assigned a value of 1 to calculate the relative ratio of activation (one-way ANOVA with Dunnett's test, Significant changes are marked with a ** $p < 0.01$, n=3).

Rap GTPases are key regulators of cell migration (Asha et al., 1999; Lin et al., 2010b), and my data showed that LPA stimulation increased the activation of Rap2B in monocytic cell line (THP-1 cells) and the activation of Rap1B in primary monocytes. Therefore, LPA may promote monocyte migration through activating Rap GTPases.

3.2.3.3 Quantitative analysis of the Ras and Rap small GTPase activity in monocytes stimulated by LPA-induced platelet releasate

The effect of LPA-induced platelet releasate on monocytes was inspected by quantitative analysis of the activation of Ras and Rap GTPases (Figure 3-5). The activation of Rap1B and

Rap2B in monocytes with two-minute platelet releasate stimulation was significantly increased. Platelet releasate stimulation did not significantly affect the activation of Rap1A and Ras GTPases. LPA stimulation only increased the activation of Rap1B, whereas LPA-induced platelet releasate stimulation elevated the activation of both Rap1B and Rap2B. Therefore, the increase of Rap2B activity may be caused by platelet releasate, while the increase of Rap1B activity could also be attributed by the action of residual LPA in the releasate.

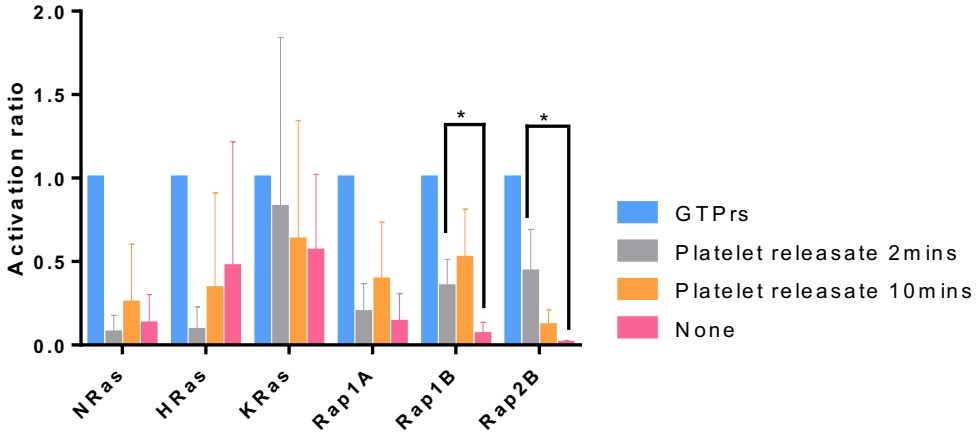

Figure 3-5. Two-minute LPA-induced platelet releasate stimulation increased the activity of Rap1B and Rap2B in monocytes.

Monocytes were treated with platelet releasate for 2 minutes or 10 minutes. The activity levels of small GTPases in GTPγs-treated monocyte lysate were assigned a value of 1 to calculate the relative ratio of activation (one-way ANOVA with Dunnett's test, Significant changes are marked with a * $p < 0.05$, n=3).

3.2.3.4 Activity level of the Ras and Rap small GTPases in response to inhibitor treatment

To further prove the effect of LPA-induced platelet releasate on Rap small GTPases, the activation of Rap GTPases in platelet releasate-stimulated monocytes with or without the addition of an anti-CXCL12 blocking antibody was studied (Table 3-4). The activation of

Rap1A, Rap1B, and Rap2B was significantly decreased in monocytes stimulated by platelet releasate in the presence of the anti-CXCL12 antibody compared to stimulation with platelet releasate alone. These results showed that LPA-induced platelet releasate activated both Rap1 and Rap2 in monocytes through CXCL12, which supports my hypothesis. The anti-CXCL12 antibody inhibited the effect of LPA-induced platelet releasate on Rap GTPases. The inhibition of Rap1A, Rap1B, and Rap2B was ~40%, ~50%, and ~90%, respectively. Rap1A displayed a PR + Inhibitor/resting activation ratio greater than 1.0, indicating that the inhibiting effect of anti-CXCL12 on it is incomplete. Although the PR + Inhibitor/resting activation ratios of Rap1B and Rap2B were also greater than 1.0, the inhibition effect of anti-CXCL12 on them is uncertain due to the large standard deviations. Ras GTPases were not significantly affected by anti-CXCL12 treatment. Therefore, Rap GTPases in monocytes are main targets of platelet releasate.

Table 3-4. CXCL12 antibody treatment significantly reduced the activation of Rap1A, Rap1B, and Rap2B in platelet releasate-stimulated monocytes.

Protein name	PR + Inhibitor/PR	PR + Inhibitor/None	Inhibition effect
NRas	2.11±1.17	-	-
HRas	0.93±0.12	6.22±8.83	-
KRas	0.28±0.49	0.27±0.49	-
Rap1A	0.61±0.1 **	4.74±0.78	Partial inhibition
Rap1B	0.46±0.19 **	2.79±2.7	-
Rap2B	0.088±0.175 ***	6.25±16.54	-

Notes: PR: monocytes were treated with platelet releasate; PR + Inhibitor: monocytes were treated with platelet releasate in the presence of the inhibitor (CXCL12 antibody); None: monocytes without treatment. Monocytes were stimulated with platelet releasate in the presence or absence of inhibitor for 2 minutes. The ratios of activity levels of small GTPases in different samples were compared with 1. (one-way ANOVA with Dunnett's test, Significant changes are marked with a ** $p < 0.01$, *** $p < 0.001$, n=4).

3.3 Conclusions

This study demonstrated that treating monocytes with LPA-induced platelet releasate resulted in the rapid activation of both Rap1 and Rap2. The following conclusions were reached.

First, four types of effect binding domains, GST-RalGDS-RBD, GST-Rhotekin-RBD, GST-Raf1-RBD and GST-PAK1-PBD, were prepared and their utility for precipitating small GTPases in monocytes was validated. With this, the quantitative multiplexed small GTPase activity assay was also suitable for monocytes.

Second, eleven small GTPases, NRas, HRas, KRas, RhoA, RhoC, Rap1A, Rap1B, Rap2B, Rac1, Rac2, and Cdc42, were expressed in monocytes, but most of them have lower basal activation levels than what was observed in platelets. Also, the MRM assay was validated, but it has the limitation that an increased number of transitions in each run would decrease its sensitivity.

Third, LPA-induced platelet releasate could activate both Rap1 and Rap2 in monocytes through CXCL12, and the effect of platelet releasate could be inhibited by anti-CXCL12 antibody.

Chapter 4: Quantitative analysis of the cAMP/cGMP interactome in platelets

4.1 Introduction

The main physiological function of platelets is to contribute to the hemostatic process after vessel endothelium damage (Gachet, C., 2006; Huo et al., 2004). They are also involved in inflammation and atherosclerosis (Lievens et al., 2011; Huo et al., 2004; Kaplan et al., 2011) and the activation of platelets is an important component of atherothrombosis (Davi et al., 2007). Most agonists that activate platelets work through binding to membrane G-protein-coupled receptors (Offermanns, S., 2006). These receptors are coupled to G proteins in platelets and in turn activate their downstream intracellular signaling pathways. Receptors for platelet inhibitors (endothelial prostacyclin and adenosine) are coupled to the G protein G_s to stimulate adenylyl cyclase(AC)-dependent cAMP synthesis (Li et al., 2010). Nitric oxide (NO) directly activates soluble guanylyl cyclase (sGC) to raise the level of cGMP. Cyclic nucleotides (cAMP and cGMP) stimulate the protein kinases PKA and PKG to phosphorylate a broad panel of substrate proteins such as VASP, resulting in inhibition of platelet activation and aggregation. Scavenger receptor, CD36, in platelet membrane is identified as a receptor for oxidized low-density lipoprotein (oxLDL) and oxidized phosphatidylcholines (oxPCs). However, how oxLDL/oxPC affects platelets through binding to CD36 is not clear (Figure 4-1).

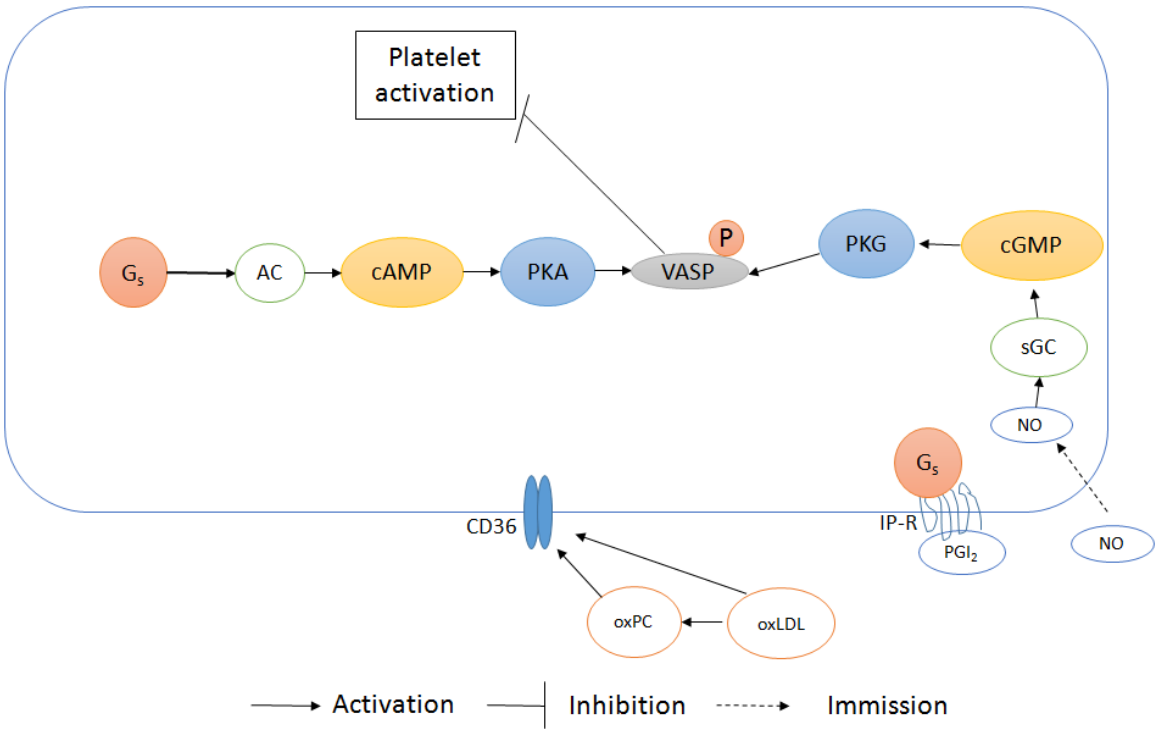

Figure 4-1. Cyclic AMP and cyclic GMP pathways in platelets.
Both oxPC and oxLDL bind to CD36.

Cyclic nucleotide signaling is compartmentalized in platelets (Wilson et al., 2008). To achieve spatial specificity, localized cAMP interacts with A-kinase anchoring proteins (AKAPs) through PKA. AKAPs can localize active PKA to its substrates to form subcellular cAMP signaling compartments. Other signaling components such as phosphodiesterases (PDEs) control localized cAMP signaling not only spatially but also timewise (Mongillo et al., 2004). PDEs degrade platelet cyclic nucleotides and provide a negative feedback loop for cyclic nucleotide signaling. Three PDEs, PDE2A, PDE3A, and PDE5A, are expressed in platelets. cGMP regulates all of these three PDEs. cGMP-stimulated PDE2A and cGMP-inhibited PDE3A can degrade both cAMP and cGMP, but they mainly regulate cAMP. cGMP-stimulated PDE5A only hydrolyzes cGMP (Haslam et al., 1999; Conti et al., 1999) (Figure 4-2).

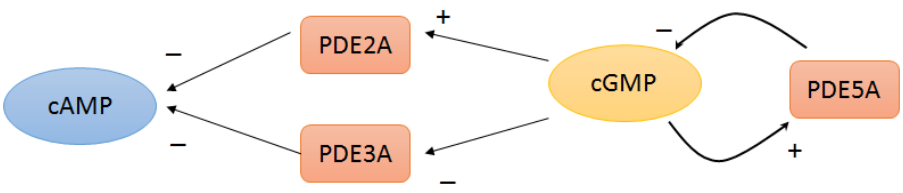

Figure 4-2. Phosphodiesterases in platelets.

cGMP activates PDE2A and PDE5A resulting in the degradation of cAMP and cGMP, respectively. cGMP inhibits PDE3A which degrades cAMP.

Previous studies have shown that oxLDL and oxPC are able to bind platelets via CD36 and promote platelet activation (Korporaal et al., 2007; Wraith et al., 2013; Nergiz-Unal, et al., 2011; Podrez et al., 2007). The mechanism of the activation of platelets by oxPC/oxLDL is through inhibition of the cGMP/PKG signaling pathway (Magwenzi et al., 2015). However, oxLDL inhibits platelet function through increasing cAMP (Korporaal et al., 2005). Our lab also checked the effect of PAPC and oxPCs on platelets and found that KDdiA-PC and POV-PC, two types of oxPC species, were able to increase both cAMP and cGMP levels without inducing platelet aggregation. (Li, 2016). Although platelet reactivity modulated by oxPC has been studied, the response of platelets at the level of anchoring proteins and cyclic nucleotide regulated proteins (PDEs) is not well understood.

To reveal the response of cAMP/cGMP binding proteins in platelets with KDdiA-PC and POV-PC stimulation, I decided to develop and apply a targeted quantitative chemical proteomics approach. In this approach, immobilized cAMP and cGMP beads were utilized to enrich low abundant signaling proteins, and stable isotope dimethyl labeling was employed to quantitatively analyze the specific spatial-temporal alterations of cyclic nucleotide regulated proteins in platelets upon oxPC stimulation. Therefore, the first objective of this chapter was to develop the

quantitative chemical proteomics approach. The second objective was to validate this approach. The third objective was to monitor downstream changes of cAMP/cGMP binding proteins in platelets upon KDdiA-PC and POV-PC stimulation by using this approach.

4.2 Results and discussion

4.2.1 General workflow

The general workflow of the cAMP/cGMP interactome pull-down and identification is shown in Figure 4-3. cAMP/cGMP beads were incubated with cell lysate to precipitate cyclic nucleotide signaling proteins. Beads were subsequently washed by adenosine diphosphate (ADP) and guanosine diphosphate (GDP) to get rid of non-specific binding proteins and then the enriched cAMP/cGMP binding proteins were eluted and subjected to 12% SDS-PAGE electrophoresis. After in-gel digestion, digested peptides were analyzed by LC-MS/MS for protein identification.

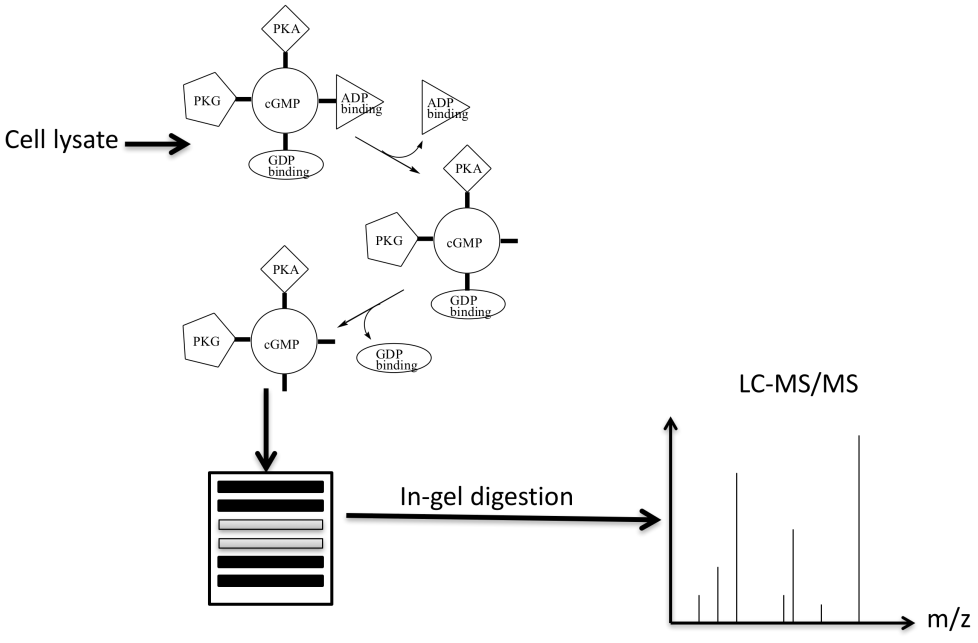

Figure 4-3. Workflow of enrichment and identification of cAMP and cGMP interactors in THP-1 cells or platelets.

4.2.2 Development of the cAMP/cGMP interactome pull-down assay and validation of dimethyl labeling quantitation

4.2.2.1 Optimization of the cAMP/cGMP interactome pull-down procedure

In the quantitative chemical proteomics approach, two immobilized cyclic nucleotides, 2-AHA-cAMP and 2-AH-cGMP beads, are used to precipitate cAMP/cGMP binding proteins. To obtain more specific information on proteins interacting with cAMP/cGMP and reduce the amount of non-specific binding proteins, the 2-AH-cGMP beads that were incubated with THP-1 cell lysate were eluted sequentially with ADP, GDP, cGMP, and cAMP solutions. The proteins in the eluted fractions were separated on the SDS-PAGE gel (Figure 4-4).

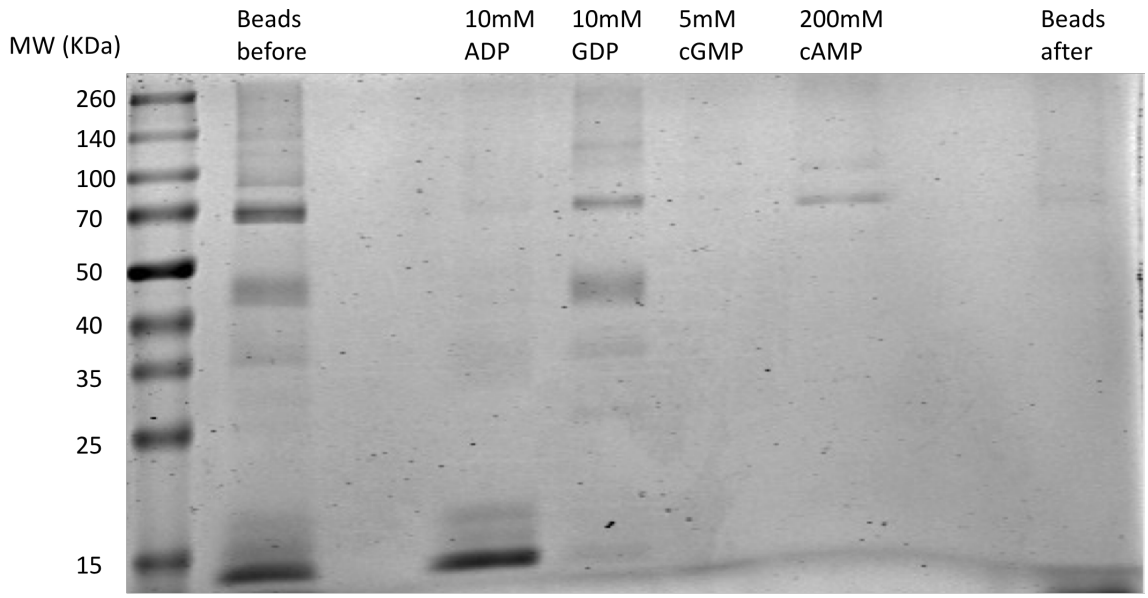

Figure 4-4. SDS-PAGE gel of THP-1 lysate treated with 2AH-cGMP beads and sequentially eluted with ADP, GDP, cGMP and cAMP.

Beads before was the pulled down fraction before sequential elution and *beads after* was the PKA/PKG enriched fraction remaining on the beads.

Each lane was cut into 4 gel pieces, digested, and the peptides in each fraction were extracted and analyzed by LC-MS/MS on an orthogonal quadrupole - time of flight mass spectrometer (Q-TOF) for protein identification and label-free quantitation. Because larger proteins yield more peptides resulting in a higher MASCOT score, the relative abundance of a protein cannot directly be inferred from its protein MASCOT score. Instead, a protein filtration method that took into account the molecular weight of each protein, was used to semi-quantitatively determine the relative abundance of the proteins in the data set (Table 4-1). The filtration method was as follows: At least 10 unique peptides were required for large proteins (MW≥ 100kDa); MW/10 unique peptides were required for medium proteins (40kDa ≤MW< 100kDa); At least 4 unique peptides were required for small proteins (MW< 40kDa). Using the stringent filtration settings noticeably reduced the number of proteins and increased the accuracy of protein identification.

Table 4-1. The number of proteins in each sample before and after protein filtration.

Sample	Beads before	ADP	GDP	cGMP	cAMP	Beads after
Before filtration	174	31	38	31	51	51
After filtration	80	12	19	13	20	23

After applying the filtration method, the most abundant pulled-down proteins in each eluent were identified and classified based on their ligand binding properties. Proteins were divided into eight categories: cAMP, cGMP, AMP/ADP/ATP, GMP/GDP/GTP, DNA/RNA, Co-enzyme, Cytoskeletal, and Unknown (Figure 4-5). Comparing the percentage of cAMP/cGMP binding proteins in the *Beads before* fraction (4% cAMP-binding and 1% cGMP-binding) to that in the *Beads after* fraction (9% cAMP-binding and 4% cGMP-binding) revealed that cAMP/cGMP

binding proteins were enriched after sequential elution. The high percentage of ADP and GDP binding proteins in the ADP elution (50% AMP/ADP/ATP-binding) and the GDP elution (32% GMP/GDP/GTP-binding) fractions proved that competitive binding of ADP and GDP was able to elute most ADP and GDP binding proteins (i.e. non-specific binding proteins). Also, no cAMP/cGMP binding proteins were found in both fractions after ADP and GDP elution, which demonstrated that ADP/GDP only removed non-specific binding proteins. In contrast, cAMP elution (15% cAMP-binding) and cGMP elution (16% cAMP-binding and 8% cGMP-binding) competitively eluted most of cAMP/cGMP binding proteins.

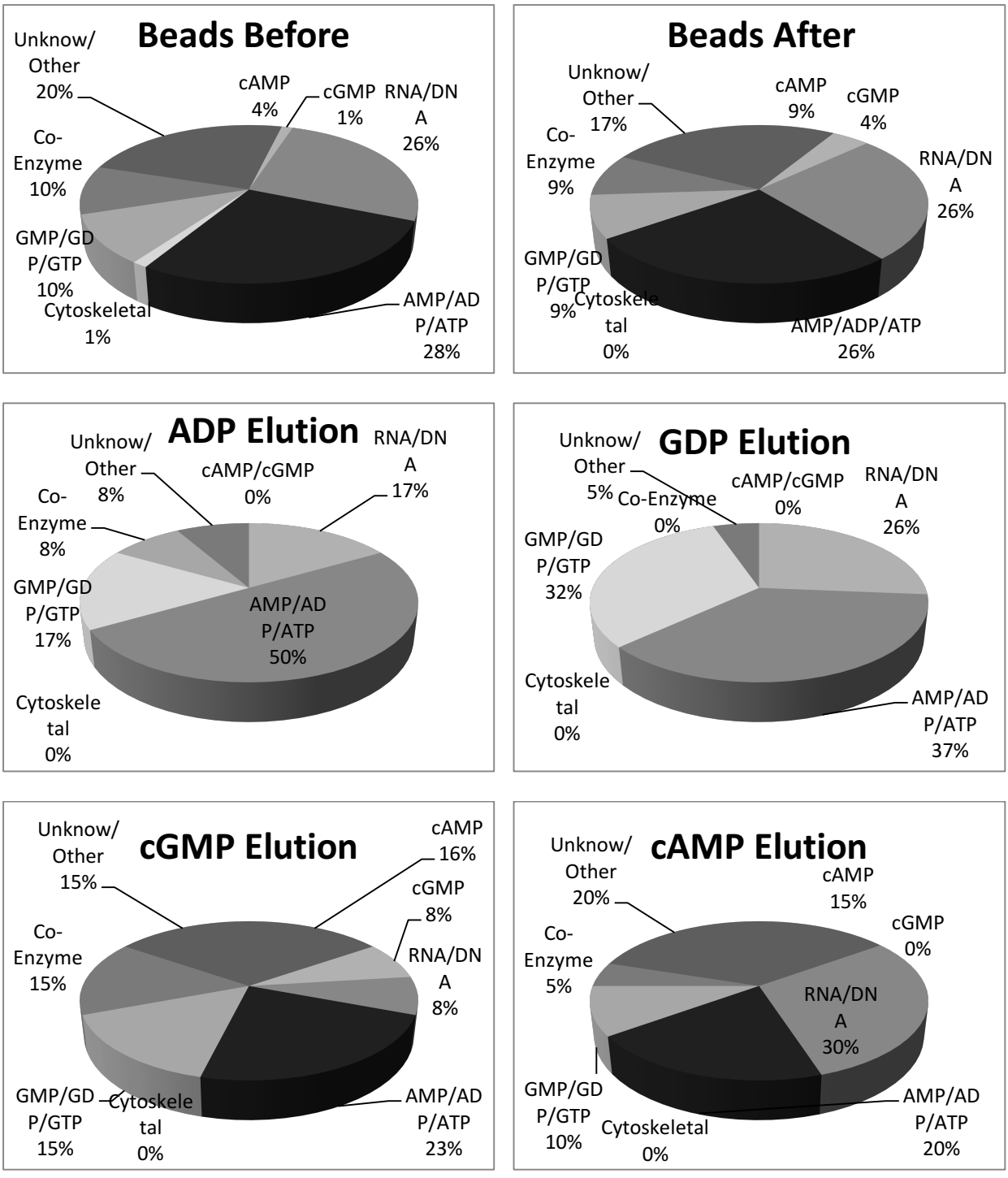

Figure 4-5. Classification of pulled down proteins from each elution based on their ligand binding properties.

The cAMP- and cGMP-binding proteins identified in each fraction are shown in Table 4-2. Six cAMP/cGMP-interacting proteins were precipitated from THP-1 lysate but two low abundant

proteins, AKAP2 and AKAP11, were lost during sequential elution. Since elution with ADP and GDP could efficiently remove non-specific binding proteins, ADP/GDP treatment was used as the first step in all subsequent experiments.

Table 4-2. cAMP/cGMP binding proteins found in each sample.

	Samples					
Proteins	**Beads before**	**ADP**	**GDP**	**cGMP**	**cAMP**	**Beads after**
PKA-RIα	√			√	√	√
PKA-RIIα	√			√	√	√
PDE1B	√			√	√	√
PKA-RIIβ	√				√	
AKAP2	√					
AKAP11	√					

4.2.2.2 Addition of a dimethyl labeling step to the enrichment method

To introduce an alternative quantitation approach, stable isotope dimethyl labeling was validated for its compatibility with the enrichment method. Using this combination, cAMP/cGMP binding proteins were identified and quantitatively analyzed after labeling equal amounts of THP-1 cell lysate with two different labels (light and heavy) and mixing them (Table 4-3). Nine cAMP-interacting proteins, PKA-RIα, PKA-RIIα, PKA-RIIβ, AKAP 2, AKAP 8, AKAP 1, AKAP 9, AKAP 7, PKA-Cβ, and one cGMP-interacting protein, PDE1B, were identified. The amount of each protein precipitated from equal amounts of THP-1 cell lysate was almost identical ($H/L \approx 1$). This result indicated the general suitability of isotopic dimethyl labelling quantitation in my workflow. In table 4-3, each heavy/light ratio is reported with four significant numbers because the peak areas measured by mass spectrometry have a precision of five significant figures.

Table 4-3. Determine the ratio of cAMP/cGMP binding proteins in equal amount of THP-1 cell lysate to prove the quantification efficiency of stable isotope dimethyl labeling.

	In solution digestion and dimethyl labeling	
Proteins	**Proteins found**	**H/L ratio**
PKA-RIα	√	0.937
PKA-RIIα	√	0.994
PDE1B	√	0.939
PKA-RIIβ	√	0.977
AKAP 2	√	1.010
AKAP 8	√	1.044
AKAP 1	√	1.011
AKAP 9	√	0.961
AKAP 7	√	0.935
PKA-Cβ	√	1.045

Notes: THP-1 lysate was incubated with cGMP beads to pull down cAMP/cGMP binding proteins. After in-solution digestion, sample was separated to two fractions. One fraction was labeled "light" and the other fraction was labeled "heavy".

4.2.3 Validation of the chemical proteomics pull-down assay in platelets

Following its optimization and validation in THP-1 cell lysate, the newly developed pull-down assay was employed to analyze the cAMP/cGMP interactome in human platelets, the main focus. ADP and GDP was pre-incubated with platelet lysate before adding 2-AHA-cAMP and 2-AH-cGMP beads. After washing with ADP/GDP solution and lysis buffer, proteins remaining on the beads were eluted and run on an SDS-PAGE gel. The resulting gel is shown in Figure 4-6. In-gel digestion and LC-MS/MS analysis were performed to obtain a list of pulled-down platelet proteins. After protein filtration, the most abundant proteins (P1-P71) were identified. They are listed in Table 4-4.

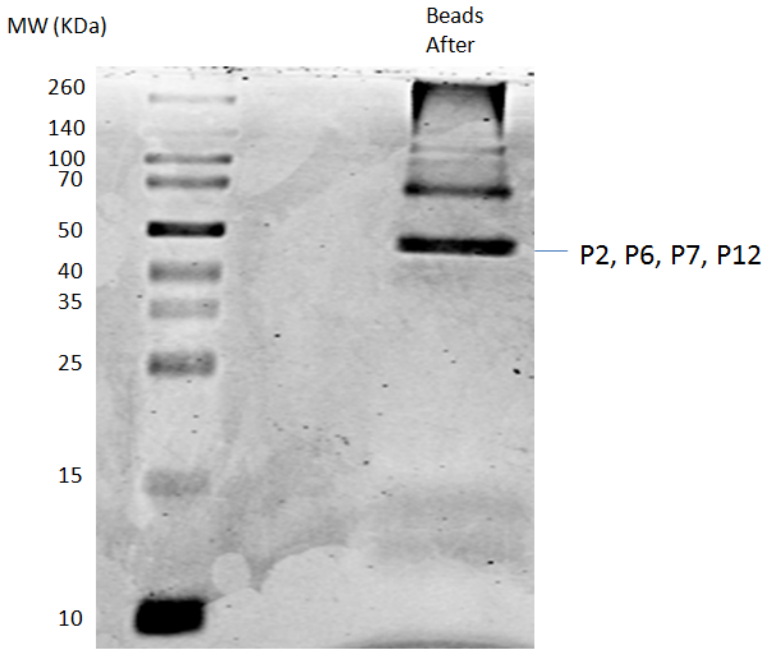

Figure 4-6. SDS-PAGE gel of the PKA/PKG enriched fraction precipitated from platelets.

Table 4-4. Abundant proteins pulled down from platelets. Ordered according to MASCOT score.

No.	Protein name	Accession No.	Binds	MW [kDa]	Coverage	Unique peptides	MASCOT score
P1	cGMP-specific 3',5'-cyclic phosphodiesterase	O76074	cGMP	99.9	62.97	96	57358.9
P2	cAMP-dependent protein kinase type I-alpha regulatory subunit	P10644	cAMP	43	76.12	46	55339.86
P3	Actin, cytoplasmic 1	P60709	ATP	41.7	52.53	15	47212.74
P4	Glycogen debranching enzyme	P35573	ADP	174.7	76.63	123	43160.41
P5	cGMP-dependent protein kinase 1	Q13976	cGMP	76.3	64.98	60	30205.64
P6	cAMP-dependent protein kinase type II-alpha regulatory subunit	P13861	cAMP	45.5	83.17	41	29492.56
P7	cAMP-dependent protein kinase type II-beta regulatory subunit	P31323	cAMP	46.3	79.67	39	24704.44
P8	Protein MRVI1	H0YI08	cGMP	89.6	54.81	43	17783.14
P9	cGMP-dependent 3',5'-cyclic phosphodiesterase	O00408	cGMP	105.6	57.49	46	13425.32
P10	Clathrin heavy chain 1	Q00610	other	191.5	35.1	59	8031.75
P11	Glutaryl-CoA dehydrogenase, mitochondrial	Q92947	CoA	48.1	52.51	16	6499
P12	cAMP-dependent protein kinase type I-beta regulatory subunit	P31321	cAMP	43	38.85	20	4933.86
P13	Glycogen phosphorylase, liver form	P06737	ADP	97.1	32.47	30	4599.64
P14	cGMP-dependent 3',5'-cyclic phosphodiesterase (Fragment)	F5H130	cGMP	15.3	75	10	4103.12
P15	Galectin-3-binding protein	Q08380	unknown	65.3	38.8	18	3760.47
P16	Mitogen-activated protein kinase 1	P28482	ATP	41.4	41.11	14	3565.79
P17	Glycogen [starch] synthase, muscle	P13807	other	83.7	30.53	19	3360.38
P18	Complement factor H	P08603	other	139	30.38	25	3194.97

No.	Protein name	Accession No.	Binds	MW [kDa]	Coverage	Unique peptides	MASCOT score
P19	Short/branched chain specific acyl-CoA dehydrogenase, mitochondrial	P45954	CoA	47.5	34.49	15	3092.91
P20	Tubulin beta-1 chain	Q9H4B7	GTP	50.3	31.93	10	2987.66
P21	Histone H1.4	P10412	DNA	21.9	32.42	10	2950.26
P22	Calcium-transporting ATPase	B4E2Q0	ATP	104.6	29.28	19	2847.15
P23	Glycogen phosphorylase, brain form	P11216	other	96.6	23.84	20	2538.29
P24	Histone H2B type 1-C/E/F/G/I	P62807	DNA	13.9	68.25	9	2437.2
P25	Integrin-linked protein kinase	Q13418	ATP	51.4	40.27	17	2315.5
P26	Coagulation factor XIII A chain	P00488	other	83.2	18.72	12	2314.92
P27	Tubulin alpha-4A chain	P68366	GTP	49.9	41.96	13	2209.3
P28	Integrin beta-3	P05106	unknown	87	25.25	15	2115.08
P29	Histone H1.3	P16402	DNA	22.3	32.13	10	2076.23
P30	Heat shock cognate 71 kDa protein	P11142	ATP	70.9	29.26	18	1942.45
P31	Filamin-A	P21333	Cytoskeletal	280.6	14.51	24	1825.34
P32	Sarcoplasmic/endoplasmic reticulum calcium ATPase 3	Q93084	ATP	113.9	19.37	17	1769.73
P33	Zinc-binding alcohol dehydrogenase domain-containing protein 2	Q8N4Q0	NADP	40.1	24.4	10	1625.83
P34	Integrin alpha-IIb	P08514	other	113.3	21.94	19	1552.22
P35	Tubulin beta chain	P07437	GTP	49.6	43.92	13	1505.48
P36	cGMP-dependent protein kinase 2	Q13237	cGMP	87.4	13.52	11	1410.07
P37	Histone H2A type 1-H	Q96KK5	DNA	13.9	49.22	4	1247.75
P38	Tubulin beta-4B chain	P68371	DNA	49.8	34.38	11	1229.97
P39	Isobutyryl-CoA dehydrogenase, mitochondrial	Q9UKU7	CoA	45	26.75	10	1185.94
P40	Mitogen-activated protein kinase 3	P27361	ATP	43.1	20.84	8	1129.78
P41	Serine/threonine-protein kinase B-raf (Fragment)	H7C560	ATP	41.9	16.53	5	1120.45

No.	Protein name	Accession No.	Binds	MW [kDa]	Coverage	Unique peptides	MASCOT score
P42	Myosin-9	P35579	ATP	226.4	9.08	11	1095.59
P43	Inositol 1,4,5-trisphosphate receptor type 1	Q14643	cGMP	313.7	9.35	22	1094.52
P44	Protein S100-A6	P06703	other	10.2	50	4	1065.79
P45	Histone H1.5	P16401	DNA	22.6	30.97	8	999.64
P46	cAMP-dependent protein kinase catalytic subunit beta	P22694	cAMP	40.6	22.22	8	987.78
P47	Histone H3 (Fragment)	K7EK07	DNA	14.9	29.55	4	816.99
P48	Talin-1	Q9Y490	other	269.6	6.69	10	787.24
P49	Ig gamma-1 chain C region	A0A087WYC5	unknown	52.4	32.21	11	769.73
P50	Heterogeneous nuclear ribonucleoproteins A2/B1	P22626	RNA	37.4	20.4	5	692.29
P51	Histone H4	P62805	DNA	11.4	45.63	5	663.58
P52	Plasminogen	P00747	other	90.5	13.58	9	620.57
P53	Calcium/calmodulin-dependent protein kinase type 1	Q14012	ATP	41.3	19.46	4	611.06
P54	Heat shock 70 kDa protein 1A/1B	P08107	ATP	70	12.95	8	609.42
P55	A-kinase anchor protein 7 isoform gamma	Q9P0M2	cAMP	39.5	27.87	8	542.41
P56	A-kinase anchor protein 9	A0A0A0MRE9	cAMP	362.4	4.25	9	538.33
P57	Lysyl oxidase homolog 3	E7END4	other	77.1	16.79	8	527.84
P58	Tripartite motif-containing protein 4	Q9C037	other	57.4	21.2	10	504.01
P59	LIM and senescent cell antigen-like-containing domain protein 1	P48059	other	37.2	14.46	5	498.09
P60	Ig gamma-2 chain C region	P01859	other	35.9	29.14	7	480.95
P61	Ig kappa chain C region	P01834	other	11.6	80.19	4	433.43
P62	Inositol 1,4,5-trisphosphate receptor type 2	Q14571	cGMP	307.9	3.55	10	424.46
P63	Short-chain specific acyl-CoA dehydrogenase, mitochondrial	P16219	CoA	44.3	10.19	4	390.25
P64	Lamin-B1	P20700	unknown	66.4	8.02	6	359.41
P65	Ig lambda-2 chain C regions (Fragment)	A0A075B6L0	other	11.3	37.74	4	331.58

No.	Protein name	Accession No.	Binds	MW [kDa]	Coverage	Unique peptides	MASCOT score
P66	Endonuclease domain-containing 1 protein	O94919	other	55	11.4	5	328.12
P67	Fibrinogen gamma chain	P02679	other	51.5	15.89	5	321.64
P68	Glycogen synthase kinase-3 beta	P49841	ATP	46.7	13.1	4	290.14
P69	Lamin B2, isoform CRA_a	J9JID7	unknown	69.9	12.9	7	274.24
P70	Four and a half LIM domains 1 (Fragment)	Q5JXI8	other	29.1	31.91	6	258.62
P71	A-kinase anchor protein 10, mitochondrial	E7EMD6	cAMP	67.7	5.63	2	193.48

The largest band on the gel contained PKA-RI (P2, P12) and PKA-RII (P6, P7), which indicated that PKAs were abundant proteins in platelets and well retained in the protocol. As before, all enriched cAMP/cGMP-binding proteins in platelets were classified (Figure 4-7), which illustrated that the performance was comparable to that achieved with THP-1 cell lysates.

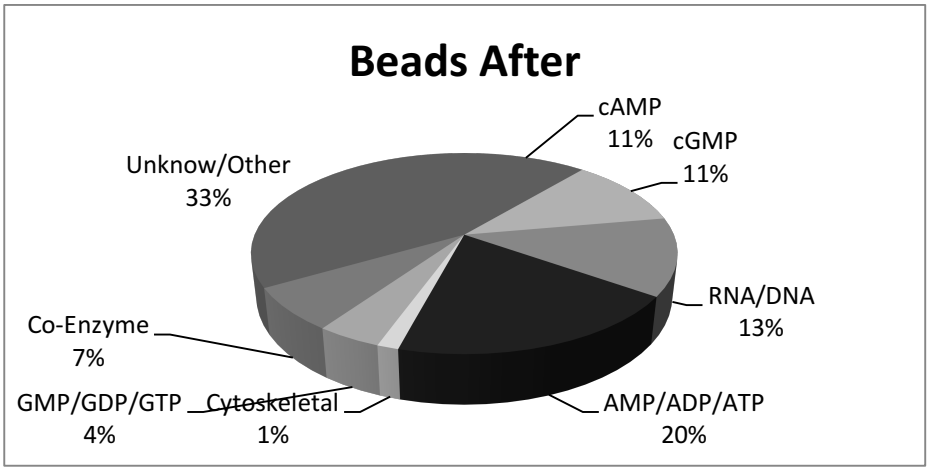

Figure 4-7. Classification of pulled down proteins from the PKA/PKG enriched fraction remaining on the beads based on their ligand binding properties.

The enriched cAMP and cGMP binding proteins are also listed in Table 4-5. All four types of PKAs (RIα, RIβ, RIIα, and RIIβ) and two types of PKGs (I and II) were present in the dataset. Only two of three PDEs were observed, as PDE3A was missing which may be because of its membrane-associated localization. Besides primary interactors (PKA-R, PKG, PDEs), some secondary interactors (AKAPs, PKA-C, MRVI1, IP_3-Rs) were also captured in this experiments. For example, the inositol-1,4,5-trisphosphate receptor-associated cGMP kinase substrate, MRVI1, combines with the PKGI and the inositol 1,4,5-trisphosphate receptor type 1 (IP_3-RI) to form a macromolecular complex (Ammendola et al., 2001). Although they are very low abundant, all of them were detected. Therefore, the newly developed quantitative chemical proteomics approach can be used to efficiently purify cAMP and cGMP binding proteins.

Table 4-5. cAMP/cGMP signaling proteins found in platelets.

cAMP-dependent protein kinase type I-alpha regulatory subunit	PKA-RIα
cAMP-dependent protein kinase type I-beta regulatory subunit	PKA-RIβ
cAMP-dependent protein kinase type II-alpha regulatory subunit	PKA-RIIα
cAMP-dependent protein kinase type II-beta regulatory subunit	PKA-RIIβ
cGMP-dependent protein kinase 1	PKGI
cGMP-dependent protein kinase 2	PKGII
cGMP-specific 3',5'-cyclic phosphodiesterase	PDE5A
cGMP-dependent 3',5'-cyclic phosphodiesterase	PDE2A
cAMP-dependent protein kinase catalytic subunit beta	PKA-Cβ
A-kinase anchor protein 7	AKAP7
A-kinase anchor protein 9	AKAP9
Protein MRVI1	MRVI1
Inositol 1,4,5-trisphosphate receptor type 1	IP_3-RI
Inositol 1,4,5-trisphosphate receptor type 2	IP_3-RII
A kinase anchor protein 10, mitochondrial	AKAP10

4.2.4 The response of the cAMP/cGMP interactome in platelets with KDdiA-PC and POV-PC stimulation

Previous studies demonstrated that the effect of oxPCs on platelets is controversial but associated with cAMP/cGMP signaling. To determine how oxPCs affect the components of cAMP/cGMP signaling pathway, the quantitative chemical proteomics approach was applied to monitor the changes of cAMP/cGMP downstream signaling proteins in platelets with KDdiA-PC and POV-PC stimulation. The workflow is displayed in Figure 4-8. Equal amount of resting, KDdiA-PC and POV-PC treated platelets were lysed and incubated with cAMP and cGMP (1:1) beads. Pulled-down cyclic nucleotide signaling proteins were subjected to in-solution digestion and then

labeled with light, intermediate, and heavy formaldehyde. Labeled peptides were mixed in 1:1:1 ratio followed by LC-MS/MS analysis for protein identification and quantitation.

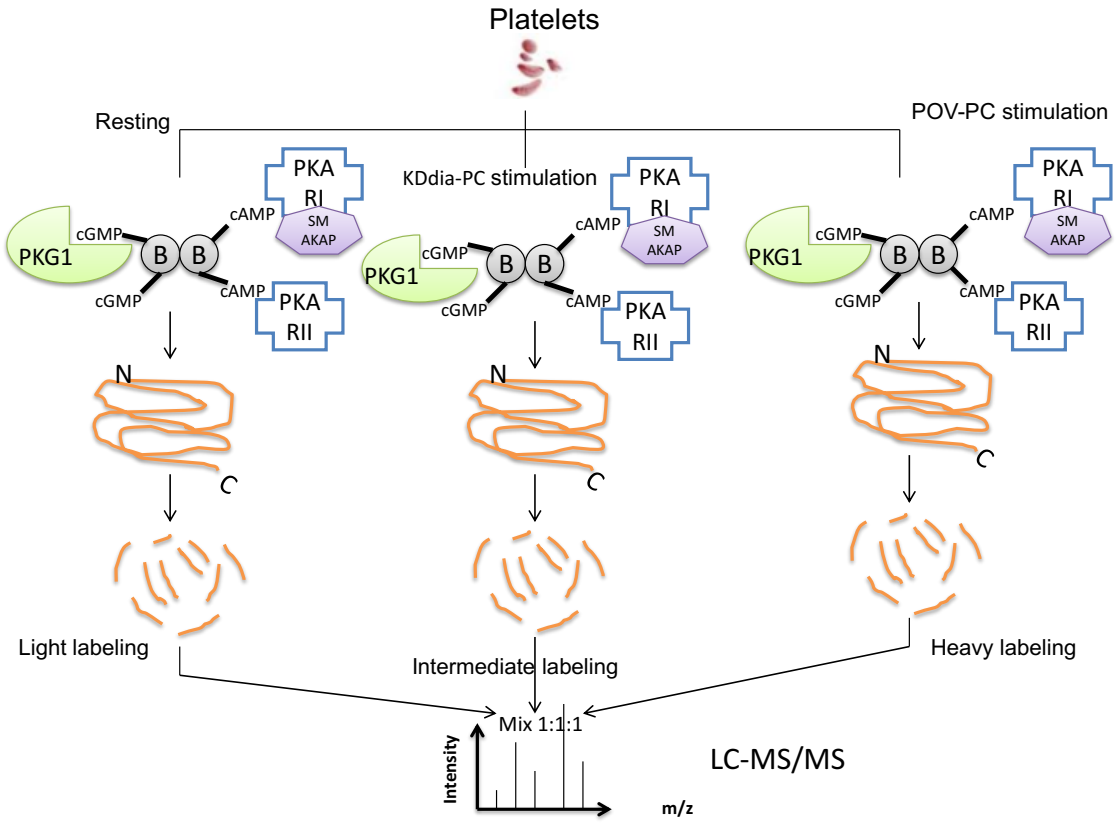

Figure 4-8. Workflow of enrichment and quantitation of cAMP and cGMP interactors in resting and KDdiA-PC/POV-PC stimulated platelets.

Based on the experimental result of our lab that KDdiA-PC and POV-PC increased both cAMP and cGMP levels in platelets (Li, 2016), I hypothesized that lower amounts of PKA and PKG would be precipitated by cAMP/cGMP beads from platelets upon KDdiA-PC or POV-PC treatment.

The cAMP/cGMP signaling proteins showed in Table 4-5 were precipitated from all of the platelets that were isolated from 50ml whole blood. For comparing the cAMP/cGMP interactors in resting platelets to those in KDdiA-PC and POV-PC stimulated platelets, the platelets isolated from 50ml whole blood had to be divided into three equal portions to prepare the three samples. Therefore, some very low abundant cAMP/cGMP interactors could not be identified and quantified.

Comparing to the cAMP/cGMP binding proteins in resting platelets, the amount of the primary interactors PDE2A, PKA-RIα and -RIIα in POV-PC-stimulated platelets decreased significantly (Figure 4-9). Also, the amount of the secondary interactor small membrane AKAP, a PKA-RI binding protein, decreased significantly upon POV-PC stimulation revealing the reduction of PKA-RIα. The amount of PDE2A and PKA-RIα in KDdiA-PC stimulated platelets decreased slightly (ratio 0.77 and 0.65 respectively), but the change is not significant (p value 0.064 and 0.055 respectively). PKA-RIIβ, PDE5A, and PKG1 did not exhibit an alternation upon both KDdiA-PC and POV-PC stimulation.

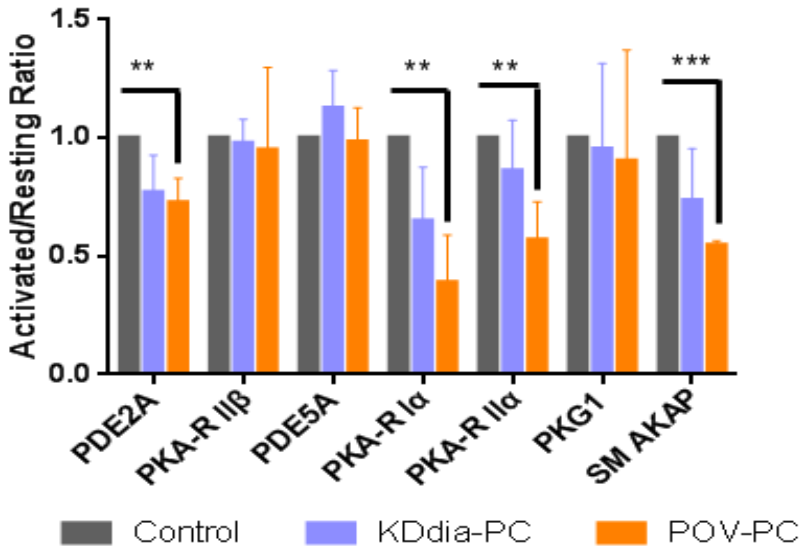

Figure 4-9. POV-PC stimulation reduced the amount of PDE2A, PKA-RIα, PKA-RIIα and small membrane AKAP in platelets.

Platelets were treated with 5μM KDdia-PC or POV-PC for 15 minutes. (one-way ANOVA with Dunnett's test, Significant changes are marked with a ** for $p < 0.01$ and *** for $p < 0.001$, n=4).

The decrease of PKA-RIα and -RIIα in POV-PC-stimulated platelets indicated that the intracellular cAMP level was increased, as more cAMP bound to PKA caused more PKA to dissociate and RIα and RIIα to decrease. Furthermore, cAMP binding released the catalytic subunit PKA-C to activate downstream proteins, hence the overall PKA activity in POV-PC-treated platelets increased. However, the intracellular cGMP level was not changed since the amount of PKG1 remain same after KDdiA-PC or POV-PC stimulation. These findings do not completely match my hypothesis, but are in agreement with the earlier report that oxidized LDL concentration-dependently inhibits collagen-stimulated platelet aggregation through increasing the formation of cAMP but not cGMP (Chou, et al., 2004). The amount of PDE2A precipitated by the beads decreased significantly in platelets with POV-PC stimulation. Decreased affinity towards cAMP/cGMP, in solution or on the beads, or lower availability in the soluble proteome

could cause the cAMP level increase since PDE2A mainly hydrolyses cAMP. Nevertheless, the cAMP/cGMP interactors in KDdiA-PC-activated platelets did not show any significant response, which demonstrated that different oxPCs have different effect on cAMP/cGMP binding proteins.

As the cAMP/cGMP interactors in POV-PC-activated platelets showed significant response, they were further investigated. To determine if the POV-PC affects the components of the cGMP pathway and how it affects them, I used the soluble guanylyl cyclase (sGC)-specific inhibitor ODQ, 1H-[1,2,4]oxadiazolo-[4,3-a]quinoxalin-1-one, to inhibit sGC by reducing cGMP synthesis in POV-PC-treated platelets. ODQ was pre-incubated with platelets before POV-PC stimulation. The amount of PKA-RIIβ, PDE5A, PKG1, and PKA-RIβ in POV-PC-stimulated platelets decreased significantly upon ODQ treatment (Table 4-6). All of these cAMP/cGMP binding proteins displayed a POV + Inhibitor/resting abundance ratio of around 1.0, indicating complete inhibition.

Table 4-6. The sGC inhibitor ODQ significantly suppressd the effect of POV-PC on PDE5A, PKA-RIβ, PKA-RIIβ, and PKGI in platelets.

Protein name	POV + Inhibitor/POV	POV + Inhibitor/None	Inhibition effect
PDE2A	0.763 ± 0.205	0.91 ± 0.692	-
PKA-RIIβ	0.842 ± 0.077 ***	1.02 ± 0.289	Complete inhibition
PDE5A	0.838 ± 0.149 *	0.857 ± 0.248	Complete inhibition
PKA-RIα	0.903 ± 0.201	1.157 ± 0.395	-
PKA-RIIα	1.025 ± 0.113	1.028 ± 0.156	-
PKGI	0.748 ± 0.183 **	0.903 ± 0.417	Complete inhibition
small membrane AKAP	1.115 ± 0.262	1.205 ± 0.12	-
PKA-RIβ	0.925 ± 0.007 **	0.755 ± 0.163	Complete inhibition

Notes: POV: platelets were treated with POV-PC; POV + Inhibitor: platelets were treated with POV-PC in the presence of ODQ; None: platelets without treatment. The ratios of the amount of the pulled-down proteins in platelets with different treatments are calculated and compared with 1 (one-way ANOVA with Dunnett's test, Significant changes are marked with a * $p < 0.05$, ** $p < 0.01$, *** $p < 0.001$, n=6).

Upon ODQ treatment, the amount of PKG1 in POV-PC-stimulated platelets decreased significantly. The reduction of PKG1 indicated that the intracellular cGMP level in POV-PC- and ODQ-treated platelets was higher than that in POV-PC-stimulated platelets. Moreover, PKG1 demonstrated a POV + Inhibitor/resting abundance ratio of around 1.0, revealing that the cGMP level did not change in platelets with POV-PC and ODQ treatment. This result implies that the cGMP level decreases in platelets upon POV-PC stimulation.

Another interesting observation is that the amount of PKA-RIIβ and PKA-RIβ in POV-PC-stimulated platelets decreased significantly upon ODQ treatment. The reduced amounts of PKA-RIIβ and PKA-RIβ indicated that the intracellular cAMP level also increased upon ODQ treatment. Since ODQ only inhibits sGC, not AC, the ODQ treatment should not affect the cAMP level. This effect of ODQ treatment on cAMP proved the cross-talk between the cAMP and cGMP signaling pathways. The cAMP and cGMP cross-communication is facilitated by

PDE2A and PDE3A. Upon ODQ treatment, the intracellular cGMP level in POV-PC stimulated platelets was increased. There are two scenarios: cGMP may decrease the cAMP level through activating PDE2A resulting in an increase in the PKA-RIβ and PKA-RIIβ, or cGMP may increase cAMP level by suppressing PDE3A resulting in a decrease in the PKA-RIβ and PKA-RIIβ. The result of the PKA-RIβ and PKA-RIIβ reduction revealed that cGMP regulated the cAMP level mainly through PDE3A in this condition. However, PDE2A was also involved in cAMP regulation. Upon POV-PC stimulation, PDE2A decrease without cGMP alternation leaded to the cAMP level elevation resulting in a decrease in the PKA-RIα and RIIα. This proves that PDE2A and PDE3A are present in different compartments of the platelets (Colman, R. W., 2004). Cyclic GMP can regulate the cAMP level, but the change of platelet cAMP level has no effect on the cGMP pathway (Wangorsch et al., 2011). Therefore, POV-PC not only affects the cAMP level directly but also indirectly through affecting cGMP.

My data also showed that the amount of affinity-enriched PDE5A decreased significantly in POV-PC-stimulated platelet in the presence of ODQ. PDE5A specifically degrades cGMP. Therefore, the intracellular cGMP level in POV-PC-and ODQ-treated platelets was higher than that in POV-PC-stimulated platelets, which matches my previous result that the cGMP level decreased in platelets upon POV-PC stimulation.

4.3 Conclusions

In this study, a targeted quantitative chemical proteomics approach was developed, and it was used to determine the the response of cAMP/cGMP interactome in platelets with KDdiA-PC or POV-PC stimulation. The following conclusions were reached.

First, ADP and GDP elution could efficiently remove non-specific binding proteins without disturbing cAMP/cGMP binding proteins.

Second, stable isotope dimethyl labeling was validated for its compatibility with the enrichment method.

Third, the newly developed pull-down assay was validated by precipitating cAMP/cGMP binding proteins in platelets. Some very low abundant secondary interactors such as MRVI1, PKGI and IP_3-RI could be purified by using this assay. Therefore, this enrichment method was efficient for precipitation of cAMP/cGMP binding proteins.

Fourth, comparing to cAMP/cGMP binding proteins in resting platelets, the amount of PKA-RIα and PKA-RIIα in POV-PC-stimulated platelets decreased, which indicated the increase of the intracellular cAMP level in platelets with POV-PC stimulation. Upon ODQ treatment, the amount of PKG1 in POV-PC-stimulated platelets decreased, which indicated the increase of the intracellular cGMP level in POV-PC-stimulated platelets with ODQ treatment. The amount of PKG1 in POV-PC-and ODQ-treated platelets and in resting platelets was almost identical, which implies the decrease of the cGMP level in platelets with POV-PC stimulation.

Fifth, upon ODQ treatment, the amount of PKA-RIIβ and PKA-RIβ in POV-PC-stimulated platelets decreased, which indicated the increase of the cAMP level in POV-PC-and ODQ-treated platelets. Therefore, ODQ, as a sGC inhibitor, affected the cAMP level through affecting the cGMP level, which proved the cross-talk between the cAMP and cGMP signaling pathways.

Chapter 5: Conclusions and future work

In this thesis, I studied the effect of platelet releasate on monocytes and explored the impact on platelet activation imparted by oxPC. To reach these aims, two proteomics methods, a quantitative multiplexed small GTPase activity assay and a targeted quantitative chemical proteomics approach, were employed.

The quantitative multiplexed small GTPase activity assay is a combination of functional proteomics and MRM targeted quantitative proteomics. Using this assay, multiple active small GTPases can be quantified in parallel and from a single sample run, and different small GTPase isoforms can be distinguished. The targeted quantitative chemical proteomics approach is a combination of chemical proteomics and stable isotope dimethyl labeling quantitative proteomics. Using this approach, several cAMP/cGMP binding proteins can be quantified and, in some cases, low abundant secondary interactors can also be precipitated and identified.

In this thesis, the quantitative multiplexed small GTPase activity assay was employed to precipitate multiple active small GTPase isoforms in monocytes and quantify their activity change with platelet releasate treatment. Upon platelet releasate stimulation, the activation levels of Rap1B and Rap2B in monocytes increased. After an anti-CXCL12 blocking antibody treatment, the activation levels of all Rap small GTPases, Rap1A, Rap1B, and Rap2B, in platelet releasate-stimulated monocytes were significantly decreased. These results suggest that LPA-induced platelet releasate activates Rap GTPases in monocytes through CXCL12. Since Rap GTPases are associated with monocyte migration, CXCL12 in platelet releasate might become a potential drug target. Therefore, this finding can potentially be developed into an effective

strategy to control monocyte transmigration in atherosclerosis and atherosclerotic lesion formation.

The platelet releasate consists of a large number of cytokines and chemokines, which promote monocyte migration and induce monocyte differentiation. Some small GTPases in monocytes may also be involved in monocyte differentiation. Therefore, the quantitative multiplexed small GTPase activity assay can be used as a general tool to explore cytokines and chemokines as potential drug targets to prevent undesirable monocyte differentiation in the future.

The targeted quantitative chemical proteomics approach was developed for studying the effect of oxPC on cAMP/cGMP interactome in platelets. Multiple cAMP/cGMP binding proteins in platelets could be precipitated and enriched, and their response to oxPC treatment was monitored by dimethyl labeling quantification. Upon POV-PC stimulation, the amount of the primary interactors PDE2A, PKA-RIα and RIIα, and the amount of the secondary interactor small membrane AKAP (smAKAP) precipitated from platelets decreased. The reduced association of the PKA-RIα and RIIα to PKA-C indirectly indicated that intracellular cAMP in platelets increased with POV-PC treatment. However, incubation with the sGC inhibitor ODQ decreased the amount of PKA-RIIβ, PDE5A, PKG1, and PKA-RIβ in POV-PC-stimulated platelets significantly. The reduction of PKG1 is consistent with the increase of intracellular cGMP in POV-PC-stimulated platelets with ODQ treatment, which implies that the cGMP level in platelets decreases upon POV-PC stimulation. Furthermore, the effect of ODQ on PKA-RIβ and PKA-RIIβ demonstrated the cross-talk between the cAMP and cGMP signaling pathways. All these findings could be explained by cyclic nucleotide regulated protein PDEs. PDE2A

hydrolyzes cAMP. Therefore, the decrease of PDE2A leads to the increase of the cAMP level in POV-PC-stimulated platelets. PDE5A degrades cGMP. Therefore, the decrease of PDE5A results in the increase of the cGMP level in POV-PC-and ODQ-stimulated platelets. cGMP regulates the cAMP level through PDE2A and PDE3A.

Based on the findings above, a pathway of how oxLDL/oxPC affects platelets through binding to CD36 can be proposed, in which CD36 is coupled to an unknown protein (or peptide) and in turn activates AC and inhibits sGC resulting in an increase of the cAMP level and a decrease of the cGMP level. Miller et al. (2010) demonstrated that amyloid-β (Aβ) peptides inhibit NO-cGMP signaling in a CD36-dependent manner. Therefore, amyloid-β might be the unknown protein that connects CD36 and the cAMP/cGMP pathway (Figure 5.1), but further analysis is needed to confirm this in the future.

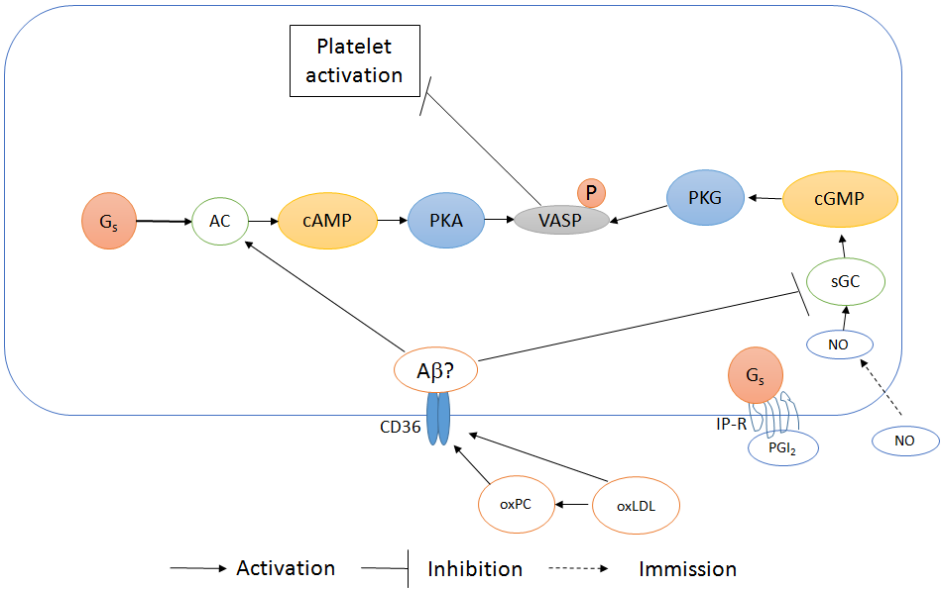

Figure 5-1. The mechanism of oxLDL/oxPC affects platelets through cyclic AMP and cyclic GMP pathways.

Platelets play key roles in thrombosis and hemostasis. Therefore, preventing accidental platelet activation and maintaining the balance between activation and inhibition are important. Various pharmacological treatments related to cAMP signaling in platelets are used for this purpose. Those antiplatelet drugs include cyclooxygenase inhibitors (Aspirin), ADP receptor inhibitors (Clopidogrel), Phosphodiesterase inhibitors (Cilostazol), and integrin αIIbβ3 inhibitors (Tirofiban). Platelet drugs applied in combination can decrease drug dosage and undesirable side effects like bleeding (Lobato et al., 2006). Platelet drug combinations can not only be inhibitor-inhibitor, but inhibitor-activator and activator-activator as well. However, how to combine those different drugs is a big challenge for clinical research. To find effective drug combinations, a full systems model of platelets is needed. Hence, the detailed understanding of the interactions between PDEs and cAMP/cGMP levels, and their effects on platelet activation and inhibition have clinical significance. Future work will extend the cAMP/cGMP interactor study to cover more low abundant downstream effector proteins.

There are two limitations in this study. First, not all 11 active small GTPases in monocytes were present in sufficient quantity to be detected by MRM assay. During the pulldown procedure, the active small GTPases were pulled down with the binding domains and separated by SDS-PAGE from the co-eluting binding domains that were non-covalently attached to the glutathione resin. Some proteins might also have been lost during in-gel digestion. If the binding domains can be covalently linked to the glutathione resin by crosslinking, the SDS-PAGE and in-gel digestion steps can be replaced by in-solution digestion to increase protein recovery. Second, some very low abundant cAMP/cGMP secondary interactors were identified but could not be quantified due to insufficient numbers of platelets. This proved that the protein purification part of the targeted

quantitative chemical proteomics approach was efficient. Since MRM assays can specifically and sensitively quantify targeted proteins, replacing dimethyl labeling and combining MRM with the chemical proteomics step can potentially improve the sensitivity of this approach.

In this thesis I studied the function of platelets and monocytes in atherosclerosis. Both LPA and oxPC are oxLDL derivatives and components of atherosclerotic plaques. Numerous reports have pinpointed LPA as a platelet agonist, which implies that the major downstream signaling pathway of LPA-stimulated platelet activation may be G_q, $G_{12/13}$, or G_i. In contrast, the effect of oxPC on platelets is still under debate, and it has been suggested that the major downstream signaling pathway of oxPC in platelets may be G_s due to the compartmentalization character of cyclic nucleotide signaling. However, there are still some connections between the different G protein pathways; for example, G_i inhibits cAMP synthesis. Therefore, LPA and oxPC may actually share some signaling pathways to affect platelets. There is a scenario in which platelets are challenged by both LPA and oxPC, a situation that may in fact exist during atherosclerotic plaque rupture. They may affect platelet activation antagonistically or synergistically, and their effect on cAMP/cGMP interactome in platelets can be analyzed by the targeted quantitative chemical proteomics approach. Their effect (through platelet releasate) on the change in activity of multiple small GTPases in monocytes can also be quantified by the quantitative multiplexed small GTPase activity assay.

In conclusion, this study has added to our knowledge of the function of platelets and monocytes as well as their interactions. This information can potentially contribute to the discovery of more

efficient therapies for atherosclerosis. In addition, the proteomics tools employed in this research may expand their application in other areas, including cancer research.

Bibliography

Aebersold, R., Mann, M., 2016. Mass-spectrometric exploration of proteome structure and function. Nature 537(7620), 347-355.

Alberts, B., 1998. The cell as a collection of protein machines: preparing the next generation of molecular biologists. Cell 92(3), 291-294.

Altelaar, A. F., Munoz, J., Heck, A. J., 2013. Next-generation proteomics: towards an integrative view of proteome dynamics. Nature Reviews Genetics 14(1), 35-48.

Amisten, S., Braun, O. O., Bengtsson, A., Erlinge, D., 2008. Gene expression profiling for the identification of G-protein coupled receptors in human platelets. Thrombosis Research 122(1), 47-57.

Ammendola, A., Geiselhoringer, A., Hofmann, F., Schlossmann, J., 2001. Molecular determinants of the interaction between the inositol 1,4,5-trisphosphate receptor-associated cGMP kinase substrate (IRAG) and cGMP kinase Iβ. The Journal of Biological Chemistry 276, 24153-24159.

Anderson, N. L., Anderson, N. G., 1998. Proteome and proteomics: New technologies, new concepts, and new words. Electrophoresis 19(11), 1853-1861.

Aoki, J., Taira, A., Takanezawa, Y., Kishi, Y., Hama, K., Kishimoto, T., Mizuno, K., Saku, K., Taguchi, R., Arai, H., 2002. Serum lysophosphatidic acid is produced through diverse phospholipase pathways. The Journal of Biological Chemistry 277, 48737-48744.

Arora, K., Sinha, C., Zhang, W., Ren, A., Moon, C. S., Yarlagadda, S., Naren, A. P., 2013. Compartmentalization of cyclic nucleotide signaling: a question of when, where, and why? Pflügers Archiv: European Journal of Physiology 465(10), 1397-1407.

Arthur, W. T., Quilliam, L. A., Cooper, J. A., 2004. Rap1 promotes cell spreading by localizing Rac guanine nucleotide exchange factors. The Journal of Cell Biology 167(1), 111-122.

Asha, H., de Ruiter, N. D., Wang, M. G., Hariharan, I. K., 1999. The Rap1 GTPase functions as a regulator of morphogenesis in vivo. The EMBO Journal 18(3), 605-615.

Ashraf, M. Z., Kar, N. S., Podrez, E. A., 2008. Oxidized Phospholipids: Biomarker for Cardiovascular Diseases. The International Journal of Biochemistry & Cell Biology 41(6), 1241-1244.

Badimon, L., Padró, T., Vilahur, G., 2012. Atherosclerosis, platelets and thrombosis in acute ischaemic heart disease. European Heart Journal: Acute Cardiovascular Care 1(1), 60-74.

Bandoh, K., Aoki, J., Taira, A., Tsujimoto, M., Arai, H., Inoue, K., 2000. Lysophosphatidic acid (LPA) receptors of the EDG family are differentially activated by LPA species. Structure-activity relationship of cloned LPA receptors. FEBS Letters 478(1-2), 159-165.

Beck, S., Michalski, A., Raether, O., Lubeck, M., Kaspar, S., Goedecke, N., Baessmann, C., Hornburg, D., Meier, F., Paron, I., Kulak, N. A., Cox J., Mann, M., 2015. The impact II, a very high resolution quadrupole time-of-flight instrument for deep shotgun proteomics. Molecular and Cellular Proteomics 14(7), 2014-2029.

Ben-David, Y., Letwin, K., Tannock, L., Bernstein, A., Pawson, T., 1991. A mammalian protein kinase with potential for serine/threonine and tyrosine phosphorylation is related to cell cycle regulators. The EMBO Journal 10(2), 317-325.

Blair, P., Flaumenhaft, R., 2009. Platelet alpha-granules: basic biology and clinical correlates. Blood Reviews 23(4), 177-189.

Boersema, P. J., Aye, T. T., van Veen, T. A., Heck, A. J., Mohammed, S., 2008. Triplex protein quantification based on stable isotope labeling by peptide dimethylation applied to cell and tissue lysates. Proteomics 8(22), 4624-4632.

Boersema, P. J., Raijmakers, R., Lemeer, S., Mohammed, S., Heck, A. J., 2009. Multiplex peptide stable isotope dimethyl labeling for quantitative proteomics. Nature Protocols 4(4), 484-494.

Boisvert, F. M., Ahmad, Y., Gierliński, M., Charrière, F., Lamont, D., Scott, M., Barton, G., Lamond, A. I., 2012. A quantitative spatial proteomics analysis of proteome turnover in human cells. Molecular & Cellular Proteomics 11(3), M111.011429.

Bos, J. L., 2005. Linking Rap to cell adhesion. Current Opinion in Cell Biology 17(2), 123-128.

Broijersen, A., Hamsten, A., Eriksson, M., Angelin, B., Hjemdahl, P., 1998. Platelet activity in vivo in hyperlipoproteinemia—importance of combined hyperlipidemia. Journal of Thrombosis and Haemostasis 79(2), 268-275.

Cary, L. A., Cooper, J. A., 2000. Signal transduction: Molecular switches in lipid rafts. Nature 404, 945-947.

Chatterjee, M., Gawaz, M., 2013. Platelet-derived CXCL12 (SDF-1α): basic mechanisms and clinical implications. Journal of Thrombosis and Haemostasis 11(11), 1954-1967.

Chatterjee, M., SNI von Ungern-Sternberg, Seizer, P., Schlegel, F., Büttcher, M., Sindhu, N. A., Müller, S., Mack, A., Gawaz, M., 2015. Platelet-derived CXCL12 regulates monocyte function, survival, differentiation into macrophages and foam cells through differential involvement of CXCR4-CXCR7. Cell Death and Disease 6, e1989.

Chen, R., Roman, J., Guo, J., West, E., McDyer, J., Williams, M. A., Georas, S. N., 2006. Lysophosphatidic acid modulates the activation of human monocyte-derived dendritic cells. Stem Cells and Development 15(6), 797-804.

Cherfils, J., Zeghouf, M., 2013. Regulation of Small GTPases by GEFs, GAPs, and GDIs. Physiological Reviews 93(1), 269-309.

Chien, C. T., Bartel, P. L., Sternglanz, R., Fields, S., 1991. The two-hybrid system: a method to identify and clone genes for proteins that interact with a protein of interest. Proceedings of the National Academy of Sciences of the United States of America 88(21), 9578-9582.

Chou, D. S., Hsiao, G., Shen, M. Y., Fong, T. H., Lin, C. H., Chen, T. F., Sheu, J. R., 2004. Low concentration of oxidized low density lipoprotein suppresses platelet reactivity in vitro: an intracellular study. Lipids 39(5), 433-440.

Chun, J., Goetzl, E. J., Hla, T., Lgarashi, Y., Lynch, K. R., Moolenaar, W., Pyne, S., Tigyi, G., 2002. International union of pharmacology. XXXIV. Lysophospholipid receptor nomenclature. Pharmacological Reviews 54(2), 265-269.

Colman, R. W., 2004. Platelet cyclic adenosine monophosphate phosphodiesterases: Targets for regulating platelet-related thrombosis. Seminars in Thrombosis and Hemostasis 30(4), 451-460.

Conti, M., Jin, S. L., 1999. The molecular biology of cyclic nucleotide phosphodiesterases. Progress in Nucleic Acid Research and Molecular Biology 63, 1-38.

Cox, J., Mann, M., 2008. MaxQuant enables high peptide identification rates, individualized p.p.b.-range mass accuracies and proteome-wide protein quantitation. Nature Biotechnology 26(12), 1367-1372.

Crouse, J. R. 3rd, Raichlen, J. S., Riley, W. A., Evans, G. W., Palmer, M. K., O'Leary, D. H., Grobbee, D. E., Bots, M. L., METEOR Study Group, 2007. Effect of rosuvastatin on progression of carotid intima-media thickness in low-risk individuals with subclinical atherosclerosis: the METEOR Trial. The Journal of the American Medical Association 297(12), 1344-1353.

Cui, M. Z., 2012. Lysophosphatidic acid effects on atherosclerosis and thrombosis. Journal of Clinical Lipidology 6(4), 413-426.

Dangel, O., Mergia, E., Karlisch, K., Groneberg, D., Koesling, D., Friebe, A., 2010. Nitric oxide-sensitive guanylyl cyclase is the only nitric oxide receptor mediating platelet inhibition. Journal of Thrombosis and Haemostasis 8(6), 1343-1352.

Daub, K., Seizer, P., Stellos, K., Krämer, B. F., Bigalke, B., Schaller, M., Fateh-Moghadam, S., Gawaz, M., Lindemann, S., 2010. Oxidized LDL-activated platelets induce vascular inflammation. Seminars in Thrombosis and Hemostasis 36(2), 146-156.

Davi, G., Patrono, C., 2007. Platelet activation and atherothrombosis. New England Journal of Medicine 357(24), 2482-2494.

Delprato, A., 2012. Topological and Functional Properties of the Small GTPases Protein Interaction Network. PLoS ONE 7(9), e44882.

Fenn, J. B., Mann, M., Meng, C. K., Wong, S. F., Whitehouse, C. M., 1989. Electrospray ionization for mass spectrometry of large biomolecules. Science 246(4926), 64-71.

Furie, B., Furie, B. C., 2005. Thrombus formation in vivo. The Journal of Clinical Investigation 115(12), 3355-3362.

Gachet, C., 2006. Regulation of platelet functions by P2 receptors. Annual Review of Pharmacology and Toxicology 46, 277-300.

Gawaz, M., Langer, H., May, A. E., 2005. Platelets in inflammation and atherogenesis. Journal of Clinical Investigation 115(12), 3374-3384.

Gerber, S. A., Rush, J., Stemman, O., Kirschner, M. W., Gygi, S. P., 2003. Absolute quantification of proteins and phosphoproteins from cell lysates by tandem MS. Proceedings of the National Academy of Sciences of the United States of America 100(12), 6940-6945.

Ghattas, A., Griffiths H. R., Devitt, A., Lip, G. Y., Shantsila, E., 2013. Monocytes in coronary artery disease and atherosclerosis: where are we now? Journal of the American College of Cardiology 62(17), 1541-1551.

Gleissner, C. A., Shaked, I., Erbel, C., Bockler, D., Katus, H. A., Ley, K., 2010. CXCL4 downregulates the atheroprotective hemoglobin receptor CD163 in human macrophages. Circulation Research 106(1), 203-211.

Graves, P. R., Haystead, T. A. J., 2003. A functional proteomics approach to signal transduction. Recent Progress in Hormone Research 58, 1-24.

Gustin, C., Van Steenbrugge, M., Raes, M., 2008. LPA modulates monocyte migration directly and via LPA-stimulated endothelial cells. American Journal of Physiology - Cell Physiology 295, C905-C914.

Halvorsen, B., Smedbakken, L. M., Michelsen, A. E., Skjelland, M., Bjerkeli, V., Sagen, E. L., Tasken, K., Bendz, B., Gullestad, L., Holm, S., Biessen, E. A., Aukrust, P., 2014. Activated platelets promote increased monocyte expression of CXCR5 through prostaglandin E2-related mechanisms and enhance the anti-inflammatory effects of CXCL13. Atherosclerosis 234(2), 352-359.

Haserück, N., Erl, W., Pandey, D., Tigyi, G., Ohlmann, P., Ravanat, C., Gachet, C., Siess, W., 2004. The plaque lipid lysophosphatidic acid stimulates platelet activation and platelet-monocyte aggregate formation in whole blood: involvement of P2Y1 and P2Y12 receptors. Blood 103(7), 2585-2592.

Haslam, R. J., Dickinson, N. T., Jang, E. K., 1999. Cyclic nucleotides and phosphodiesterases in platelets. Thrombosis and Haemostasis 82(2), 412-423.

Hazen S. L., 2008. Oxidized phospholipids as endogenous pattern recognition ligands in Innate Immunity. The Journal of Biological Chemistry 283, 15527–15531.

Hsu, J., Huang, S., Chow, N., Chen, S., 2003. Stable-Isotope Dimethyl Labeling for Quantitative Proteomics. Analytical Chemistry 75(24), 6843-6852.

Huo, Y., Ley, K. F., 2004. Role of platelets in the development of atherosclerosis. Trends in Cardiovascular Medicine 14(1), 18-22.

Jose, P. A., Felder, R. A., Felder, C. C., Chan, W. Y., 1990. Molecular-biology of adrenergic and dopamine-receptors and the study of developmental nephrology. Pediatric Nephrology 4(6), 679-685.

Kaplan, Z. S., Jackson, S. P., 2011. The role of platelets in atherothrombosis. Hematology American Society of Hematology Education Program 2011, 51-61.

Karas, M., Hillenkamp, F., 1988. Laser desorption ionization of proteins with molecular masses exceeding 10,000 daltons. Analytical Chemistry 60(20), 2299-2301.

Khandoga, A. L., Fujiwara, Y., Goyal, P., Pandey, D., Tsukahara, R., Bolen, A., Guo, H., Wilke, N., Liu, J., Valentine, W. J., Durgam, G. G., Miller, D. D., Jiang, G., Prestwich, G. D., Tigyi, G., Siess, W., 2008. Lysophosphatidic acid-induced platelet shape change revealed through $LPA_{1\text{-}5}$ receptor-selective probes and albumin. Platelets 19(6), 415-427.

Khosrovi-Eghbal, A., 2012. Exploring the interaction environment of blood cells : proteomic analysis of platelet releasate and platelet-monocyte interaction. Master thesis. The University of British Columbia, Vancouver, Canada

Klages, B., Brandt, U., Simon, M. I., Schultz, G., Offermanns, S., 1999. Activation of G_{12}/G_{13} results in shape change and Rho/Rho-kinase-mediated myosin light chain phosphorylation in mouse platelets. The Journal of Cell Biology 144(4), 745-754.

Kocher, T., Superti-Furga, G., 2007. Mass spectrometry-based functional proteomics: from molecular machines to protein networks. Nature Methods 4(10), 807-815.

Kondrat, R. W., McClusky, G. A., Cooks, R. G., 1978. Multiple reaction monitoring in mass spectrometry/mass spectrometry for direct analysis of complex mixtures. Analytical Chemistry 50(14), 2017-2021.

Korporaal, S. J. A., Gorter, G., Van Rijn, H. J. M., Akkerman, J. N., 2005. Effect of oxidation on the platelet-activating properties of low-density lipoprotein. Arteriosclerosis, Thrombosis, and Vascular Biology 25(4), 867-872.

Korporaal, S. J. A., Van Eck, M., Adelmeijer, J., Ijsseldijk, M., Out, R., Lisman, T., Lenting, P. J., Van Berkel, T. J. C., Akkerman, J. N., 2007. Platelet activation by oxidized low density lipoprotein is mediated by CD36 and scavenger receptor-A. Arteriosclerosis, Thrombosis, and Vascular Biology 27(11), 2476-2483.

Kroll, M. H., Hellums, J. D., Mclntire, L. V., Schafer, A., Moake, J. L., 1996. Platelets and shear stress. Blood 88(5), 1525-1541.

Kunjathoor, V. V., Febbraio, M., Podrez, E. A., Moore, K. J., Andersson, L., Koehn, S., Rhee, J. S., Silverstein, R., Hoff, H. F., Freeman, M. W., 2002. Scavenger receptors class A-I/II and CD36 are the principal receptors responsible for the uptake of modified low density lipoprotein leading to lipid loading in macrophages. The Journal of Biological Chemistry 277(51), 49982-49988.

Lam, F. W., Vijayan, K. V., Rumbaut, R. E., 2015. Platelets and their interactions with other immune cells. Comprehensive Physiology 5(3), 1265-1280.

Larance, M., Lamond, A. I. 2015. Multidimensional proteomics for cell biology. Nature Reviews Molecular Cell Biology 16, 269-280.

Lee, H., Liao, J. J., Graeler, M., Huang, M. C., Goetzl, E. J., 2002. Lysophospholipid regulation of mononuclear phagocytes. Biochimica et Biophysica Acta 1582(1-3), 175-177.

Lewis, T. S., Hunt, J. B., Aveline, L. D., Jonscher, K. R., Louie, D. F., Yeh, J. M., Nahreini, T. S., Resing, K. A., Ahn, N. G., 2000. Identification of novel MAP kinase pathway signaling targets by functional proteomics and mass spectrometry. Molecular Cell 6(6), 1343-1354.

Li, R., 2016. A novel inhibitory mechanism of oxPC identified on platelet activation and its association with ROS. PhD thesis. The University of British Columbia, Vancouver, Canada

Li, R., Klockenbusch, C., Lin, L., Jiang, H., Lin, S., Kast, J., 2016. Quantitative protein sulfenic acid analysis identifies platelet releasate-induced activation of integrin beta (2) on monocytes via NADPH oxidase. Journal of Proteome Research 15(12), 4221-4233.

Li, Z., Delaney, M. K., O'Brien, K. A., Du, X., 2010. Signaling during platelet adhesion and activation. Arteriosclerosis, Thrombosis, and Vascular Biology 30(12), 2341-2349.

Lievens, D., von Hundelshausen, P., 2011. Platelets in atherosclerosis. Journal of Thrombosis and Haemostasis 106(5), 827-838.

Lin, C. L., Chen, C. N., Chen, J. H., Lee, H., 2006. Lysophospholipids increase IL-8 and MCP-1 expressions in human umbilical cord vein endothelial cells through an IL-1-dependent mechanism. Journal of Cellular Biochemistry 99(4), 1216-1232.

Lin, K. B., Tan, P., Freeman, S. A., Lam, M., McNagny, K. M., Gold, M. R., 2010a. The Rap GTPases regulate the migration, invasiveness and in vivo dissemination of B-cell lymphomas. Oncogene 29(4), 608-615.

Lin, K. B. L., Freeman, S. A., Gold, M. R., 2010b. Rap GTPase-mediated adhesion and migration. Cell Adhesion & Migration 4(3), 327-332.

Link, A. J., Eng, J., Schieltz, D. M., Carmack, E., Mize, G. J., Morris, D. R., Garvik, B. M., Yates, J. R. 3rd, 1999. Direct analysis of protein complexes using mass spectrometry. Nature Biotechnology 17(7), 676-682.

Lobato, E. B., Beaver, T., Muehlschlegel, J., Kirby, D. S., Klodell, C., Sidi, A., 2006. Treatment with phosphodiesterase inhibitors type III and V: milrinone and sildenafil is an effective combination during thromboxane-induced acute pulmonary hypertension. British Journal of Anaesthesia 96(3), 317-322.

MacLean, B., Tomazela, D.M., Shulman, N., Chambers, M., Finney, G.L., Frewen, B., Kern, R., Tabb, D.L., Liebler, D.C., MacCoss, M.J., 2010. Skyline: an open source document editor for creating and analyzing targeted proteomics experiments. Bioinformatics 26(7), 966-968.

Magwenzi, S., Woodward, C., Wraith, K. S., Aburima, A., Raslan, Z., Jones, H., McNeil, C., Wheatcroft, S., Yuldasheva, N., Febbriao, M., Kearney, M., Naseem, K., 2015. Oxidised LDL activates blood platelets through CD36-NADPH oxidase-mediated inhibition of the cGMP/Protein kinase G signaling cascade. Blood 125, 2693-2703.

Mahajan, S., Tuteja, N., 2005. Cold, salinity and drought stresses: An overview. Archives of Biochemistry and Biophysics 444(2), 139-158.

Margarucci, L., Roest, M., Preisinger, C., Bleijerveld, O. B., van Holten, T. C., Heck, A. J., Scholten, A., 2011. Collagen stimulation of platelets induces a rapid spatial response of cAMP and cGMP signaling scaffolds. Molecular Biosystems 7(7), 2311-2319.

Martínez-Aguilar, J., Molloy, M. P., 2013. Label-free selected reaction monitoring enables multiplexed quantitation of S100 protein isoforms in cancer cells. Journal of Proteome Research 12(8), 3679-3688.

Martino, A., Volpe, E., Baldini, P. M., 2006. The influence of lysophosphatidic acid on the immunophenotypic differentiation of human monocytes into dendritic cells. Haematologica 91(9), 1273-1274.

May, A. E., Seizer, P., Gawaz, M., 2008. Platelets: inflammatory firebugs of vascular walls. Arteriosclerosis, Thrombosis, and Vascular Biology 28(3), s5-10.

McClelland, S., Cox, C., O'Connor, R., de Gaetano, M., McCarthy, C., Cryan, L., Fitzgerald, D., Belton, O., 2010. Conjugated linoleic acid suppresses the migratory and inflammatory phenotype of the monocyte/macrophage cell. Atherosclerosis 211(1), 96-102.

McLeod, S. J., Li, A. H. Y., Lee, R. L., Burgess, A. E., Gold, M. R., 2002. The Rap GTPases regulate B cell migration toward the chemokine stromal cell-derived factor-1 (CXCL12): potential role for Rap2 in promoting B cell migration. The Journal of Immunology 169(3) 1365-1371.

Mendes-Silverio, C. B., Leiria, L. O., Morganti, R. P., Anhê, G. F., Marcondes, S., Mónica, F. Z., De Nucci, G., Antunes, E., 2012. Activation of haem-oxidized soluble guanylyl cyclase with BAY 60-2770 in human platelets lead to overstimulation of the cyclic GMP signaling pathway. PloS One 7(11), e47223.

Miller, T. W., Isenberg, J. S., Shih, H. B., Wang, Y., Roberts, D. D., 2010. Amyloid-β inhibits No-cGMP signaling in a CD36- and CD47-dependent manner. PloS One 5(12), e15686.

Mongillo, M., McSorley, T., Evellin, S., Sood, A., Lissandron, V., Terrin, A., Huston, E., Hannawacker, A., Lohse, M. J., Pozzan, T., Houslay, M. D., Zaccolo, M., 2004. Fluorescence resonance energy transfer-based analysis of cAMP dynamics in live neonatal rat cardiac myocytes reveals distinct functions of compartmentalized phosphodieaterases. Circulation Research 95(1), 67-75.

Monti, M., Orrù, S., Pagnozzi, D., Pucci, P., 2005. Functional proteomics. Clinica Chimica Acta 357(2), 140-150.

Monti, M., Cozzolino M., Cozzolino, F., Tedesco, R., Pucci, P., 2007. Functional proteomics: protein-protein interactions in vivo. The Italian Journal of Biochemistry 56(4), 310-314.

Moro, M. A., Russell, R. J., Cellek, S., Lizasoain, I., Su, Y., Darley-Usmar, V. M., Radomski, M. W., Moncada, S., 1996. cGMP mediates the vascular and platelet actions of nitric oxide: confirmation using an inhibitor of the soluble guanylyl cyclase. Proceedings of the National Academy of Sciences of the USA 93, 1480-1485.

Munro, J. M., Cotran, R. S., 1988. The pathogenesis of atherosclerosis: atherogenesis and inflammation. Laboratory Investigation 58(3), 249-261.

Naseem, K. M., Goodall, A. H., Bruckdorfer, K. R., 1997. Differential effects of native and oxidatively modified low-density lipoproteins on platelet function. Platelets 8(2-3), 163-173.

Neer, E. J., 1995. Heterotrimeric G proteins: organizers of transmembrane signals. Cell 80(2), 249-257.

Nergiz-Unal, R., Lamers, M. M., Van Kruchten, R., Luiken, J. J., Cosemans, J. M., Glatz, J. F., Kuijpers, M. J., Heemskerk, J. W., 2011. Signaling role of CD36 in platelet activation and thrombus formation on immobilized thrombospondin or oxidized low-density lipoprotein. Journal of Thrombosis and Haemostasis 9(9) 1835-1846.

Nishizuka, Y., 1984. The role of protein kinase C in cell surface signal transduction and tumour promotion. Nature 308, 693-698.

Nityanand, S., Pande, I., Bajpai, V. K., Singh, L., Chandra, M., Singh, B. N., 1993. Platelets in essential hypertension. Thrombosis Research 72(5), 447-454.

Noguchi, K., Ishii, S., Shimizu, T., 2003. Identification of p2y9/GPR23 as a novel G protein-coupled receptor for lysophosphatidic acid, structurally distant from the Edg family. The Journal of Biological Chemistry 278(28), 25600-25606.

Nowak, J., Murray, J. J., Oates, J. A., FitzGerald, G. A., 1987. Biochemical evidence of a chronic abnormality in platelet and vascular function in healthy individuals who smoke cigarettes. Circulation 76(1), 6-14.

Offermanns, S., 2006. Activation of platelet function through G protein-coupled receptors. Circulation Research 99(12), 1293-1304.

Ong, S. E., Blagoev, B., Kratchmarova, I., Kristensen, D. B., Steen, H., Pandey, A., Mann, M., 2002. Stable isotope labeling by amino acids in cell culture, SILAC, as a simple and accurate approach to expression proteomics. Molecular & Cellular Proteomics 1(5), 376-386.

Pamukcu, B., Lip, G. Y., Devitt, A., Griffiths, H., Shantsila, E., 2010. The role of monocytes in atherosclerotic coronary artery disease. Annals of Medicine 42(6), 394-403.

Pamuklar, Z., Lee, J. S., Cheng, H., Panchatcharam, M., Steunhubl, S., Morris, A. J., Charnigo, R., Smyth, S. S., 2008. Individual heterogeneity in platelet response to lysophosphatidic acid. Arteriosclerosis, Thrombosis, and Vascular Biology 28(3), 555-561.

Podrez, E. A., Byzova, T. V., Febbraio, M., Salomon, R. G., Ma, Y., Valiyaveettil, M., Poliakov, E., Sun, M., Finton P. J., Curtis, B. R., Chen, J., Zhang, R., Silverstrin, R. L., Hazen, S. L., 2007. Platelet CD36 links hyperlipidemia, oxidant stress and a prothrombotic phenotype. Nature Medicine 13(9) 1086-1095.

Podrez, E. A., Poliakov, E., Shen, Z., Zhang, R., Deng, Y., Sun, M., Finton, P. J., Shan, L., Gugiu, B., Fox, P. L., Hoff, H. F., Salomon, R. G., Hazen, S. L., 2002a. Identification of a novel family of oxidized phospholipids that serve as ligands for the macrophage scavenger receptor CD36. The Journal of Biological Chemistry 277, 38503–38516.

Podrez, E. A., Poliakov, E., Shen, Z., Zhang, R., Deng, Y., Sun, M., Finton, P. J., Shan, L., Febbraio, M., Hajjar, D. P., Silverstein, R. L., Hoff, H. F., Salomon, R. G., Hazen, S. L., 2002b. A novel family of atherogenic oxidized phospholipids promotes macrophage foam cell formation via the scavenger receptor CD36 and is enriched in atherosclerotic lesions. The Journal of Biological Chemistry 277, 38517–38523.

Puig, O., Caspary, F., Rigaut, G., Rutz, B., Bouveret, E., Bragado-Nilsson, E., Wilm, M., Séraphin, B., 2001. The tandem affinity purification (TAP) method: a general procedure of protein complex purification. Methods 24(3), 218-229.

Qin, J., Fenyo, D., Zhao, Y., Hall, W. W., Chao, D. M., Wilson, C. J., Young, R. A., Chait, B. T., 1997. A strategy for rapid, high-confidence protein identification. Analytical Chemistry 69(19), 3995–4001.

Rainger, G. E., Chimen, M., Harrison, M. J., Yates, C. M., Harrison, P., Watson, S. P., Lordkipanidze, M., Nash, G. B., 2015. The role of platelets in the recruitment of leukocytes during vascular disease. Platelets 26(6), 507-520.

Rall, T. W., Sutherland, E. W., 1958. Formation of a cyclic adenine ribonucleotide by tissue particles. The Journal of Biological Chemistry 232, 1065–1076.

Rao, V. S., Srinivas, K., Sujini, G. N., Sunand Kumar, G. N., 2014. Protein-Protein Interaction Detection: Methods and Analysis. International Journal of Proteomics 2014, 147648.

Rappsilber, J., Mann, M., Ishihama, Y., 2007. Protocol for micro-purification, enrichment, pre-fractionation and storage of peptides for proteomics using Stage Tips. Nature Protocols 2(8), 1896-1906.

Ray, R., Rai, V., 2017. Lysophosphatidic acid converts monocytes into macrophages in both mice and humans. Blood 129(9), 1177-1183.

Rendu, F., Brohard-Bohn, B., 2001. The platelet release reaction: granules' constituents, secretion and functions. Platelets 12(5), 261-273.

Retzer, M., Essler, M., 2000. Lysophosphatidic acid-induced platelet shape change proceeds via Rho/Rho kinase-mediated myosin light-chain and moesin phosphorylation. Cell Signal 12(9-10), 645-648.

Rizza, C., Leitinger, N., Yue, J., Fischer, D. J., Wang, D. A., Shih, P. T., Lee, H., Tigyi, G., Berliner, J. A., 1999. Lysophosphatidic acid as a regulator of endothelial/leukocyte interaction. Laboratory Investigation 79(10), 1227-1235.

Roach, P. J., Cao, Y., Corbett, C. A., DePaoli-Roach, A. A., Farkas, I., Fiol, C. J., Flotow, H., Graves, P. R., Hardy, T. A., Hrubey, T. W., Viskupic, E., Zhang, W., 1991. Glycogen metabolism and signal transduction in mammals and yeast. Advances in Enzyme Regulation 31, 101-120.

Roach, P. J., 2002. Glycogen and its metabolism. Current Molecular Medicine 2(2), 101-120.
Rother, E., Brandl, R., Baker, D. L., Goyal, P., Gebhard, H., Tigyi, G., Siess, W., 2003. Subtype-selective antagonists of lysophosphatidic acid receptors inhibit platelet activation triggered by the lipid core of atherosclerotic plaques. Circulation 108(6), 741-747.

Rukoyatkina, N., Walter, U., Friebe, A., Gambaryan, S., 2011. Differentiation of cGMP-dependent and -independent nitric oxide effects on platelet apoptosis and reactive oxygen species production using platelets lacking soluble guanylyl cyclase. Thrombosis and Haemostasis 106, 922-933.

Schwamborn, J. C., Püschel, A. W., 2004. The sequential activity of the GTPases Rap1B and Cdc42 determines neuronal polarity. Nature Neuroscience 7, 923-929.

Shantsila, E., Lip, G. Y., 2009. The role of monocytes in thrombotic disorders. Insights from tissue factor, monocyte-platelet aggregates and novel mechanisms. Thrombosis and Haemostasis 102(5),916-924.

Shevchenko, A., Wilm, M., Vorm, O., Mann, M., 1996. Mass spectrometric sequencing of proteins silver-stained polyacrylamide gels. Analytical Chemistry 68(5), 850–858.

Shevchenko, A., Wilm, M., Mann, M., 1997. Peptide sequencing by mass spectrometry for homology searches and cloning of genes. Journal of Protein Chemistry 16(5), 481–490.

Shevchenko, A., Tomas, H., Havlis, J., Olsen, J. V., Mann, M., 2006. In-gel digestion for mass spectrometric characterization of proteins and proteomes. Nature Protocols 1(6), 2856-2860.
Siess, W., Tigyi, G., 2004. Thrombogenic and atherogenic activities of lysophosphatidic acid. Journal of Cellular Biochemistry 92(6), 1086-1094.

Silverstein, R. L., Febbraio, M., 1992. Identification of lysosome-associated membrane protein-2 as an activation-dependent platelet surface glycoprotein. Blood 80(6), 1470-1475.

Simon, D. I., Ezratty, A. M., Francis, S. A., Rennke, H., Loscalzo, J., 1993. Fibrin(ogen) is internalized and degraded by activated human monocytoid cells via Mac-1 (CD11b/CD18): a non- plasmin fibrinolytic pathway. Blood 82(8), 2414-2422.

Simons, K., Toomre, D., 2000. Lipid rafts and signal transduction. Nature Reviews Molecular Cell Biology 1, 31-39.

Singhal, M., Resat, H., 2007. A domain-based approach to predict protein-protein interactions. BMC Bioinformatics 8(1), 199.

Smedbakken, L. M., Halvorsen, B., Daissormont, I., Ranheim, T., Michelsen, A. E., Skjelland, M., Sagen, E. L., Folkersen, L., Krohg-Sorensen, K., Russell, D., etc., 2012. Increased levels of the homeostatic chemokine CXCL13 in human atherosclerosis - Potential role in plaque stabilization. Atherosclerosis 224(1), 266-273.

Smith, L. M., Kelleher, N. L. & The Consortium for Top Down Proteomics, 2013. Proteoform: a single term describing protein complexity. Nature Methods 10(3), 186-187.

Smolenski, A., 2012. Novel roles of cAMP/cGMP-dependent signaling in platelets. Journal of Thrombosis and Haemostasis 10(2), 167-176.

Smyth, S. S., Cheng, H., Miriyala, S., Panchatcharam, M., Morris, A. J., 2008. Roles of lysophosphatidic acid in cardiovascular physiology and disease. Biochimica et Biophysica Acta 1781(9), 563-570.

Stephen, J., Emerson, B., Fox, K. A., Dransfield, I., 2013. The uncoupling of monocyte-platelet interactions from the induction of proinflammatory signaling in monocytes. The Journal of Immunology 191(11), 5677-5683.

Takai, Y., Sasaki, T., and Matozaki, T., 2001. Small GTP-binding proteins. Physiological Reviews 81(1), 153–208.

Takasago, T., Imagawa, T., Furukawa, K., Ogurusu, T., Shigekawa, M., 1991. Regulation of the cardiac ryanodine receptor by protein kinase-dependent phosphorylation. Journal of Biochemistry 109(1), 163-170.

Thomas, M. R., Storey, R. F., 2015. The role of platelets in inflammation. Thrombosis and Haemostasis 114(3), 449-458.

Tian, J., Gu, X., Sun, Y., Ban, X., Xiao, Y., Hu, S., Yu, B., 2012. Effect of statin therapy on the progression of coronary atherosclerosis. BMC Cardiovascular Disorders 12:70

Tran, J. C., Zamdborg, L., Ahlf, D. R., Lee, J. E., Catherman, A. D., Durbin, K. R., Tipton, J. D., Vellaichamy, A., Kellie, J. F., Li, M., Wu, C., Sweet, S. M., Early, B. P., Siuti, N., LeDuc, R. D., Compton, P. D., Thomas, P. M., Kelleher, N. L., 2011. Mapping intact protein isoforms in discovery mode using top-down proteomics. Nature 480(7376), 254-258.

Tsimikas, S., 2006. Oxidative biomarkers in the diagnosis and prognosis of cardiovascular disease. American Journal of Cardiology 98(11A), 9P-17P.

Tuteja, N., 2009. Signaling through G protein coupled receptors. Plant Signaling & Behavior 4(10), 942-947.

van Gils, J. M., Zwaginga, J. J., Hordijk, P. L., 2009. Molecular and functional interactions among monocytes, platelets, and endothelial cells and their relevance for cardiovascular diseases. Journal of Leukocyte Biology 85(2), 195-204.

Varga-Szabo, D., Pleines, I., Nieswandt, B., 2008. Cell adhesion mechanisms in platelets. Arteriosclerosis, Thrombosis, and Vascular Biology 28(3), 403-412.

Walton, K. A., Cole, A. L., Yeh, M., Subbanagounder, G., Krutzik, S. R., Modlin, R. L., Lucas, R. M., Nakai, J., Smart, E. J., Vora, D. K., Berliner, J. A., 2003. Specific phospholipid oxidation products inhibit ligand activation of toll-like receptors 4 and 2. Arteriosclerosis, Thrombosis, and Vascular Biology 23, 1197–1203.

Wangorsch, G., Butt, E., Mark, R., Hubertus, K., Geiger, J., Dandekar, T., Dittrich, M., 2011. Time-resolved in silico modeling of fine-tuned cAMP signaling in platelets: feedback loops, titrated phosphorylations and pharmacological modulation. BMC Systems Biology 5, 178.

Wennerberg, K., Rossman K. L., Der, C. J., 2005. The Ras superfamily at a glance. Journal of Cell Science 118(Pt 5), 843-836.

Wilson, L. S., Elbatarny, H. S., Crawley, S. W., Bennett, B. M., Maurice, D. H., 2008. Compartmentation and compartment-specific regulation of PDE5 by protein kinase G allows selective cGMP-mediated regulation of platelet functions. Proceedings of the National Academy of Sciences of the USA 105(36), 13650-13655.

Wong, J. W., Cagney, G., 2010. An overview of label-free quantitation methods in proteomics by mass spectrometry. Methods in Molecular Biology 604, 273-283.

Wraith, K. S., Magwenzi, S., Aburima, A., Wen, Y., Leake, D., Naseem, K. M., 2013. Oxidized low-density lipoproteins induce rapid platelet activation and shape change through tyrosine kinase and Rho kinase-signaling pathways. Blood 122(4), 580-589.

Yan, G. R., He, Q. Y., 2008. Functional proteomics to identify critical proteins in signal transduction pathways. Amino Acids 35(2), 267-274.

Yang, J., Zhang, L., Yu, C., Yang, X., Wang, H., 2014. Monocyte and macrophage differentiation: circulation inflammatory monocyte as biomarker for inflammatory diseases. Biomarker Research 2(1), 1.

Yang, Z., 2002. Small GTPases: Versatile Signaling Switches in Plants. The Plant Cell 14 Suppl, S375-388.

Yokoyama, S., Ikeda, H., Haramaki, N., Yasukawa, H., Murohara, T., Imaizumi, T., 2005. Platelet P-selectin plays an important role in arterial thrombogenesis by forming large stable platelet-leukocyte aggregates. Journal of the American College of Cardiology 45(8), 1280-1286.

Yost, R. A., Enke, C. G., 1978. Selected ion fragmentation with a tandem quadrupole mass spectrometer. Journal of the American Chemical Society 100(7), 2274-2275.

Young, M. H., 2010. Atherosclerotic cardiovascular disease beginning in childhood. Korean Circulation Journal 40(1), 1-9.

Zhang, C. C., Li, R., Jiang, H., Lin, S., Rogalski, J. C., Liu, K., Kast, J., 2015. Development and application of a quantitative multiplexed small GTPase activity assay using targeted proteomics. Journal of Proteome Research 14(2), 967-976.

Zhang, G., Xiang, B., Dong, A., Skoda, R. C., Daugherty, A., Smyth, S. S., Du, X., Li, Z., 2011. Biphasic roles for soluble guanylyl cyclase (sGC) in platelet activation. Blood 118(13), 3670-3679.

Zhao Y., Brandish, P. E., Di Valentin, M., Schelvis, J. P., Babcock, G. T., Marletta, M. A., 2000. Inhibition of soluble guanylate cyclase by ODQ. Biochemistry 39(35), 10848-10854.

Zimman, A., Titz, B., Komisopoulou, E., Biswas, S., Graeber, T. G., Podrez, E. A., 2014. Phosphoproteomic analysis of platelets activated by pro-thrombotic oxidized phospholipids and thrombin. PLOS ONE 9(1), e84488.

Zoughlami, Y., Voermans, C., Brussen, K., van Dort, K. A., Kootstra, N. A., Maussang, D., Smit, M. J., Hordijk, P. L., van Hennik, P. B., 2012. Regulation of CXCR4 conformation by the small GTPase Rac1: implications for HIV infection. Blood 119, 2024-2032.